Thesis

LONG-TERM CELLULAR EFFECTS OF CHRONIC EXPOSURE TO NANOMATERIALS

LANGZEITEFFEKTE VON NANOMATERIALIEN AUF ZELLEN NACH CHRONISCHER EXPOSITION

submitted by

Bakk. rer. nat., MSc.

Maria FRÖHLICH (formerly MRAKOVCIC**)**

for the academic degree of

Doctor of Medical Sciences

(Dr. scient. med.)

at the

Medical University of Graz

Center for Medical Research

under the supervision of

Prof. Dr. med. Dipl. Biochem. Eleonore FRÖHLICH

2013

To my family

Eidesstattliche Erklärung

Ich erkläre ehrenwörtlich, dass ich die vorliegende Arbeit selbstständig angefertigt und abgefasst, und jene Personen und Institutionen, die am Zustandekommen der Forschungsdaten beteiligt waren, namentlich genannt habe. andere als die angegebenen Quellen habe ich nicht verwendet und die den benutzten Quellen wörtlich oder inhaltlich entnommenen Stellen habe ich als solche kenntlich gemacht. Die Arbeit an der Dissertation und daraus entstandener Publikation wurde gemäß den Regeln der „Good Scientific Practice“ durchgeführt.

Graz, am 18.04.2013

Declaration

I hereby declare that this thesis is my own original work and that I have fully acknowledged by name all those individuals and organisations that have contributed to the research for this thesis. Due acknowledgement has been made in the text to all other material used. Throughout this thesis and in all related publications I followed the guidelines of “Good Scientific Practice”.

April 18th, 2013

Acknowledgements

This project was performed at the Center for Medical Research of the Medical University of Graz, Austria. The work was funded by the Austrian Science Fund FWF [P22576-B18] and the Austrian Research Promotion Agency FFG; Research and Technology Development in the Project Cluster NANO-HEALTH.

I would like to thank my supervisor PD. Dr. Eleonore Fröhlich for providing me the opportunity to work on this topic. I appreciate her guidance as well as her efforts very much. Furthermore, I would like to acknowledge the advice, technical assistance, and the nice working atmosphere of all co-workers of the Core facility Microscopy: Markus Absenger, Tatjana Kueznik, and Claudia Meindl.

I want to thank Mag. Regina Riedl for her help in the statistical evaluation of the data. The cooperation of Dr. Eva Roblegg and her co-workers, especially Sandra Blass of the Institute of Pharmaceutical Sciences of the Karl-Franzens-University of Graz is highly appreciated.

I would like to express my gratitude to my family, especially my husband for supporting me all the time and making my studies possible.

TABLE OF CONTENTS

ABBREVIATIONS

(E)NM(s)	(engineered) nanomaterial(s)
NP(s)	nanoparticle(s)
nm	nanometer
µm	micrometer
cm	centimeter
PPP	plain polystyrene particle
PS	polystyrene
(MW)CNT(s)	(multi-walled) carbon nanotube(s)
CNT-COOH	carboxylated carbon nanotubes
R25	red fluorescent PPP of 25 nm
HUVEC	human unmbilical vein endothelial cell
sec	second
min	minute
hrs	hours
d	day
O / N	overnight
g	gravitation
rpm	Rotations per minute
µg	microgramm
ng	nanogramm
pg	picogramm
ml	milliliter
DMEM	Dulbecco's modified Eagle‘s Medium
PBS	phosphate buffered saline
HBSS	Hanks‘ Balanced Salt Solution
Mg^{2+}	magnesium ions
Ca^{2+}	calcium ions
EDTA	ethylene diamine tetraacetic acid
FBS	fetal bovine serum
P / S	penicillin / streptomycin
mM	millimolar

EtOH	ethanol
GEM™	Global Eucaryotic Microcarrier
MTS	3-(4,5-dimethylthiazol-2-yl)-5-(3-carboxymethoxyphenyl)-2-(4-sulfophenyl)-2H-tetrazolium
ELISA	Enzyme-linked immunosorbent assay
OD	optical density
LDH	lactate dehydrogenase
U	unit
IC_{50}	inhibitory concentration where 50% of enzymes are blocked
CYP(450)	cytochrome P450
ROS	reactive oxygen species
IL	interleukin
BSA	bovine serum albumin
poly-HEMA	poly-(2-hydroxyethyl methacrylate)
LPS	lipopolisaccharide
RT	room temperature
HRP	horse radish peroxidase
Tris	Tris (hydroxymethyl) aminomethane
HCl	hydrogen chloride
NaCl	sodium chloride
SDS	sodium dodecyl sulfate
PARP	poly (ADP-ribose) polymerase

LIST OF FIGURES

LIST OF TABLES

ABSTRACT

Nano-sized materials could find multiple applications in medical diagnosis and therapy. One main concern is that engineered nanoparticles, similar to combustion-derived nanoparticles, may cause adverse effects on human health by accumulation of entire particles or their degradation products. Chronic cytotoxicity must therefore be evaluated.

In order to establish a model for chronic cytotoxicity testing, plain polystyrene nanoparticles (20 and 200 nm), the endothelial cell line EAhy 926, as representatives for epithelial cells, as well as THP-1 cells, representing immune cells, were used. Culturing was performed in a microcarrier cell culture system for anchorage-dependent cells (BioLevitator^{TM}) and a bioreactor culturing system for in suspension growing cells (CELLine CL350). Viability, mode of action assays, and cytokine secretion served as read-out parameters. The established system was used for cytotoxicity testing of > 50 nm short plain and carboxyl-functionalized multi-walled carbon nanotubes. Cells were cultured for four weeks and exposed to doses of polystyrene particles, which were not cytotoxic upon 24 hours of exposure. In addition, fluorescent polystyrene particles were applied in order to investigate their sub-cellular localization. For comparison, these particles were also studied in regularly sub-cultured cells, a method that has traditionally been used to assess chronic cellular effects.

Culturing by using both, microcarrier and bioreactor culture methods, produced very high cell densities. After four weeks of exposure, the number of EAhy 926 cells exposed to 20 nm polystyrene particles decreased by 60% as compared to untreated controls. Fluorescent particles were mainly localized in the lysosomes of the exposed cells. When tested in sub-cultured cells, the same particles decreased cell numbers to 80% of the untreated controls. Dose-dependent decreases in cell numbers were also noted after exposure of microcarrier cultured cells to 50 nm short functionalized multi-walled carbon nanotubes, but not upon exposure to plain nanotubes of the same size. Our findings support that necrosis, but not apoptosis, contributed to cell death of the exposed cells in the microcarrier culture system.

In contrast, exposure of THP-1 monocytes to polystyrene particles in bioreactor cultures, revealed unreliable findings. Not only the reaction to the particles, but

also growth of untreated THP-1 cells in the bioreactor showed great variations between the experiments. The uptake of fluorescent particles was very poor; only one out of 1000 cells was found to contain particles. When sub-cultured cells were exposed to polystyrene particles, the cell number was reduced as expected in a dose- and size-dependent manner. Here, too, necrosis, following an inflammatory response, contributed to cell death of exposed monocytes. However, exposure to both types of carbon nanotubes showed no changes in cell proliferation, and induced no release of cytokines as compared to untreated cells.

In conclusion, the established microcarrier model for anchorage-dependent cells appears to be more sensitive for the identification of cellular effects upon prolonged and repeated exposure to nanoparticles than traditional sub-culturing. In contrast, long-term effects on monocytes are superiorly assessed in sub-cultured cells than in bioreactor cultures. While polystyrene particles partially induce adverse effects on both cell types, carbon nanotubes seemed to be less harmful. These findings could prove short carbon nanotubes to be suitable for applications in biomedical applications.

ZUSAMMENFASSUNG

In der heutigen Zeit werden verschiedene Nanomaterialien immer häufiger zu unterschiedlichen Zwecken (in der Medizin, der pharmazeutischen und kosmetischen Industrie, usw.) angewandt. Großes Interesse besteht darin, sowohl industriell hergestellte, als auch natürlich vorkommende Nanopartikel, hinsichtlich ihrer Verträglichkeit zu untersuchen. Da Nanopartikel oder deren Abbauprodukte in Zellen akkumulieren können, muss neben einer akuten Schädigung auch die langzeitliche Zytotoxizität untersucht werden.

Zur Untersuchung der Langzeittoxizität nach chronischer Exposition von Endothelzellen und Monozyten, wurden, im Rahmen der vorliegenden Arbeit, zwei Methoden zur Langzeitkultivierung etabliert und mit konventionellen Methoden verglichen: eine *„microcarrier“* (dt. Mikroträger) Zellkultur für Endothelzellen (BioLevitator^{TM}) und eine Bioreaktor Zellkultur für Monozyten (CELLine CL350). Die Zellen wurden über einen Zeitraum von vier Wochen kultiviert. Als Modellpartikel wurden nicht-funktionalisierte Polystyrol-Nanopartikel, mit einem Durchmesser von 20 und 200 nm, verwendet. Zusätzilch wurde die intrazelluläre Lokalisierung der Partikel mittels fluoreszenter Polystyrolpartikel (20 nm) untersucht. Nach Etablierung der geeigneten Methode wurden auch zelluläre Effekte nach Behandlung mit kurzen Kohlenstoffnanoröhren (engl. *carbon nanotubes*, CNTs), mit einem Durchmesser von > 50 nm, untersucht.

Nach Behandlung der *„microcarrier“* Kulturen mit 20 nm Nanopartikeln reduzierte sich die Zellzahl um etwa 60%. In konventionellen Kulturen verringerte sich diese jedoch nur um 20%. Funktionalisierte CNTs führten ebenfalls zu einer dosisabhängigen Abnahme der Zellzahlen. Diese Änderungen wurden hauptsächlich durch nekrotischen Zelltod hervorgerufen.

Im Gegensatz zu den Endothelzellen, wurden bei Monozyten aussagekräftigere Ergebnisse mittels konventioneller Methoden erzielt. Auch hier nahm die Zellzahl nach Behandlung mit Polystyrolpartikel ab. Dieser Effekt war jedoch dosis- und größenabhängig. Zellnekrose aufgrund einer entzündlichen Reaktion verursacht durch Nanopartikel konnte dabei als wichtigster Mechanismus identifiziert werden. Interessanterweise konnten bei der Behandlung von Monozyten mit CNTs hingegen keine Änderungen festgestellt werden.

Während sich für die Untersuchung der langzeitlichen Wirkung von unterschiedlichen Nanomaterialien auf Endothelzellen die *„microcarrier“* Zellkultivierung als geeignete Methode herausstellte, konnte für Monozyten nur die konventionelle Technik angewandt werden. Es konnte gezeigt werden, dass Polystyrolpartikel zum Teil erhebliche Schäden an Zellen hervorrufen können. Eine Exposition mit CNTs schien jedoch harmloser zu sein. Diese Erkenntnisse unterstützen somit die unbedenkliche Anwendung von kurzen CNTs sowohl in verschiedenen biomedizinischen, als auch in anderen Produkten.

1. INTRODUCTION

1.1 Nanomaterials and Nanotechnology

The prefix “nano” (greek: *nanos* = dwarf) refers to nanometer (nm) which is 1 x 10^{-9} meter (Arora *et al*., 2012). Nanomaterials (NMs) are either natural, or engineered, or accidental structures with at least one dimension that ranges from 1 – 100 nm (Nel *et al*., 2006, EU). Natural or accidental particles of < 100 nm usually derive from volcano eruptions or are by-products of other processes such as fire smoke, diesel exhaustion, etc. However, the term nanoparticle (NP) refers only to engineered NMs (ENMs). Therefore, the new branch in technology dealing with engineering, characterization, and application of such materials is called nanotechnology (Hartmann *et al*., 2008). For comparison, the size distribution of different “small” objects is presented in Figure 1.

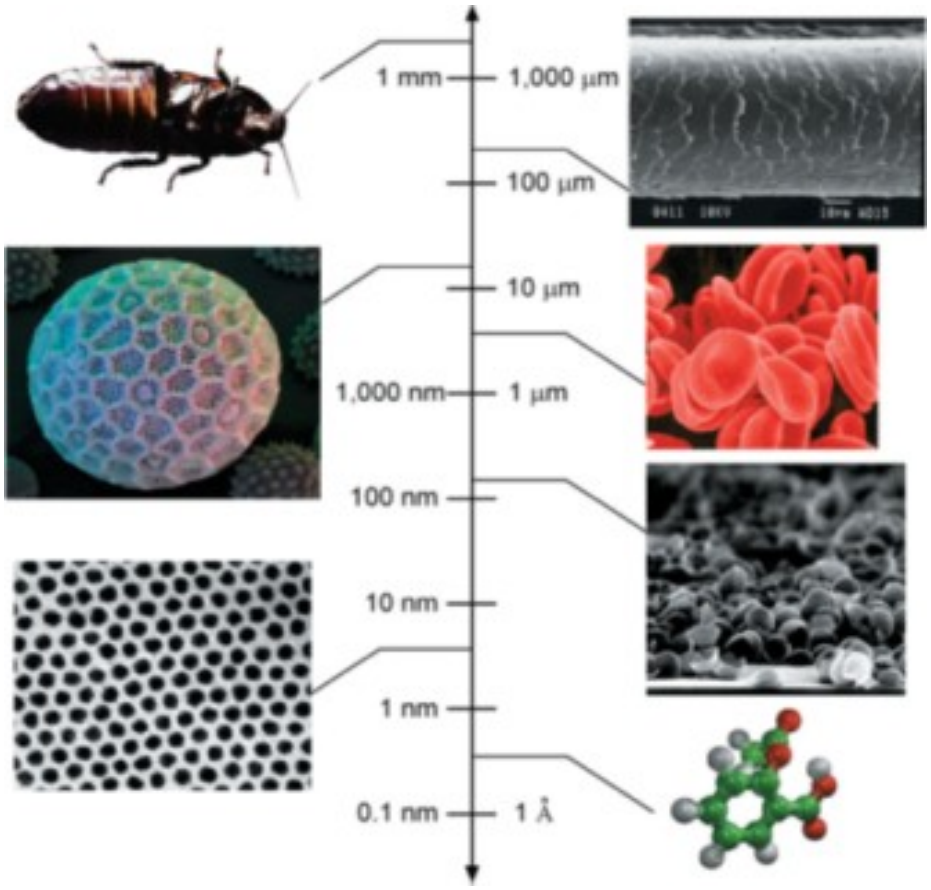

Figure 1. Sizes of different small objects. On the left (from top to bottom): a cockroach, a pollen grain, a cobalt nanocrystal superlatice; on the right side: a human hair, red blood cells, an aggregate of half-shelfs of palladium, an aspirin molecule.
From: Whiteside, Nature Nanotech. 2003

Different nanoscaled objects are presented in Figure 2.

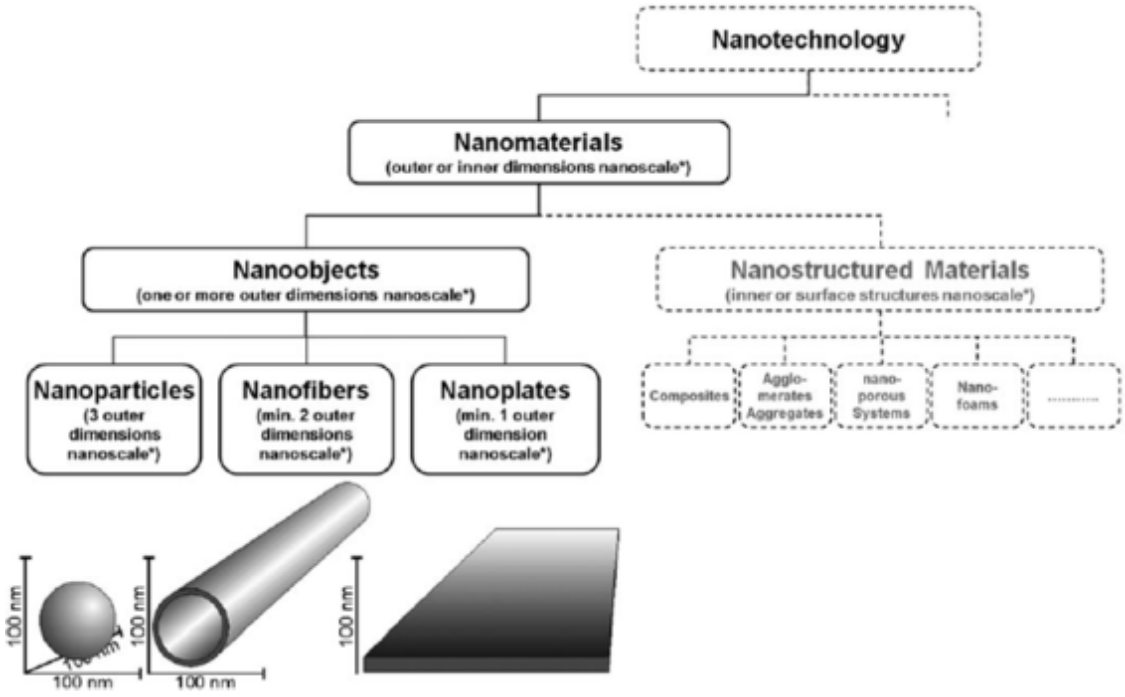

Figure 2. Definition of nanoobjects.
From: Krug and Wick, Angew. Chem. Int. Ed. 2011

Both, the biological and physical sciences share common interests in nano- and microscale structures. However, they show nanoscience in different aspects. ENMs show unique physicochemical properties when compared to their larger counterparts. In physical sciences, NPs offer quantum phenomena, such as size-dependent fluorescence, as well as remarkable physical properties, for instance electrical conductivity, etc. However, also in biological systems (e.g. cells), "nano-structures" can be found (single molecules, organelles, etc.) (Whitesides, 2003). Therefore, NPs are increasingly being used for commercial purposes such as electronics, biotechnology, cosmetics, biological / pharmaceutical / medical sciences (drug delivery, imaging contrast agents), and medicine (cancer therapy) (Arora *et al*., 2012; Ai *et al*., 2011). Due to their small size and a very high surface to volume ratio, NPs can easily interact with cell surfaces and even intracellular structures (Alexis *et al*., 2008; Hartmann *et al*., 2008; De Jong *et al*., 2008).
In Figure 3, cellular uptake mechanisms of NPs are presented.

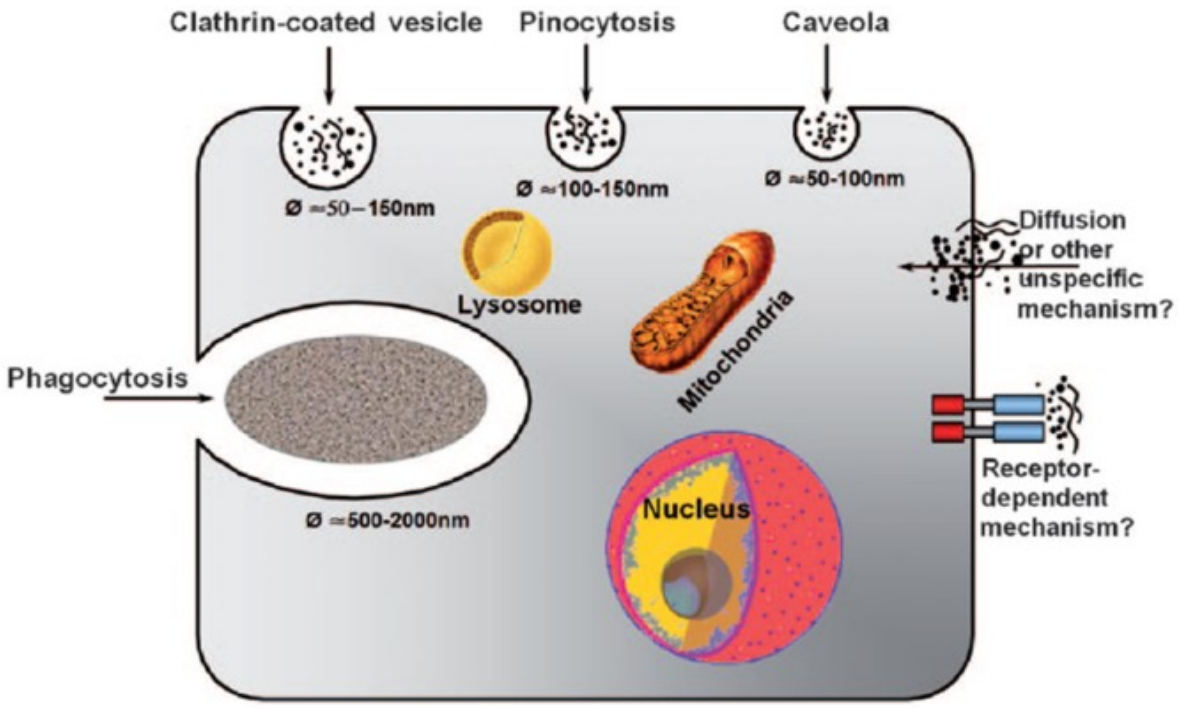

Figure 3. Cellular uptake of NPs.
From Krug and Wick, Angew. Chem. Int. Ed. 2011

1.1.1 Nanostructures in biotechnology

Several physical nano-structures can act as tools in biological applications and/ or biotechnology (Whitesides, 2003). Self-assembled monolayers allow guidance of cell behaviour, attachment, and growth. In addition, cell motility can be studied easily by applying a voltage pulse to the surface of the monolayer (Jiang *et al*., 2003). Other systems, such as optical or magnetic tweezers, provide more detailed insights into functions on the single molecule level, e.g. proteins involved in transport within cells (Knight *et al*., 2001; Block *et al*., 2003). In tissue engineering, nano- or microstructured three-dimensional scaffolds are used. Several different labelled and / or coated NPs are commercially available and are used for cell tracking, as well as for imaging.

1.1.2 NPs for drug delivery

Nanotechnology has enabled the development of combinatorial drug delivery systems using biologically targeted carriers. ENMs may be applied to enhance specificity of drug delivery, reduce toxicity, and enhance therapeutic efficacy of

drugs, as well as permit novel combinatorial therapies (e.g. in cancer therapy). One of the earliest vehicles used as drug delivery agents in cancer therapies were liposomes (Moghimi *et al*., 2005). The use of liposomes allows enhanced delivery of therapeutic agents while their cytotoxic potential is reduced. Furthermore, liposomes are amenable to surface conjugation enabling a better targeting to the desired site of action. Since then, numerous other nanoscale vehicles, such as carbon nanotubes (CNTs), dendrimers, and polymers, have been or are currently under development. Sengupta *et al*. (2005) have developed a targeted "nanocell" for the temporal release of an anti-angiogenic agent and cytotoxic chemotherapy at tumour sites demonstrating significantly enhanced efficacy.

1.1.3 NPs as imaging contrast agents

NPs have tremendous potential for imaging modalities. Specifically engineered NMs improved the specificity, sensitivity, and functionality of imaging contrast agents. In addition, such new agents are expected to act less toxic compared to traditional imaging contrast agents.

A variety of nanoscale imaging contrast agents have been developed. For instance, nanocages, CNTs, gold-speckled silica NPs have been characterized as contrast agents for photoacoustic tomography (Yang *et al*., 2007; De la Zerda *et al*., 2008; Sharma *et al*., 2008). Other NPs, such as iron oxides, are used in magnetic resonance imaging approaches. Sharma *et al*., characterized gold-speckled silica NPs as a novel multimodal imaging contrast agent. These NPs function simultaneously as contrast agents for fluorescence imaging, photo-acoustic imaging, and magnetic resonance imaging (Sharma *et al*., 2008).

1.1.4 NPs in use for cancer therapies

A wide variety of NPs, including polymers, lipids, dendrimers, as well as organometallic, and carbon-based NMs, are under investigation and development for cancer therapy and cancer imaging or diagnosis, both combined in the term "cancer nanotechnology". Nanotechnology may enable high-throughput screening analysis *in vitro*. In addition, the sensitivity and/ or specificity of *in vitro* diagnostic assays may be potentially increased by using NMs. A variety of nanoscale

systems, such as nanowires, nanotubes, cantilevers, etc., are currently being developed to have implications for clinical cancer care (Heath and Davis, 2008; Pope-Harman *et al.*, 2007). Other NPs, such as semiconductor nanocrystals or luminescent quantum dots, have been applied for enhanced tissue analysis (Bruchez *et al.*, 1998; Chan *et al.*, 2002).

The selection of a particular material for therapeutic purposes depends on the size, surface characteristics, biocompatibility, toxicity, as well as their properties in biologic systems. NPs have several properties that make them more efficient than conventional cancer therapeutics:

- NPs can act as drug delivery systems, even when loaded with different drugs in order to act as a combinatorial cancer therapy,
- NPs themselves can have therapeutic or diagnostic properties,
- Attachment to targeting ligands yield high affinity for target cancer cells, and
- NPs can bypass drug resistance mechanisms.

Even NP formulations of already established therapeutics have been integrated into cancer therapies, and clinical trials are performed. As shown by *Peer et al.* (2007), these NPs show higher efficacy and less toxicity compared to conventional drugs.

Interestingly, the use of NPs in cancer nanotechnology opens the door to new, non-invasive therapeutic strategies. This includes:

- Photothermal therapy: relies on the properties of NPs which have high absorption in the near-infrared (NIR) region. O'Neal *et al*. (2004) have demonstrated systemic thermal ablation of tumors *in vivo* following systemic injection of gold nanoshells and exposure to NIR light. Other NMs, such as nanorods, and CNTs have also been characterized as nanoscale mediators for photothermal ablation of tumors.

- NP-enhanced radiotherapy: Hainfeld *et al.* (2004) demonstrated an improved efficacy of radiation therapy on mammary carcinomas *in vivo* following intravenous administration of gold NPs. Similar results were obtained by *Chang et al.* (2008) by using an *in vivo* model of melanoma. Also in *in vitro* studies, gold NPs were demonstrated to enhance radiotherapy on tumors. Therefore, the

application of NPs in radiation therapies on cancer cells allows a dose reduction leading to reduced cytotoxicity to the surrounding tissue.

- NP-enhanced radiofrequency therapy: use of NPs in an invasive approach enables the development of a non-invasive ablation of tumor cells. Gold NPs as well as CNTs have been shown to enhance a non-invasive destruction of tumors *in vitro* and *in vivo* (Gannon *et al.*, 2008; Cardinal *et al.*, 2008; Gannon *et al.*, 2007).

- Cancer theranostics: used to simultaneously detect and treat cancer cells. Biodegradable NPs, such as iron oxides, are currently being developed as theranostic agents which allow a non-invasive diagnosis via optical/ magnetic resonance imaging, and targeted cancer therapy (Santra *et al.*, 2009). Such strategies may accelerate diagnosis and treatment of tumors, improve cure rates, while reducing side-effects of a treatment.

1.2 Nanotoxicity and nanotoxicology

The main characteristic of NPs is their small size by which their unusual physical and chemical properties (surface area, size distribution) are conditioned. Moreover, also other properties, such as chemical composition (purity, electronic properties, etc.), surface structure (functionalization, reactivity, etc.), shape, solubility, and aggregation, contribute to it (Nel *et al.*, 2006). In 2005, Oberdörster *et al.* have identified 17 different features which need to be considered when assessing NP toxicity. All these desirable physicochemical properties which make NPs suitable for biomedical applications are the same that raise concerns about adverse effects on biological systems (e.g. organs and tissues, cells, as well as sub-cellular organelles and structures) (Nel *et al.*, 2006). A short summary of the main NP classes as well as their applications and biological safety concerns, are presented in Table 1.

However, exposure to not only ENMs (e. g. industry (production process, handling), use of cosmetics and medical products containing NPs, etc.), but also natural or accidental particles (e. g. volcano eruption, air pollution, etc.) may be harmful to organisms and / or to the environment. Hence, one of the major

professional groups interested in investigating the potential risks of NMs are the occupational health staff.

NP	Application	Safety concerns	Mechanistic areas of interest
Metal NPs	Contrast agents; drug delivery	Element specific toxicity; reactive oxygen species	Excretion
Nanoshells	Hyperthermia therapy	None demonstrated	Excretion
Fullerenes	Vaccine adjuncts; hyperthermia therapy	Antibody generation	Immunotoxicity
Quantum dots	Fluorescent contrast agents	Metabolism	Intracellular/ organ distribution; excretion
Polymer NPs	Drug delivery; theraprutics	Unknown	Metabolism; immunotoxicity; complement activation
Dendrimer	Guest delivery of drug/ radiolabel dose	Metabolic path	Surface chemistry and elemental effects; complement activation
Liposome	Drug delivery; contrast agents vehicle	Hypersensitivity reactions	Complement activation

Table 1. NP classes, their application and safety concerns. Adopted from Fischer and Chan; Curr. Op. Biotech 2007.

1.2.1 Historic overview

The use of NPs in different areas has a long history. For instance, colloidal gold is used in medicine since the 1920s in treatment of tuberculosis. In addition, it has found application in the treatment of rheumatic diseases (Bhattacharya and Mukherjee, 2008; Fadeel and Garcia-Benett, 2010).

Moreover, the danger of inhaling air-borne particulate matter (smoke or fume particles) was recognized already since ancient times (Maynard and Baron, 2004). However, only researchers in the 1980s started to investigate the impact of particles with sizes in the nanometer range on human health (Oberdörster *et al*., 1990; Ferin *et al*., 1990). About those times, a new type of NM was discovered - CNTs (Iijima, 1991). In the 1990s, associations between NP inhalation and diseases of the respiratory and / or cardiovascular system were uncovered (Dockery *et al*., 1993). In addition, more concerns arose about the effects of the inhalation of CNTs - or nanoscale fibres in general- on human health (Coles, 1992).

Since nanoscaled materials act differently compared to their larger counterparts, the need of a specific category in toxicological sciences raised. Even when made of inert elements such as gold, NPs become highly (re)active or catalytic when approaching the nanoscale (Ai *et al*., 2011). This is mainly caused by the very high surface to volume ratio (Xia *et al*., 2006). Therefore, in 2004, Ken Donaldson and his colleagues named this new branch of science “nanotoxicology” (Donaldson *et al*., 2004). As presented in Figure 4, the principle components of this branch include the production, physicochemical and biological characterization, as well as risk assessment and risk management.

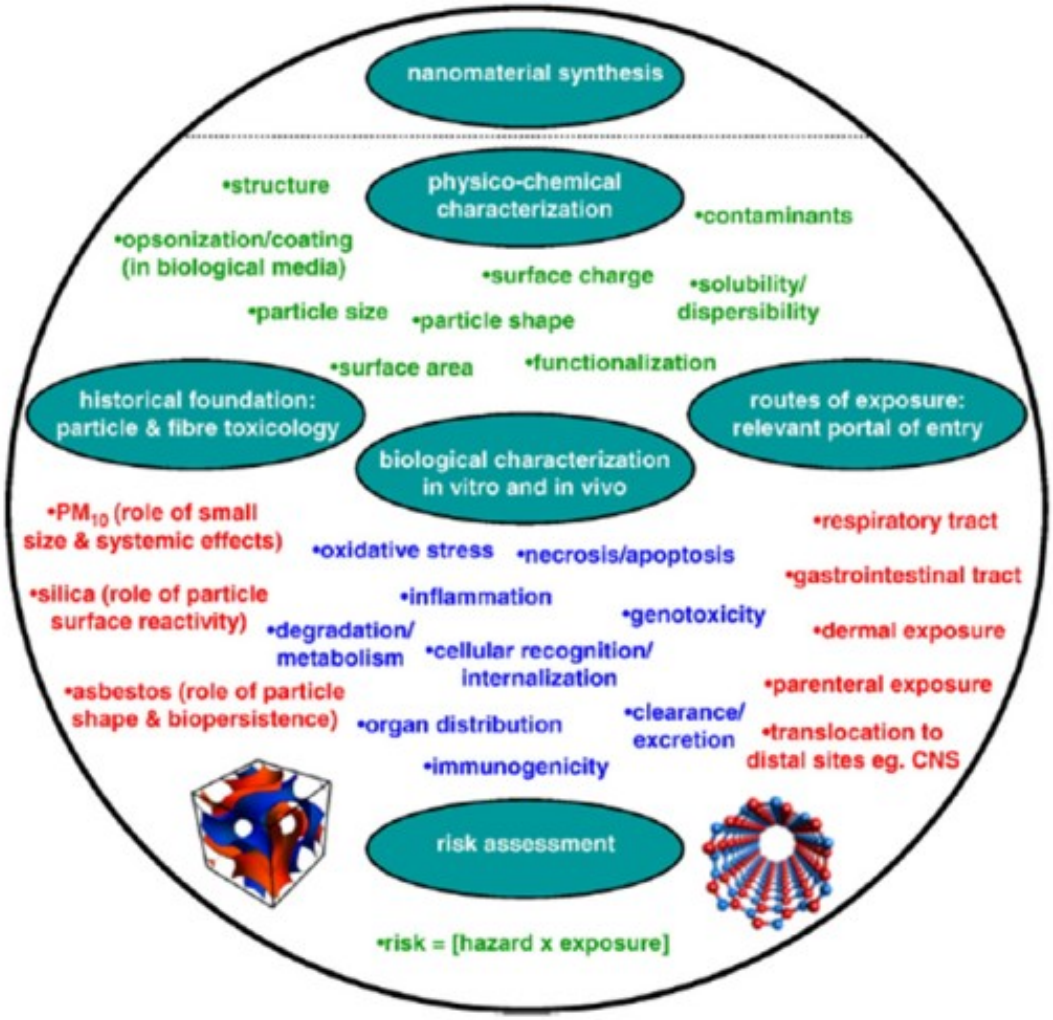

Figure 4. Overview of the interdisciplinary science named nanotoxicology.
From: Fadeel and Garcia-Benett, Adv. Drug Deliv. Rev. 2010

1.2.2 Physicochemical characteristics important for toxicity

The most important properties for particle toxicity are: size and chemical composition (Ai *et al*., 2011). However, other determinants, such as coating, particle shape, surface, aggregation state, etc., are also influencing the potential biological effect of a NP (Schlesinger 1995; Chithrani *et al*., 2006; Lockman *et al*., 2004; Wick *et al*., 2007).

By decreasing the particle size, more chemical molecules may attach to its surface. Hence, the reactivity and toxic potential are enhanced (Linkov *et al*., 2008; Hyuk *et al*., 2009). In 2009, Hyuk *et al*. have demonstrated that the ability of NPs to cross the mucosal barrier is size-dependent: the smaller the NPs, the more they were detected in the lymphatic tissue of the intestine.

In addition, the surface of a NP is also discussed to play an important role in toxicity. Reactive groups linked to the surface of an NP, may influence the interaction with biological materials. Also other features, such as hydrophobicity / hydrophilicity of a NP, may be used to estimate the toxic potential. As demonstrated for silica NPs, surface modifications could influence the cytotoxicity, inflammogenicity, and fibrogenicity (Schins *et al*., 2002), thus leading to fibrosis and lung cancer. As proposed by Fubini in 1997, these effects may be caused by the appearance of surface radicals and reactive oxygen species. However, some surface modifications, such as coating, can reduce the toxicity of NPs (e.g. iron NPs).

Moreover, the shape of NPs was demonstrated to influence the biological effects. In 2007, Pal *et al*. have investigated the interaction of silver NPs with bacteria, and they could show that the NPs undergo a shape-dependent interaction. HeLa cells have been demonstrated to rather uptake spherical gold NPs than gold nanorods (Chithrani *et al*., 2006). In the case of fibres (e.g. anatase titanium dioxide, CNTs), it has been shown that long structures are more prone to initiate inflammatory responses in lung tissue than short particles. Moreover, the length of a fibre is related to its toxicity as it might be an indication for its bio-persistence (Donaldson *et al*., 2004; Hamilton *et al*., 2009). Similar to asbestos fibres, long persistent fibres initiate pathogenic effects, while short and / or non-persistent fibres undergo phagocytosis (Donaldson *et al*., 2004). In addition, contamination with heavy metals (e.g. iron, etc.) is an important issue in assessing toxicity of CNTs. The

metals are originally used as scaffolds in the synthesis process and already have been documented to exert toxicity (Donaldson et al., 2006).

Possible biological effects caused by the physicochemical properties of different NPs are presented in Table 2.

Physicochemical property		Toxicokinetic findings	Biological effects
Size	15nm gold NP	Most widespread organ distribution	Biodistribution of NPs
	15 and 50nm gold NP	Pass blood-brain barrier	Blood-brain barrier permeability
	50nm QDs	Receptor-mediated endocytosis	
	1 – 10nm silver NP	Penetration inside bacteria	
Shape	Open-ended SWCNTs	Blocking of ion channels	Spherical SWCNTs less reactive
	Spherical gold NPs	Higher uptake	Reduced uptake of rod-shaped
	Carbon-based NPs	Stimulate human platelet aggregation; accelerate the rate of vascular thrombosis	Biological reactivity: mixed carbon NPs > SWCNTs > MWCNTs
Chemical composition	Incorporation of 1% manganese doping into titania NPs	Increase in UV-A absorption; reduction in free radical generation	
	Metal traces associated with commercial CNTs	Dose- and time-dependent increase of intracellular ROS; decrease of mitochondrial membrane potential	More reactive compared to purified CNTs
	QDs core metalloid complexes of cadmium	Can cross blood-brain barrier and placenta; systematical distribution to all tissues	Probable carcinogen
	Metal (oxide) NPs	Different cytotoxicity patterns	Reduce cell proliferation; induce cell death
Surface charge	Positively charged dendrimers	Increased deposition into tissues	Neutral dendrimers show reduced deposition
	Coating of silica NPs with aluminium lactate	Inhibition of DNA strand brakeage and formation of 8-hydroxy-deoxyguanosine	Reduction in genotoxicity
Surface area to volume ratio	TiO2 (300 cm^2)	Increased lymph-node burdens	Inflammation
	Ultrafine carbon black NPs (270m^2/g)	Increased pulmonary toxicity	Higher reactivity than larger NPs (22m^2/g)
Aggregation state	Rope-like CNTs	Induction of cytotoxicity	More reactive than well dispersed CNTs

Table 2. Biological effects due to physicochemical properties. Adopted from Arora *et al.*, Toxicol. Appl. Pharmacol. 2012

1.2.3 Routes of exposure

The human body has several interfaces for direct substance exchange with the environment (Figure 5). The four most important organs with regard to the uptake of NPs are the skin, bloodstream, respiratory tract, and gastrointestinal tract.

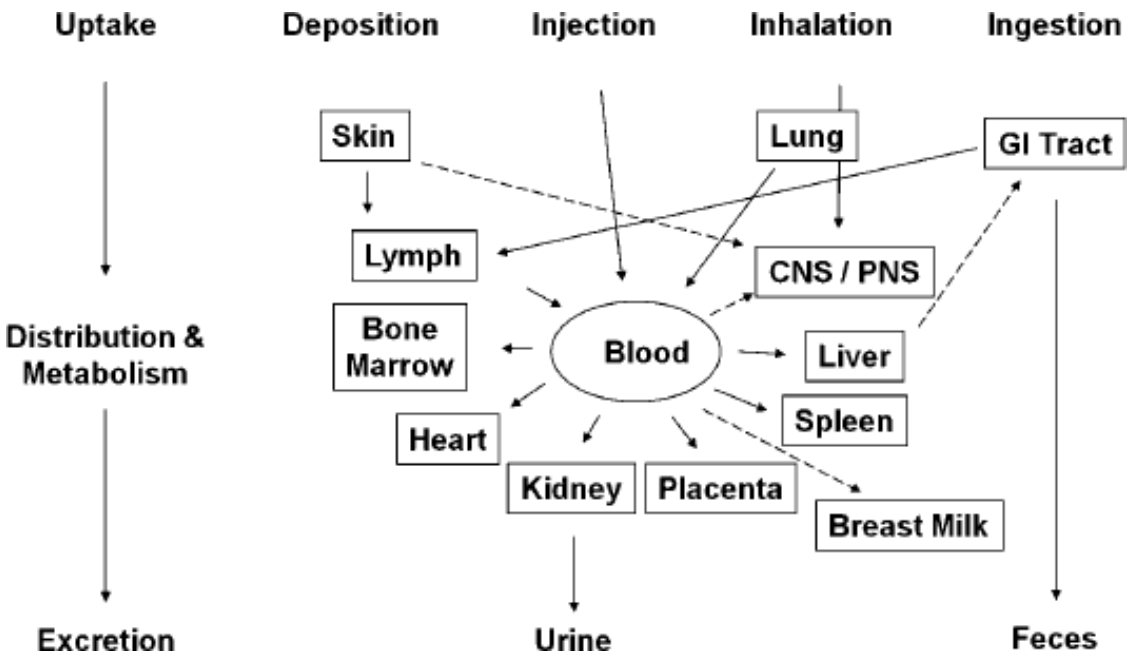

-Figure 5. Exposure routes and bio-distribution of NPs in the body.
From Krug and Wick, Angew. Chem. Int. Ed. 2011

- Dermal exposure: the healthy skin is an important barrier. It is a 1.5 – 2 m² organ which is composed of three layers: epidermis, dermis, and subcutis. The first cell layer of the epidermis is the corneal layer (= *stratum corneum*). It mainly consists of dead epithelial cells (= keratinocytes) representing the first mechanical barrier for NPs. The dermis (= *corium*) is located beneath the epidermis and consists of connective tissue. It contains hair follicles, sweat glands, and perspiratory glands. These two layers are separated by a basal membrane. Blood vessels and nerves (e.g. lammelar bodies) are located in the loose connective and adipose tissue of the subcutis (Figure 6).

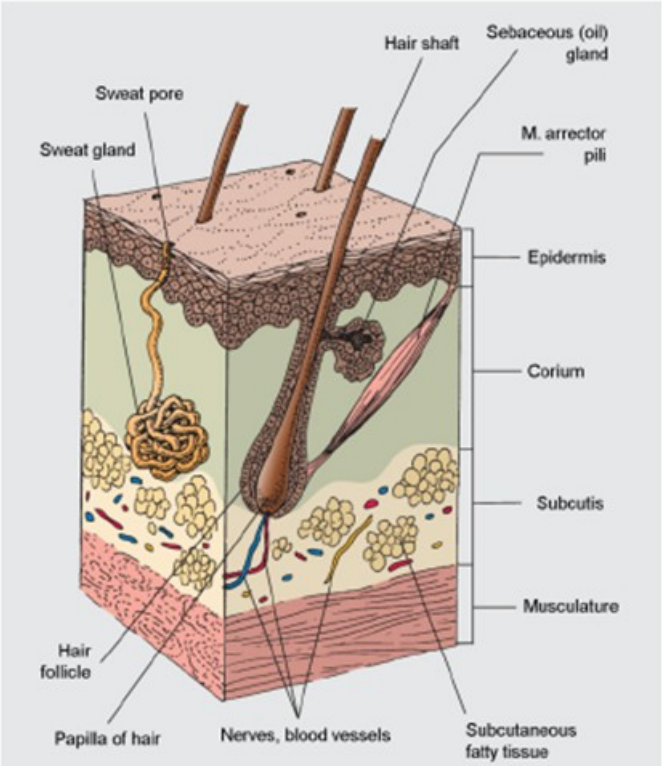

Figure 6. Skin model.
From Roblegg et al., EuroNanoTox Letters 2009

There are three major exposure scenarios: air pollution, application of cosmetics containing NPs, and application of nanotechnology in textile industry (Roblegg *et al.*, 2009). So far, not many exposure studies on healthy skin were performed. However, some studies could show titanium dioxide (TiO_2) NPs, which are used in sunscreens, to be found in the first two cell layers of keratinocytes or even in hair follicles (Tinkle *et al.*, 2003). As shown by Ryman-Rasmussen *et al.* in 2003, the penetration of NPs into the skin depends on their size as well as the applied surface coatings of the NPs. In addition, studies on toxicological effects of exposing diseased or stressed skin to several kinds of NPs must be performed.

- Exposure to injected NPs: injection of NPs is mainly used in diagnosis and therapies. Nanoscale imaging contrast agents, as well as transport vehicles in cancer therapies are currently under investigation. The NPs are either injected directly into the target organ or into the bloodstream from where they can be easily distributed.

Injection of NPs is the choice when biological barriers, such as the skin, gastro-intestinal tract, etc. need to be bypassed. However, other types of barriers, such as the blood-brain-barrier (BBB) or the placenta of pregnant women become more

relevant (Helland *et al.*, 2008; Wick *et al.*, 2010). The ability of NPs to pass the BBB is exploited to transport anti-cancer drugs into the brain.

However, when investigating NPs for their administration into the bloodstream, the potential effects on different functions need to be evaluated (Abdelmoez *et al.*, 2010). In 2008, Mayer *et al.* investigated the effects of carboxyl-functionalized polystyrene particles on hemocompatibility. The authors could show that small and positively charged NPs caused thrombocyte and granulocyte activation and hemolysis, as well as the activation of the complement system, respectively. In addition, they showed negatively charged NPs > 60 nm to be less hematotoxic.

- Inhalation: organs with respect to the entry and distribution of inhaled NPs are the nasal cavity, the trachea, and the lung (Figure 7).

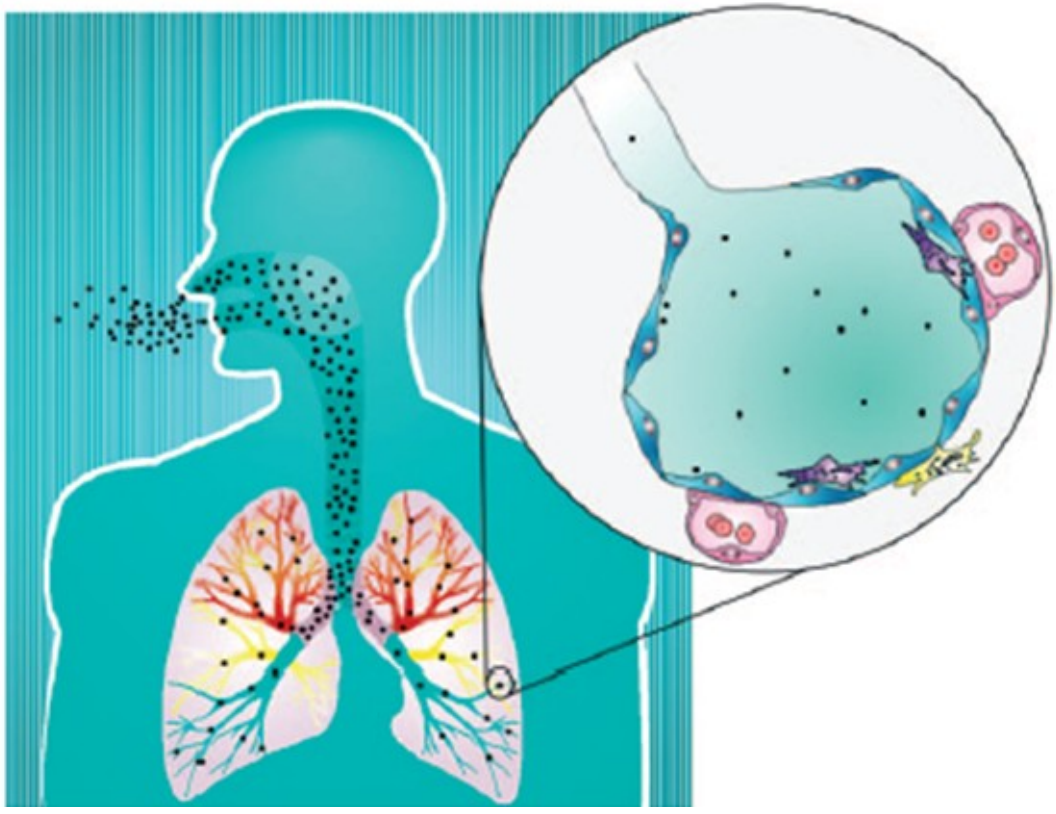

Figure 7. Inhalation of particles.
From Krug and Wick, Angew. Chem. Int. Ed. 2011

Larger particles or aggregates (> 50 µm) deposit on the nasal mucosa and are therefore under investigation as effective drug delivery vehicles. However, some studies reported a translocation of NPs into the brain via the olfactory nerve (Oberdörster *et al.*, 2004; Elder *et al.*, 2006). Other studies demonstrated

morphological and cellular expression of free radical formation in microglia (= brain macrophages) of mice exposed to small NPs (Long *et al.*, 2006).

Large particles are mostly removed by mucociliary transport (Krug and Wick, 2011). The transport of a NP into the lung depends on the particle size: the smaller the particle, the higher is the probability of its transport. Particles < 2.5 µm can be transported into the alveoli. Once present, the particles are removed by phagocytosis resulting from the activation of lung macrophages (Borm *et al.*, 2006). This may further lead to tissue damage and systemic effects due to the inflammation of the lung. Furthermore, the translocation of NPs to the blood vessels (Geiser *et al.*, 2005) and the distribution to other organs may result in cardiovascular effects (Hoet *et al.*, 2004).

If NPs are not sufficiently cleared they could be deposited in the interstitium, thus leading to oxidative stress reactions and inflammation. Moreover, oxidative damage may occur due to the production of free radicals, similar to the manifestation of exposure to asbestos fibres (Donaldson *et al.*, 2004). The clearance of NPs from the respiratory tract depends on the physicochemical properties of the particles. In addition, the health status of the organ is of high importance: the clearance mechanisms are extremely efficient as long as they are not chronically overstressed (e.g. by dust in workplaces, by smoking, etc.) (Krug and Wick, 2011).

- Ingestion: NPs can enter the gastrointestinal tract either through food and water, by application of medications and / or other consumer products, or can be swallowed unknowingly after mucociliary clearance has occurred (Oberdörster *et al.*, 2005).

While some studies report no uptake at all, some others reported absorption of NPs through the intestinal wall (Volkheimer, 1974). Here, too, the size of the NPs seems to be the most important physicochemical property (Jani *et al.*, 1990). However, due to coating of NPs also larger particles can penetrate the intestinal mucosa, thus enabling the application of oral “nano-therapeutics” with enhanced efficacy of encapsulated drugs (Gradauer *et al.*, 2012; Gradauer *et al.*, 2013).

1.2.4 Cytotoxicity screening assays

When investigating the toxicity of agents, such as chemicals, NPs, etc., cell-based assays are often applied before experiments are performed in animals. Compared to *in vivo* testing, *in vitro* assays are less expensive and easier to control and reproduce. Moreover, because of the urging need to develop alternatives to animal testing, cellular assays become more attractive.
For assessing the toxicity of NPs, mainly cells of the respective organ (e.g. lung, skin, immune system, etc.) are used. Endpoints such as cytotoxicity, proliferation, and genotoxicity are evaluated (Hillegass *et al*., 2010).

- Cytotoxicity assays: The easiest assay to evaluate cytotoxicity is the visual inspection of the cells using bright-field microscopy (Fiorito *et al*., 2006). However, colorimetric methods are used more frequently. Cytotoxicity is often accompanied with a loss of membrane integrity. Assays such as neutral red, Trypan blue, and the LIVE / DEAD viability test are based on cell staining – live and dead cells are distinguished according to the different staining patterns (Lewinski *et al*., 2008). Loss of membrane integrity may also lead to leakage of the cellular content (e.g. lactate dehydrogenase, LDH); the amount of released LDH is proportional to the number of damaged cells (Haslam *et al*., 2000).
Another group of methods include the determination of the cell death mechanism. A major part of assays rely on the enzymatic cleavage of a tetrazolium salt by the mitochondrial dehydrogenase. This reaction can occur only in living cells (Mosmann, 1983). The most commonly used tests are the MTT, MTS and WST (-1 and -8) viability assays. In addition to assessing the mitochondrial activity, assays on detecting activated effector caspases such as caspase-3 and caspase-7 may give more insights on the mode of cell death of NPs (Ott *et al*., 2002).
Other, sub-lethal effects of NPs, including oxidative stress, lipid peroxidation, and inflammation are combined in a third group of cell damage. Oxidative stress is mostly detected by the glutathione (GSH) assay. The assay can also be used when determining lipid peroxidation. In addition, other methods such as the thiobarbituric acid (TBA) assay can be used. Inflammation, however, is mainly determined by detecting pro-inflammatory cytokines (e.g. IL1-ß, IL6, TNFα, etc.) and chemokines (e.g. IL8).

- Cell proliferation: Upon exposure to NPs, cell proliferation can occur either as a compensatory response to necrosis or apoptosis of surrounding cells, or as a mechanism in tumour promotion and progression (e.g. lung cancer following inhalation of asbestos fibres) (Hillegass *et al.*, 2010).
Different methods using different approaches (e.g. histochemistry, flow cytometry, etc.) may be performed to detect proliferating cells in a specific cell population. These methods include staining of proliferating cells by detecting Ki-67 or the Proliferating Cell Nuclear Antigen (PCNA), both proteins located specifically in proliferating cells. Other assays rely on the incorporation of [^{3}H]-thymidine or Bromodeoxyuridine (BrdU) into the DNA of dividing cells.

- Genotoxicity: NPs may act genotoxic by affecting the DNA either directly or indirectly. They can either enter the nucleus or act via mechanisms such as oxidative stress or inflammation. Different types of genotoxicity can be determined: mutagenicity, chromosomal aberration, and DNA strand breaks.
Assays on mutagenicity (e.g. Ames test, hPRT test, etc.) rely on the colony forming ability of mutated bacteria or cells, respectively, following treatment with NPs. By addition or depletion of growth medium components, the mutation ensures the survival of the cells. Another method for detecting point mutations is the measurement of oxidized guanine bases (8-OHdG) in the DNA.
Chromosomal damage is evaluated by analysing the formation of micronuclei in treated cells. As this phenomenon may also occur in untreated cells, a ratio between treated and control cells is evaluated.
DNA strand breaks can be assessed either by staining specific proteins (e.g. y-H2AX) or by gel electrophoresis on a single cell level (COMET assay).
Additionally, assay on altered gene expression following exposure to NPs may be performed. These include microarray, polymerase chain reaction (PCR) array, quantitative reverse transcriptase (qRT) –PCR, and so forth (Hillegass *et al.*, 2010).

All assays show not only certain specificity, but also have their limitations. Some NMs, in particular CNTs, may lead to unreliable findings by interacting with assay components (Krug and Wick, 2011). In 2006, Wörle-Knirsch *et al*. have shown that performance of a MTT assay when assessing cytotoxicity of CNTs lead to

erroneous results. Furthermore, metal NPs (titanium dioxide, silver, and copper NPs) have been demonstrated to interfere with the LDH assay by either inactivation or absorbion of LDH molecules (Han *et al*., 2011).

However, not only NPs but also the cells used in an assay have been shown to influence the outcomes. Fröhlich *et al*. (2012) identified the most reliable determinants of cytotoxicity to be growth pattern and the size of the used cell lines. Similar findings were shown by Xia *et al*. (2008). The authors could show that NPs act differently in different cell types. The NPs induced apoptosis in macrophages and necrosis in epithelial cells by different, cell-specific pathways which may be responsible for susceptibility or resistance to NP toxicity.

Available *in vitro* systems for different sites of entry and different endpoints are listed in Table 3.

Site of entry	Cell type	Effect	Endpoint
Lung	Epithelium	Toxicity	Trypan blue, LDH, apoptosis
		Inflammation	Gene expression, oxid. stress
		Translocation	Transfer across membranes
		Carcinogenesis	Genotoxicity, proliferation
	Macrophages	Toxicity	Trypan blue, LDH, apoptosis
		Chemotaxis	Chemotaxis
		Phagocytosis	Uptake, cytoskeletal staining
		Inflammation	Gene expression, oxid. stress
	Fibroblasts	Inflammation	Oxid. stress, cytokine profile
		Fibrosis	Collagen synthesis, proliferation
	Lung slices	Inflammation	Oxid. stress, immuno-histopathology
		Translocation	NPs across membranes
		Fibrosis	Collagen synthesis
Bloodstream	Endothelium	Inflammation	Adhesion molecules, oxid. stress
		Coagulation	Von Willebrand factor, tissue factor
	Immune cells	Immune response	Cytokine profile, adjuvant effects
Skin	Cell systems (e.g. Franz cells)	Cytotoxicity, inflammation	Cell viability, cytokine profile
	Flow-through diffusion systems	Absorption	
	Isolated skin flap model	Absorption, cytotoxicity, inflammation	Glucose utilization, cytokine profile
Gastrointestinal tract	Intestinal epithelium	Cytotoxicity	Cell viability, Trypan blue, apoptosis
		Inflammation	Oxid. stress, cytokine profile
		Translocation	Permeability
	Gastrointestinal associated lymphatic tissue (GALT)	Inflammation	Oxid. stress, cytokine profile
		Immune response	Adjuvant effects
	Buccal epithelium	Cytotoxicity	Cell viability, Trypan blue, apoptosis
		Inflammation	Oxid. stress, cytokine profile
		Translocation	Permeability

Table 3. *In vitro* assays for portal of entry testing. Adopted from Oberdörster *et al*., Part. Fibre Toxicol. 2005

1.2.5 Toxicity of polystyrene NPs

Polystyrene (PS) NPs are generally used as model particles, but not in consumer products. Since they are commercially available, well characterized NPs of distinct size, functionalization, surface charge, etc. can be purchased (Mayer *et al*., 2009). Physicochemical characterization of PS NPs usually shows that smaller NPs (< 200 nm) are more prone to aggregation when dispersed in protein containing cell culture medium than larger NPs (Mrakovcic *et al*., 2013). However, the functionalization might also influence the aggregation state (Mayer *et al*., 2009). Furthermore, addition of serum to the medium may also cause limited cytotoxicity of carboxylated PS NPs independent of the particles' size (Clift *et al*., 2010).

PS NPs induce cell damage mainly in a size-dependent manner. Only small NPs induce apoptosis and necrosis in endothelial cells (Fröhlich *et al*., 2009). However, generation of reactive oxygen species (ROS) was shown to be independent of the size. The generation of ROS was also detected in macrophages upon exposure to PS NPs (Xia *et al*., 2006). The authors could show that the NPs induced mitochondrial injury leading to toxic oxidative stress. However, no inflammation upon exposure to NPs was reported. Moreover, hemolysis, thrombocyte and granulocyte activation were reported upon exposure of blood samples *in vitro* to small PS beads (Mayer *et al*., 2009). Only functionalized NPs, however, were shown to induce platelet aggregation and this mechanism seems to depend on the surface charge. While negatively charged NPs induce an up-regulation of adhesion receptors, positively charged particles cause perturbation of the platelet membrane (McGuinnes *et al*., 2011).

In general, cationic (positively charged) NPs seem to exert higher cytotoxicity (Liu *et al*., 2011). In 2008, Xia *et al*. could show high cytotoxicity of amine-labeled NPs towards macrophages and epithelial cells. The particles caused lysosomal rupture and increased mitochondrial Ca^{2+} uptake, as well as mitochondrial damage and ATP depletion, respectively. Similar results were obtained by Bexiga *et al*. (2011). The authors demonstrated that morphological changes of the mitochondria of a human brain astrocyte cell line and the increased production of ROS lead to apoptotic cell death. In addition, cytotoxicity by disrupting the cell membrane was described (Liu *et al*., 2011; Nomura *et al*., 2013). Interestingly, Park *et al*. (2011) could not detect any cytotoxicity or cutaneous irritation of human skin *in vitro*.

In 2010, Fröhlich *et al*. investigated the influence of NPs on the drug-metabolizing cytochrome P450 (CYP) enzymes. Similar to cytotoxicity, the enzymes were influenced only by small NPs (< 60 nm). Additionally, the authors showed that the activity of the enzymes was inhibited. Moreover, the NPs increased the effects of known inhibitors of this system. Since the internalized NPs were localized in a close proximity to the endoplasmic reticulum, the authors concluded that this might facilitate the effects caused by the NPs. Internalization of NPs may lead to their localization in different cell organelles. In *in vivo* experiments, similar results were obtained. Combined exposure to PS NPs and other agents increased their effects (Yanagisawa *et al*., 2010; Shimizu *et al*., 2012). Here, too, the authors could show that the effects were much more pronounced for smaller NPs (< 50 nm).
The most important organelles with respect to uptake and accumulation of NPs are endosomes, lysosomes, and mitochondria (Fröhlich *et al*., 2012; Johnston *et al*., 2010). Moreover, PS NPs were shown to accumulate in bile canaliculi *in vitro* suggesting the elimination within bile (Johnston *et al*., 2010).

1.2.6 Toxicity of carbon-based NPs (fullerenes C60, carbon nanotubes)

The three most established carbon-based NPs are fullerenes (C_{60}), single-, and multi-walled carbon nanotubes (SWCNTs, MWCNTs). Due to their physicochemical properties, they often find application in biomedical materials and devices such as drug delivery vehicles, tissue scaffolds, and fluorescent contrast agents.

- C_{60}: C_{60} have been demonstrated to show cell-type specific cytotoxicity. While several studies show no toxicity in macrophages (Fiorito *et al*., 2006; Jia *et al*., 2005), cytotoxicity was reported for other cell lines (Sayes et al., 2004; Sayes et al., 2005). C_{60} was found to bind to cell membranes and accumulate intracellulary in different organelles including the nucleus. The aggregation on plasma membranes causing peroxidation of lipids was identified as the main mode of cell death (Sayes et al., 2005).

- CNTs: Compared to C_{60}, CNTs (especially SWCNTs) clearly show cytotoxic effects at high concentrations (Jacobsen *et al*., 2008). Functionalization of

SWCNTs, however, seems to improve the particles bio-compatibility (Sayes et al., 2006). As demonstrated by Shvedova *et al*. in 2003, longer incubation periods induced oxidative stress, altered glutathione levels, and induced nuclear and mitochondrial changes. In addition, the authors postulated that residual iron catalysts in solution may influence the toxic effect of SWCNTs. However, this is not the case for MWCNTs. Moreover, the aggregation state of the particles may also influence the displayed cytotoxicity (Wick *et al*., 2007). In order to improve their dispersion, CNTs are usually dissolved in protein-containing media (Donaldson *et al*., 2006). However, serum may enhance the expression of IL8 upon exposure of lung epithelial cells A549 to SWCNTs (Baktur *et al*., 2011). Furthermore, the authors could show that the expression of IL8 was increased already when cells were exposed to low concentration or even after removal of the particles.

For MWCNTs, similar results to those of SWCNTs were obtained. Exposure to higher concentrations and for longer time-periods, resulted in an increased uptake of the NPs, a decrease in cell viability, as well as an increased release of the pro-inflammatory chemokine IL8 (Monteiro-Riviere and Inman, 2006). Interestingly, MWCNTs are considered to be not irritating to skin *in vitro* and *in vivo* while inducing reversible conjungtival redness and discharge in rabbits (Kishore *et al*., 2009)

In *in vivo* studies, applications of high doses of CNTs induced mesotheliomas in the peritoneum, inflammatory fibrotic lesions in the lung or formation of granulomas (Becker *et al*., 2011). Upon, inhalation, CNTs may persist in the tissue either as individual nanotubes or as agglomerates, thus leading to injuries of the tissue. However, it is still not clear whether CNTs could translocate from the respiratory tract to other tissues (Ryman-Rasmussen *et al*., 2009). The bio-durability as well as the unique physicochemical properties of CNTs lead to the conclusion that they may act similar to asbestos fibres (Murr *et al*., 2005).

1.2.7 Long-term toxicity of NMs

Cytotoxicity of NPs in *in vitro* studies is mainly assessed after short-term exposure. However, in 2011, Thurnherr *et al*. investigated both, short-term and long-term cytotoxicity upon exposure of the lung epithelial cell line A549 and T-cell line

Jurkat-6 to commercial MWCNTs. In this study, the authors showed CNTs to be not overtly toxic, even after 3 months of exposure. Moreover, they noticed cellular uptake only in A549 lung cells, but not in Jurkat-6 cells (Thurnherr *et al*., 2011).

Due to the limitations of cell cultures, studies on long-term toxicity of NPs are mostly performed *in vivo*. The advantage of animal studies in assessing particle toxicity is the possibility of investigating the uptake and translocation of NPs. Furthermore, the interaction of different cell types or organs (e.g. cells of the site of entry and the immune system) can be studied in a more physiologic environment. In addition to bio-distribution, also the bio-persistence of both, degradable and non-degradable NPs may be evaluated. However, it is of high importance that appropriate animal models are used. Some effects may occur only in special models (e.g. exposure routes, gender, age, health status, etc.) (Oberdörster *et al*., 2005).

Data suggest that some NMs are not sufficiently cleared from the organism (Michalet *et al*., 2005; Thurnherr *et al*., 2011). If an organism is exposed over a long period to low concentrations of NPs, the function of cells may be compromised. Most indications for organ damage by repeated exposure to NPs were obtained in animal studies. Repeated exposure to gold NPs and magnetic NPs caused not only accumulation and histo-pathological changes in various organs but also weight loss and marked alterations in blood count (Sadauskas *et al*., 2009; Kwon *et al*., 2009; Lasagna-Reeves *et al*., 2010). Therefore, the assessment of toxic effects is becoming of outmost importance.

1.3 Long-term cell culturing

In short-term cytotoxicity studies, cell lines are usually employed, but these generally cannot be studied much longer than 72 hours in conventional culture. Subsequently, the cells need medium change and / or the cultures are in the stationary state. To assess longer time-periods, cells have been sub-cultured and again exposed to the tested compound (Thurnherr *et al*., 2011). Other systems such as bioreactors have to be used when observations over longer time-periods are needed (Pazos *et al*., 2002; Gebhardt *et al*., 2003). Dependent on their growth characteristics (adherent or in suspension), cells in bioreactors are either dispersed in medium or cultured on scaffolds, matrices or microcarriers.

In microcarrier cell cultures, anchorage-dependent cells are grown on the surface of small spheres which are maintained in stirred suspension cultures. In comparison to conventional monolayer cell culture, this technology provides the advantage that high cell densities and higher yields of cellular products such as antibodies can be obtained. Main advantages of the microcarrier system are reduced costs and reduced risk of contamination, increased culture periods without sub-culturing (Lock and Tzanakakis, 2009) as well as the imitation of the *in vivo* situation due to a more physiologic environment. This technique is therefore a good choice where cells are used for the production of biologicals, cells, cell products, and viral vaccines. Other applications include studies of cell structure, function and differentiation, enzyme-free sub-cultivation, and implantation studies (Alves *et al*., 1996; Rourou *et al*., 2007; Justice *et al*., 2009). Several cell lines (e.g. MDCK, Vero cells, COS-7, stem cells, HEK 293T) were described to grow and differentiate on microcarriers (Varani *et al*., 1998; Butler *et al*., 2000; Serra *et al*., 2009; Larson *et al*., 2010).

1.4 Aim of the study

The aim of this study was the evaluation of cellular effects upon chronic exposure of endothelial cells and monocytes to NPs over a time-period of four weeks. In order to perform long-term experiments, different cell culturing approaches had to be established and compared.

Polystyrene NPs are usually not used in consumer products, but serve as a model of non-biodegradable NPs. CNTs are bio-persistent NPs which are commonly used in different biomedical applications, such as drug delivery, or cancer therapy. Moreover, CNTs can be employed as model NPs for air pollution- derived NMs. Therefore, the assessment of long-term effects of CNTs is of high importance. Hence, the effects of exposing cells to short pristine and functionalized carbon nanotubes (CNTs) with lengths > 50 nm should be evaluated in this study.

Assessment of long-term cytotoxicity is mainly performed in animal models, usually rodents. However, when studies on long-term toxicity are performed *in vitro*, cells need to be sub-cultured and again exposed to the chemical/ compound. Here, a microcarrier cell culture system for anchorage-dependent cells, as well as a bioreactor system for in suspension growing cells, should get established and evaluated with respect to their suitability to perform long-term assays. In addition, the same assays should be performed in conventional cell cultures where cells were sub-cultured at regular intervals. In order to determine which approach is more suitable to assess long-term cytotoxic effects, the outcomes on cell density, and cell viability upon exposure to plain polystyrene NPs as model particles, should get evaluated. In addition, the cytotoxic mode of action (apoptosis and / or necrosis) of the NPs was determined. Furthermore, the internalization as well as the intracellular localization and accumulation of the NPs had to be investigated. Therefore, red fluorescent plain polystyrene NPs should get employed.

2. MATERIALS AND METHODS

2.1 Nanoparticles

For the establishment of long-term assays, plain polystyrene particles (PPP) of 20 and 200 nm (Thermo Scientific) were used. The intracellular localization of the NPs was investigated by red fluorescently labelled PPP FluoroMax red (R25) of 25 nm (Thermo Scientific). To test the suitability of the assays, short multi-walled carbon nanotubes of > 50 nm x 0.5 – 2 µm from CheapTubes Inc., USA were used. All NMs were sonicated for 20 min with an Elma S 40 sonicator before use. A summary of NMs used in this study is presented in Table 4.

Nanomaterial	abbreviation	indicated size (nm)	distributor
plain polystyrene particles	PPP 20	20	Thermo Scientific
plain polystyrene particles	PPP 200	200	Thermo Scientific
fluorescently labelled plain polystyrene particles	FluoroMax red (R25)	25	Thermo Scientific
multi-walled carbon nanotubes	MWCNT (CNT4)	> 50	CheapTubes Inc.
carboxylated multi-walled carbon nanotubes	MWCNT-COOH (CNT5)	> 50	CheapTubes Inc.

Table 4. Nanoparticles

2.2 Cell culture

2.2.1 Cells

2.2.1.1 EAhy 926

As a representative for epithelial cells, the endothelial cell line EAhy 926, kindly provided by C. S. Edgell, was used. This cell line is a hybrid developed by a fusion of human umbilical vein endothelial cells (HUVEC) and the permanent human lung

epithelial cell line A549. Moreover, the cells express the factor VIII-related antigen which is a marker for differentiated vascular endothelium (Edgell *et al*., 1983).

2.2.1.2 THP-1 [ATCC TIB-202]

The human leukemic cell line THP-1 originates from the blood of a patient with acute monocytic leukemia. The cell line shows distinct monocytic markers that are maintained during sub-culturing in a period of up to 14 month (Tsuchiya *et al*., 1980).

2.2.2 Thawing frozen cells

The cryovial containing the frozen cells was removed from the liquid nitrogen storage and was immediately placed into a 37°C water bath. The cells were thawed by gently swirling the vial until a small bit of ice is left (< 2 min). Then, the vial was transferred to a laminar flow where the cells were transferred to a falcon containing the pre-warmed growth medium. The cells were centrifuged for 4 min at 1000 g and the supernatant was aseptically decanted. The cell pellet was resuspended with 1 ml of growth medium and was transferred into a 75 cm² cell culture flask and cultivated in an incubator.

2.2.3 Cell culturing

EAhy 926 and THP-1 cells were both cultured in DMEM high glucose and RPMI 1640 growth medium, respectively, supplemented with 10% FBS, 200 mM L-glutamine, and 1% P / S. The cells were sub-cultured three times per week in a 1:3 to 1:4 ratio as well as in a density of about 3 x 10^5 cells / ml, respectively.
Adherent growing cells were sub-cultured by trypsinization. Briefly, the medium was aspirated and the cells were washed with PBS without Mg^{2+} and Ca^{2+} at RT. After aspirating the PBS, 0.05% trypsin / EDTA was added and the cells were incubated (< 5 min) at 37°C until cells detached. The reaction was stopped by the addition of growth medium. After re-suspending the cells, an aliquot depending on the ratio of sub-culturing was transferred into a new cell culture flask containing fresh growth medium.

All ingredients and disposables are summarized and presented in Table 5.

Article	Company
Cell culture material	
DMEM high glucose	PAA
RPMI 1640	PAA
FBS	PAA
L-glutamine	PAA
P / S (100x)	PAA
0.05% trypsin / EDTA	PAA
PBS	PAA
poly-HEMA	Sigma Aldrich
GEM™	Global Cell Solutions
Disposables	
Cell culture flasks	SPL Lifesciences / PAA
LeviTubes™	Global Cell Solutions / OMNI Life Science
Cell culture plates	Nunc, Greiner BioOne
Serological pipettes	Diverse companies
Pasteur pipettes	Roth
Pipette tips	Diverse companies
50 ml / 15 ml Falcon tubes	SPL Lifesciences / PAA
Safe-lock reaction micro-tubes	Eppendorf
Glasware	Roth
Devices	
Laminar flow HeraSafe	Thermo Scientific
HeraSafe incubator	
BioLevitator™	Hamilton Company
Magnet for microcarrier cultures	Global Cell Solutions
Elma S 30	ElmaSonic
Bright-field microscope	Olympus
Confocal microscope LSM510	Zeiss
SpectraMax	BMG Labtech
FLUOstar Optima	BMG Labtech
LUMIstar	BMG Labtech
CasyTT	Inovatis
Pipettes	Eppendorf
Assay reagents	
CellTiter 96 Aqueous Non-Radioactive Cell Proliferation Assay (MTS)	Promega
CytoTox-ONE Homogeneus Membrane Integrity assay (LDH)	Promega
LDH from bovine heart	Sigma Aldrich

BSA	Sigma Aldrich
Caspase 3/7-Glo Assay	Promega
ApoTox Glo Triplex Assay	Promega
EtOH 100%	Merck
ELISA Set A (IL6, IL8, IL1-ß)	BD Biosciences
ELISA Set B	BD Biosciences
Tris base	Sigma Aldrich
HCl	Sigma Aldrich
NaCl	Sigma Aldrich
Triton X-100	Sigma Aldrich
Sodium deoxycholate	Sigma Aldrich
SDS	Sigma Aldrich
Phosphatase and protease inhibitor cocktail	Roche Diagnostics
NuPage 4-12% Bis-Tris gels	Life Technologies
Staining solutions	
Hoechst 33342	Invitrogen
MitoTracker Deep Red 633	Invitrogen
ER Tracker green	Invitrogen
LysoSensor green	Invitrogen
Annexin V	ebiosciences
PI	ebiosciences
PARP	Cell Signaling Technologies
beta-Actin	Sigma Aldrich
Secondary antibodies	Cell Signaling Technologies, DAKO

Table 5. Ingredients and disposables

2.3 Long-term cell culture approaches

2.3.1 Modified conventional cell culture

In order to investigate the long-term effects of a repetitive exposure of the cells to NPs, the cells were sub-cultured once per week or, in the case of THP-1, cells were transferred into a new culture vessel. At this time-point the medium supplemented with NPs was exchanged. To avoid a growth-bias, the time-points were selected when the untreated controls have reached 100% confluence.

2.3.1.1 EAhy 926

The cells were plated at low densities (27.8 x 10^3 cells / 25 cm^2) and were incubated for 24 hrs to allow cell attachment. After this period, the medium supplemented with 20 µg/ ml PPP 20 and PPP 200 was added. For the controls, no NPs were added to the medium. The cells were then sub-cultured in a 1:10 ratio once per week for a time-period of four weeks.

2.3.1.2 THP-1

The cells were seeded in 6 well plates at densities of 5 x 10^5 cells / well. Due to the growth characteristics of the cells, the NPs were added immediately at a final concentration of 20 µg / ml and 50 µg / ml. Untreated cells and cells treated with 2% EtOH were used as negative and positive controls, respectively. Cells were used at low passage numbers.

At each time point, the cells were counted and all cells were transferred into a larger cell culture flask (25 cm^2, 75 cm^2, and 175 cm^2). At this step, the medium ± treatment agent was renewed. The experiment was stopped after 16 days when the control cells reached 100% confluence in 175 cm^2 flasks.

2.3.2 Microcarrier cell culture in the BioLevitator™

In general, 3 x 10^6 anchorage-dependent cells (EAhy 926) were seeded on 1 ml of basal membrane or collagen type IV coated microcarrier GEM™ (Figure 8 A) in a volume of 10 ml. The cells were cultured in specialized culture vessels (LeviTube™) in the bench-top bioreactor-incubator hybrid BioLevitator™ (Figure 8 B).

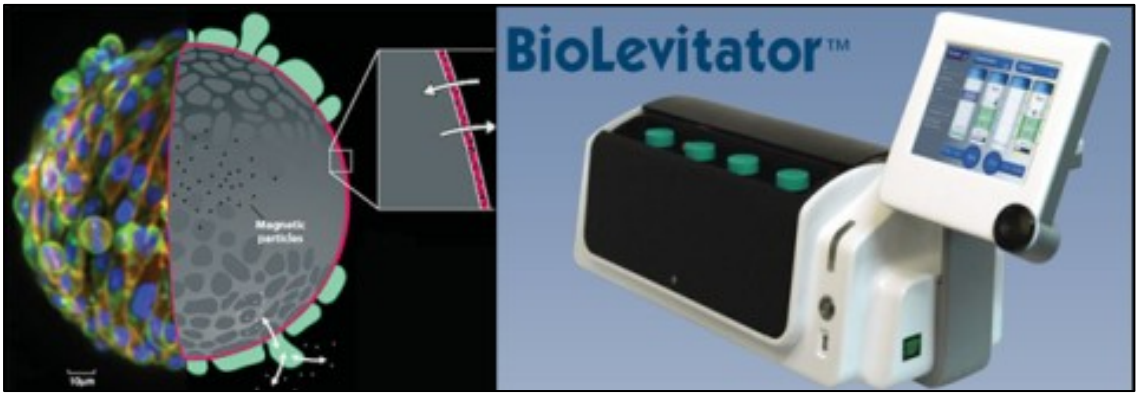

Figure 8 A. Scheme of the GEM™ **Figure 8 B. BioLevitator™**

Image courtesy by Global Cell Solutions and Hamilton Company

Prior to the inoculation, the storage buffer of the GEM™ was replaced with growth medium for the applied cell type. The GEM™ are porous beads of an alginate core coated with different proteins (e.g. gelatine, collagen type I, laminin, fibronectin, poly-L-lysine, etc.). The porous bead allows the storage of nutrients from the medium as well as cell products, e.g. growth factors that are preferably used by the cells after a medium change was performed.
The LeviTube™ was filled up with medium ± NPs after the initial inoculation phase reaching a total volume of 40 ml / LeviTube™. The medium was changed once per week. The cultures were maintained for 4 weeks without sub-culturing of the cells.

2.3.3 Culturing cells in the bioreactor CELLine

CELLine is a two-compartment bioreactor (Figure 9 A) designed for the culturing of cells producing different cell products (e.g. antibodies, vaccines) in high cell densities to ensure a rapid propagation of cells and a high amount of excreted products. The two compartments are separated by a semi-permeable membrane that allows an exchange of nutrients from the upper medium compartment and waste products from the lower cell compartment (Figure 9 B). A gas-permeable bottom membrane allows the exchange of O_2 and CO_2 in the cell compartment.

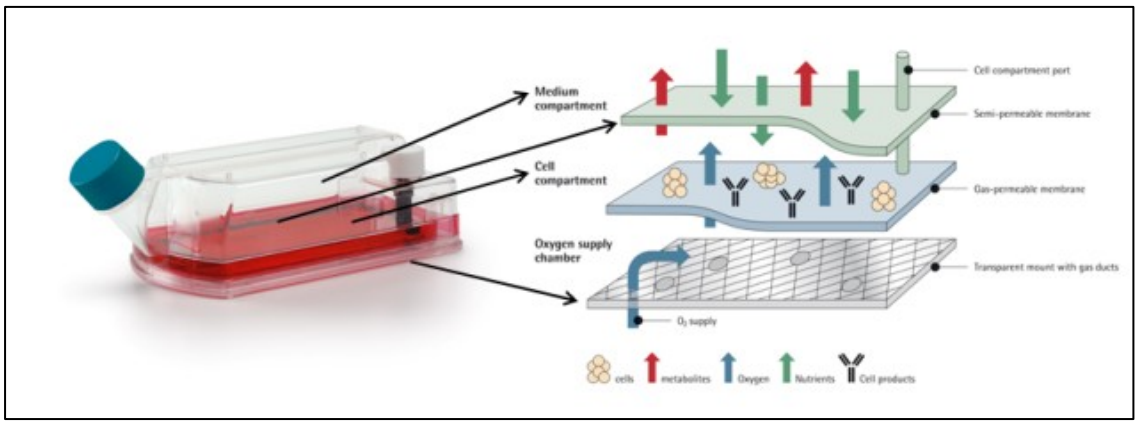

Figure 9 A. Bioreactor CELLine **Figure 9 B. Schematic representation of the two compartment system**

Image courtesy by Sartorius Stedim

The initial cell density which is suitable for maintaining cultures over a time-period of 4 weeks was figured out in a pilot experiment. Therefore, THP-1 cells were inoculated at cell densities of 10 x 10^5 cells / 10 ml, 5 x 10^5 cells / 10 ml, and 2.5 x

10^5 cells / ml into the cell compartment of the CELLine bioreactor and were cultured in a conventional incubator (HeraSafe). The medium compartments were filled with 200 ml growth medium. The cultures were maintained until the maximum cell density was reached.
In long-term exposure experiments, 2.5 x 10^5 cells / ml were inoculated. The medium in the cell chamber was immediately supplemented with NPs at final concentrations of 20 µg / ml and 50 µg / ml of PPP 20, 50 µg / ml of PPP 200, as well as with 2% EtOH. Additional 100 ml of complete growth medium was added to the medium chamber. All cultures were maintained for at least 3 weeks. Once per week, the cells were counted and the medium from the medium compartment was exchanged. The medium from the cell compartment was not changed at any time-point.

2.4 Particle characterization

The physico-chemical characterization of the NMs was performed by Dr. Eva Roblegg at the Karl-Franzens University of Graz.

Prior to exposing the cells to NMs, the particles were characterized according to their actual size and surface charge in different solvents (distilled water, medium with and without 10% serum) by dynamic light scattering on a Zetasizer 3000 (Malvern). Concentrations of 200 µg / ml of PPP and 1 µg / ml of CNTs were used.

2.5 Acute cytotoxicity assays

2.5.1 Assay on the metabolic activity

The concentrations of NMs used for the evaluation of long-term effects, were estimated by a CellTiter 96 Aqueous Non-Radioactive Cell Proliferation Assay formazan bio-reduction assay (MTS). The assay was performed according to the manufacturer's instruction. First, the cells were exposed to NMs. After exposure, the cells were stained with the staining solution at 37°C and 5% CO_2. Finally, the OD was measured on a spectral photometer SpectraMax at 490 nm.

Wells without cells but with the respective medium, in which the NMs were dissolved, were used as blank control. As positive and negative control, other cytotoxic and non-cytotoxic NPs were used, respectively. To determine the interference of the NMs with the assay compounds, an interference control containing only the highest concentration of the tested NM but no cells, was performed. When CNTs were used, the cells were washed three times with PBS prior to adding the staining solution.
In long-term experiments, the cells were exposed to concentrations where no acute damage has occurred (concentration < IC_{50}) after 24 hrs.

2.5.1.1 MTS in conventional cultures

The assay was performed in optical clear 96 well plates. A general layout for both cell types is presented in Figure 10.

M	M	M	M	M	M	M	M	M	M	M	M
B	PC	0	0	0	0	0	0	0	0	NC	IC2
B	PC	50	50	50	50	50	50	50	50	NC	IC2
B	PC	100	100	100	100	100	100	100	100	NC	IC2
IC1	PC	200	200	200	200	200	200	200	200	NC	B
IC1		400	400	400	400	400	400	400	400		B
IC1		500	500	500	500	500	500	500	500		B
M	M	M	M	M	M	M	M	M	M	M	M

Figure 10. A scheme of a general layout for a MTS assay.
M: medium; B: blank control; PC: positive control; NC: negative control; IC1/ IC2: interference controls of each NP; 0 -500: concentration range of each NP in µg/ ml.

EAhy 926 cells were seeded at cell densities of 1.4 x 10^4 cells / well. After the cells have attached (24 hrs), they were exposed to the medium ± particles for 24 hrs. THP-1 cells were plated at a density of 5 x 10^4 cells / well and were immediately exposed to nanoparticles. After 24 hrs of exposure, the cells were stained for two and for four hrs, respectively.

2.5.1.2 MTS in microcarrier cultures

The plates were coated with 5% poly-HEMA dissolved in 100% EtOH preventing cell attachment on culture plates. 10 x 10^3 cells were seeded on 5 µl GEM™ and cultured in an incubator to allow cell attachment. After 2 days, the cells were exposed to the NMs for 24 hrs. Afterwards, the cells were stained for 4 hrs and were then analyzed as described in chapter 2.5.1.

2.5.2 Assays on the mode of action of NMs

The cells were seeded in optical clear 96 well plates and were cultured O / N at 37°C and 5% CO_2 to allow cell attachment. Thereafter, the cells were treated with different concentrations of NPs for 4, 8, and 24 hrs. The mode of induction of cell death was then assessed by two assays that were performed according to the provided manuals:

- CytoTox-ONE™ Homogeneous Membrane Integrity Assay for the fluorescent detection of LDH-leakage from necrotic cells with disrupted membranes. 25 µl of the supernatant is transferred into a 96 well plate suitable for fluorescence detection. Then, an equal volume of the substrate mix is added. The plate was incubated for 10 min at RT and protected from light. The reaction was stopped by adding 0.2 volumes of the provided stopping reagent. The reaction was evaluated on a FLUOstar Optima fluorescence photometer with an excitation / emission wavelength of 544 / 590 nm.

- Caspase-Glo® 3/7 Assay for the luminescent detection of the effector caspases 3 and 7 that induce apoptosis. An equal volume of assay reagent was added to the medium and the plate was then incubated at RT for 30 min protected from light. After incubation, the whole supernatant was transferred to a 96 well plate suitable for luminescence detection and was measured on a LUMIstar Optima luminescence photometer.

A general layout for both assays is presented in Figure 11.

M	M	M	M	M	M	M	M	M	M	M	M
B	PC	0	0	0	0	0	0	0	0	NC	IC2
B	PC	50	50	50	50	50	50	50	50	NC	IC2
B	PC	100	100	100	100	100	100	100	100	NC	IC2
IC1	PC	200	200	200	200	200	200	200	200	NC	B
IC1	L	400	400	400	400	400	400	400	400	L	B
IC1	L	500	500	500	500	500	500	500	500	L	B
M	M	M	M	M	M	M	M	M	M	M	M

Figure 11. A schematic representation of the layout for the assays on apoptosis and necrosis.

M: medium; B: blank control; PC: positive control; NC: negative control; IC1/ IC2: interference controls of each NP; 0 -500: concentration range of each NP in µg/ ml; L: lysis control for LDH-assay.

2.5.3 Assay on the interleukin secretion in THP-1 cells

THP-1 cells were plated in 24 well plates in a density of 1 x 10^5 cells / well and were treated with PPP 20 and 200 for 24 hrs. Untreated cells and LPS treated cells (100 and 1000 ng / ml) were used as negative and positive controls, respectively. After incubation, the cells were transferred into centrifuge tubes and were centrifuged at 1000g for 4 min. The supernatant was then transferred into a new centrifuge tube and was used for further investigation.

The secretion of interleukins (IL) 1-ß (only upon long-term exposure), 6, and 8 was assessed by an ELISA assay. The assay was performed according to the provided instructions. First, ELISA plates were coated with the respective capture antibody and were then incubated O / N at 4°C. Prior to adding the standards and the samples, the plates were washed 3 times with < 300 µl 1 x wash buffer at RT and were blocked with 100 µl blocking solution for 60 min at RT. Afterwards, the plates were washed 3 times. In the meanwhile, the standards were prepared to range from 0 pg / ml to either 200 pg / ml (IL8), or 250 pg / ml (IL1-ß), or 300 pg / ml

(IL6). 100 µl standard and samples were incubated for 2 hrs at RT. After an additional washing step (5 times), 100 µl detection antibody coupled to a HRP was added to each well and was incubated for 60 min at RT. The last washing step was repeated 7 times. Next, 100 µl of a substrate solution was added to each well and incubated for 30 min at RT protected from light. By the addition of 50 µl stop reagent, the blue coloured substrate solution turned yellow. Then, the OD was determined on a SpectraMax at a wavelength of 450 nm.

2.6 Assessment of long-term effects

The long-term effects of NMs were evaluated by assessing following criteria:

- cellular density and viability
- induction of cell death and the mode of action
- progression of inflammation

2.6.1 Cell densities

The cellular densities and viability were assessed on an automated cell counter CasyOne (Lindl *et al*., 2005). Adherent cells were detached from their growth support by trypsinization. Briefly, the cells were washed with pre-warmed PBS and were incubated with trypsin/EDTA at 37°C until the cells have detached. 50 µl of the cell suspension has been diluted in 10 ml of an isotonic solution (Casyton; provided by the supplier) and were then counted. The cells growing in suspension were re-suspended in the culture vessel and were immediately analysed by counting 100 µl of the cell suspension.
The main settings of the CasyOne protocols are presented in Table 6.

Cell type	Cursor setting (µm)				dilution factor
	CL (*)	CR	NL (§)	NR	
Eahy 926	12.63	48.88	07.13	48.88	1 : 200
THP-1	10.00	48.88	05.86	48.88	1 : 100

* CL/ CR calculation cursor left/ right
§ NL/ NR normalization cursor left/ right

Table 6. Cursor settings of the CasyOne measuring protocols.

2.6.1.1 Counting cells from BioLevitator™ cultures

The cell detachment was performed in 24 well plates under unsterile conditions. Three wells per culture condition were used. 500 µl of each culture suspension was used for the estimation of the total cell numbers in the whole LeviTube. By placing a magnet, the microcarriers were pulled to one side of the well and the medium was removed. 500 µl of pre-warmed trypsin was added to each well and the cells were incubated for 30 min at RT. After incubation, the cells were vigorously re-suspended and counted as described in chapter 2.6.1.
The total cell numbers per LeviTube was calculated in accordance with the formula:

$$\text{Total cell number/ LeviTube} = \frac{\text{cell number/ ml x volume (ml)/ LeviTube}}{\text{volume cell suspension (ml) used for counting}}$$

2.6.1.2 Counting cells from CELLine

An aliquot of the cells was removed from the cell compartment and was placed into a 50 ml tube. After the suspension was re-suspended, an aliquot was used for counting.
The total cell numbers per bioreactor was calculated in accordance with the formula:

$$\text{Total cell number/ CELLine} = \text{cell number/ ml x volume (ml)/ CELLine}$$

2.6.2 LDH - release

In order to assess the mode of induction of cell death, the amount of LDH released from damaged cells was investigated. Briefly, an aliquot of the supernatant was collected from each culture condition and the assay was performed as described in chapter 2.5.2.

2.6.2.1 LDH - stability

In order to minimize the consumption of materials (plates, assay reagents, etc.), the stability of the enzyme at different temperatures was assessed.
For a time-period of four weeks, LDH from bovine heart was diluted to 0.002 – 0.2 U / ml in complete DMEM medium. To one half of the samples a 2% BSA solution was added to improve the storage conditions. The samples were stored at +4°C, -20°C and -80°C (Shain *et al*., 1983).
After four weeks, the frozen samples were thawed on ice and then all samples were pre-warmed to RT. The stability of the enzyme was assessed by the CytoTox-ONE^{TM} Homogeneous Membrane Integrity Assay as described in chapter 2.5.2. The data were compared to fresh LDH samples.

2.6.2.2 Assessment of necrosis in microcarrier cultures

200 µl of the supernatant of the aliquots used for cell counting were kept in reaction tubes and were stored at -80°C. At the end of each experiment, the samples were thawed on ice, pre-warmed to RT, and the assay was performed as described previously. Biological triplicates were assessed from each culture condition. In addition, each sample was evaluated in duplicates. The data from treated cultures was compared to untreated controls at each time point and was normalized to the total cell numbers per LeviTube.

2.6.2.3 Assessment of necrosis in bioreactor cultures

At each time point, each culture sample used for cell counting was centrifuged at 1000 rpm for 5 min. 1 ml of the supernatant was collected and stored at -80°C.

Here, too, the collected samples were analysed as already described in chapter 2.6.2.2. All samples were analyzed as triplicates.
The data from exposed cultures was compared to untreated cells and was also normalized to the total cell numbers in each CELLine bioreactor at each time point.

2.6.3 Induction of apoptosis in microcarrier cultures

50 µl of each culture condition was transferred into an optical clear 96 well plate. The samples were analyzed in quadruplicates. An equal amount of the assay reagent pre-warmed to RT was added to the cells. The assay was performed as already described in chapter 2.5.2. In addition, an ApoTox Glo Triplex Assay for the simultaneous detection of apoptosis, cytotoxicity and cell cycle block was performed 1 and 7 days after exposure of the cultures to PPP.
Exposed cultures were compared to the untreated control cells. Again, the data was normalized to the total cell numbers per condition at each time point.

2.6.4 Western blot analysis on PARP-1 in microcarrier cultures

In order to discriminate between apoptosis and necrosis in microcarrier cultures, a Western blot for poly (ADP-ribose) polymerase 1 (PARP-1) was performed 7 days after exposure to both, PPP and CNTs. To obtain a positive control, cells were treated with 1 µg/ ml staurosporine for 5 hours. Upon washing cells with ice-cold PBS, cell lysates were prepared in RIPA buffer (50 mM Tris-HCl pH 8.0, 150 mM NaCl, 1% Triton X-100, 0.5% sodium deoxycholate, 0.1% SDS; Sigma) overnight at 4°C with the addition of protease and phosphatase inhibitor cocktails (1 tablet each was dissolved in 10 ml RIPA buffer) (Roche Diagnostics, Austria). The protein concentration was determined photometrically by a Bradford Assay (Bio-Rad Laboratories, California). 20 µg of the protein lysate was separated by SDS-PAGE (NuPage 4- 12% Bis-Tris gels; Life Technologies, Austria) and transferred to nitrocellulose membrane (Bio-Rad). Following primary antibodies were used: PARP (dilution: 1:750; Cell Signaling Technology, Massachusetts), and as a loading control beta-Actin (diluted 1:1000; Sigma). As secondary antibody we used a goat anti-rabbit (Cell Signaling Technologies) or rabbit anti-mouse HRP-conjugated antibody, respectively (DAKO, Denmark) at a final concentration of 1

µg/ ml. An overnight incubation at 4°C was performed for both primary antibodies, followed by incubation with secondary antibodies at room temperature for 2 hours. Specific protein bands were visualized by the enhanced chemiluminescence assay (Amersham Biosciences, Germany).

2.6.5 Expression of IL in long-term cultures of THP-1 cells

For assessing the secretion of ILs, frozen samples of the supernatant from both, CELLine and conventional cell cultures, were used. All samples were thawed on ice and pre-warmed to RT. The samples were investigated in triplicates. The assay was performed according to the protocol described in chapter 2.5.3.
The exposed cultures were compared to the untreated controls and the data was normalized to the total cell amount at each time point.

2.7 Microscopy

2.7.1 Bright-field microscopy

During the whole period of culturing, the cells and especially the detachment phase of the anchorage-dependent cells from their growth supports (culture dishes, microcarriers, etc.), were monitored under a light microscope CKX41 light microscope (Olympus, Japan) using the 10x magnification lens.

2.7.2 Confocal microscopy

In addition to the general monitoring of the cells, different staining protocols were performed. All staining was then analyzed on a confocal laser scanning microscope (Zeiss) using the 40x as well as the 63x oil immersion lens. The LSM510 software was used to document the images.

2.7.2.1 Evaluation of cell proliferation on microcarriers

Proliferation of EAhy926 cells on the GEM was evaluated by nuclear staining. The staining was performed 24 hrs, 5 d, 7 d, and 14 d after inoculation.

100 µl of culture suspension was transferred into an optical clear black 96 well plate suitable for fluorescence detection. The cells were stained with Hoechst 33342 staining solution added directly to the culture at a final concentration of 5 µg / ml. The staining was performed for 15 min at RT protected from light. The images were obtained immediately after incubation with the staining solution.

2.7.2.2 Evaluation of the healthy status of endothelial cells on microcarriers (cell organelles staining)

In addition to the assessment of cellular viability on the cell counter, the healthy status of EAhy926 cells attached to GEM was determined by staining of different cell organelles (mitochondria, endoplasmic reticulum) 24 hrs after inoculation.
Here, too, 100 µl of culture suspension was co-stained with 200 nM MitoTracker DeepRed and 1 µM ER-Tracker green in an optical clear black 96 well plate. The cells on beads were washed twice with complete growth medium. The medium was replaced with HBSS buffer containing the staining solutions diluted to the appropriate final concentration. For counterstaining 5 µg / ml Hoechst 33342 solution was added to the buffer. Cell staining was performed at 37°C and 5% CO_2 for 20 min. After incubation, the solution was replaced with fresh HBSS buffer and the staining was documented as described in chapter 2.7.2.1.

2.7.2.3 Intracellular localization of NPs

EAhy926 cells were cultured on GEM in the BioLevitator as described in chapter 2.3.2. After the initial inoculation phase the LeviTube were filled up with complete growth medium supplemented with red fluorescent PPP. Here, too, the medium was changed weekly. 14 d after treatment the intracellular localization of the NPs was investigated. LysoSensor™ Green solution and Hoechst 33342 staining solution were added directly to 100 µl of culture suspension at a final concentration of 0.5 µM and 5 µg/ ml, respectively. The staining was performed at 37°C and 5% CO_2 for 5 min. The staining was documented immediately after the incubation.
In CELLine cultures of THP-1 cells, 50 µg/ ml red fluorescent PPP were added immediately. 1 day and 7 days after inoculation, 100 µl of cell suspension was analysed. Here, no counterstain was performed.

2.8 Statistical analysis

All experiments, except long-term exposure to PPP, were repeated three times. In each assay at least triplicates were performed. Data is presented as mean ± SD. The calculation was performed with Microsoft Excel software.

The statistical analysis of data of microcarrier cultures of EAhy926 treated with PPP was performed with the statistical software SPSS version 20. Therefore, the data of 5 independent experiments were compared, and a repeated measurement ANOVA was performed. For post-hoc analysis, a Bonferroni correction was conducted. A p-value < 0.05 was considered to indicate statistical significance.

3. RESULTS

3.1 Particle characterization

The hydrodynamic sizes of PPP were larger when diluted in medium, especially in the presence of FBS, than indicated by the supplier. The differences between the indicated size and the hydrodynamic radius in medium with 10% FBS, were more pronounced for the PPP 20 than for the PPP 200. Sizes of the CNTs increased markedly when protein-free medium was used. All particles were negatively charged except 200 nm PPP when dissolved in DMEM with 10% FBS.
A summary of the particle properties is presented in Table 7.

Particle	Size (nm)		ζ-potential (mV)	
	Aqua bidest.	DMEM+10% FBS	Aqua bidest.	DMEM+10% FBS
PPP 20	22.76	73.59*/12.37	-37.1	-11.7
PPP 200	211.6	224.8	-57.6	8.08
R25	22.22	58.26	-11.1	-10.3
CNT4	n.d.*	51.9	n.d.*	-7.28
CNT5	n.d.*	50.41	n.d.*	-11.0

* n.d. not determined due to aggregation

Table 7. Results of the characterization by DLS.

3.2 Acute effects on EAhy 926 cells

3.2.1 Assay on cell viability

After exposure of cells to PPP 20 for 24 hours, the cell viability was reduced in a dose-dependent manner. Addition of serum to the medium decreased the cytotoxicity of the particles (Figure 12 A, B). The estimated IC_{50} was approximately 120 µg/ ml in DMEM supplemented with 10% FBS and 30 µg/ ml in medium without FBS. PPP 200 exhibited no cytotoxicity, irrespective of the medium used (Figure 12 A, B).

Exposure of cells to CNTs dissolved in serum-containing DMEM decreased cell viability similarly to PPP 20 (Figure 12 C). The estimated IC_{50} was approximately 60 µg/ ml upon exposure to plain CNTs and approximately 125 µg/ ml upon exposure to CNT-COOH.

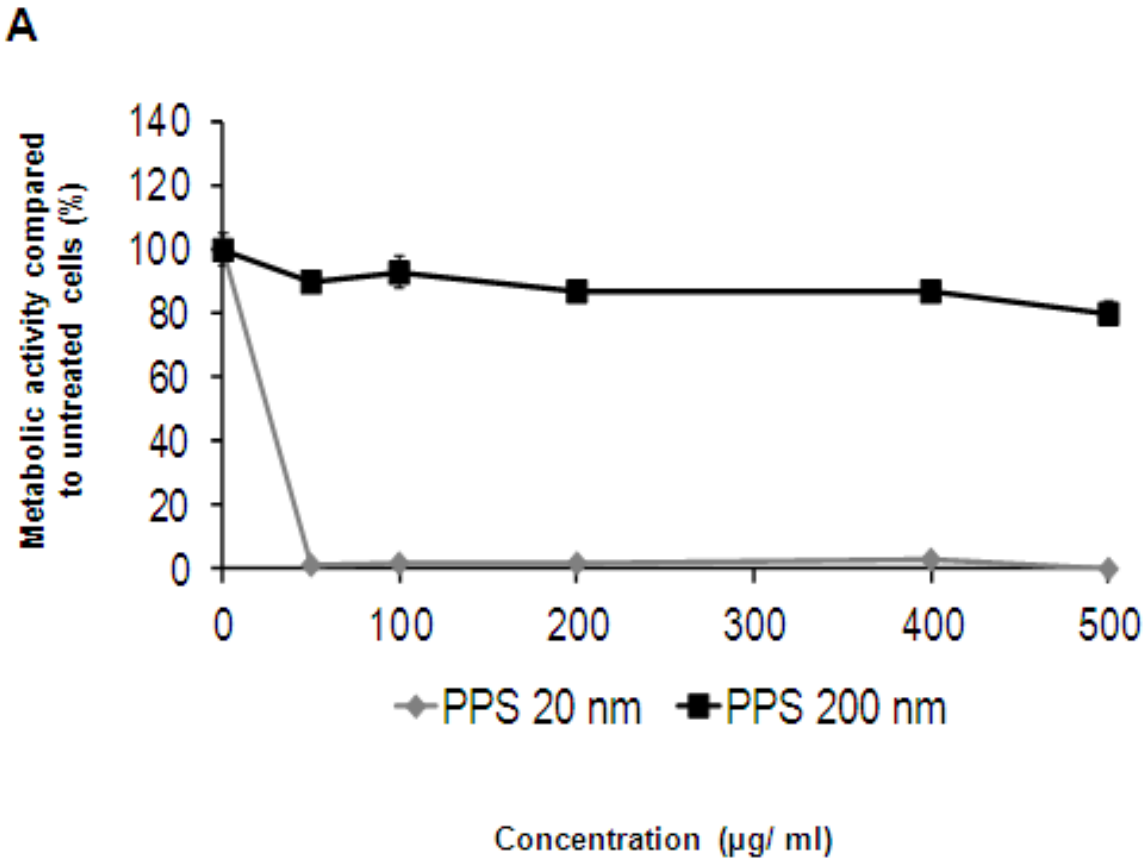

B

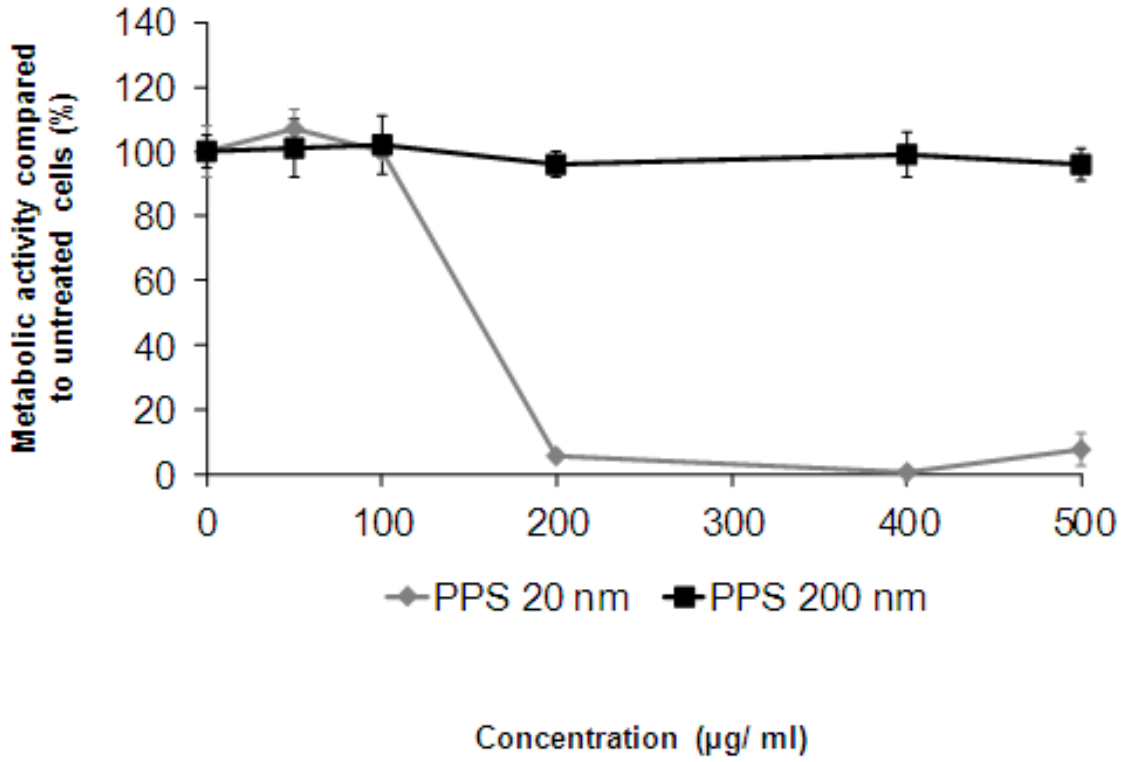
Metabolic activity compared to untreated cells (%)
140
120
100
80
60
40
20
0
0
100
200
300
400
500
PPS 20 nm
PPS 200 nm
Concentration (µg/ ml)

C

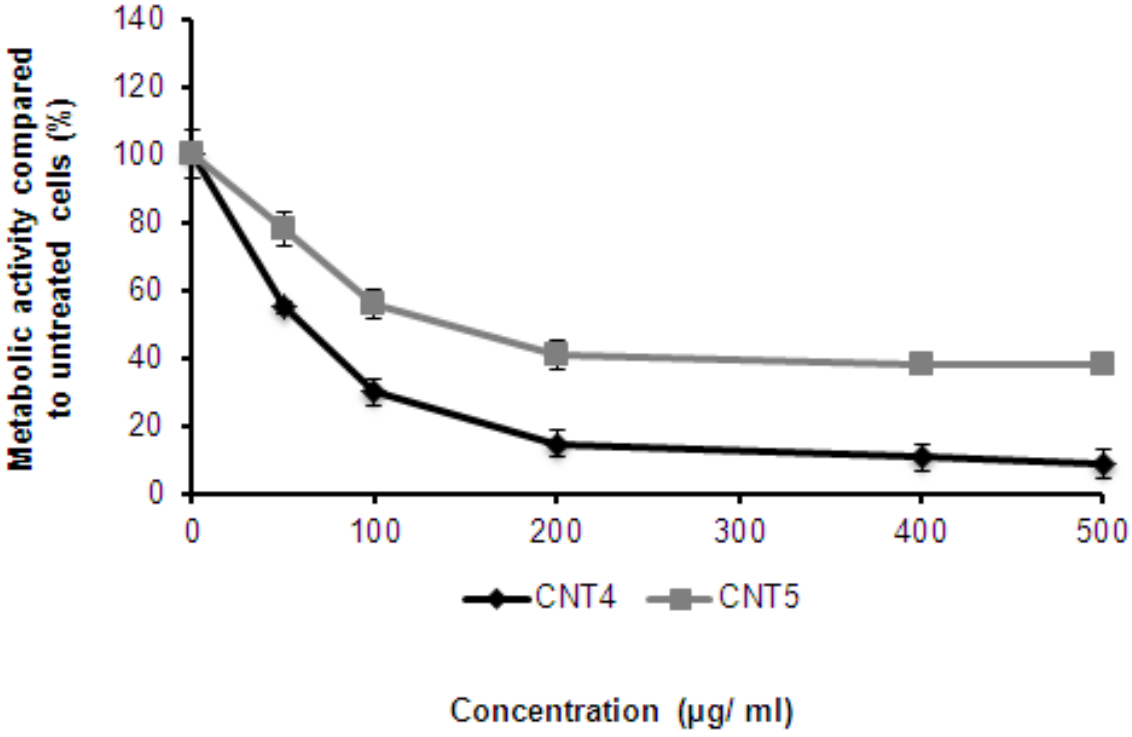
Metabolic activity compared to untreated cells (%)
140
120
100
80
60
40
20
0
0
100
200
300
400
500
CNT4
CNT5
Concentration (µg/ ml)

Figure 12. Metabolic activity of EAhy 926 cells.

20 nm PPP decreased cell viability in a dose-dependent manner in medium without **(A)** and with **(B)** 10% FBS. No changes were observed when 200 nm PPP were applied. Exposure to CNTs resulted in a reduction of the metabolic activity of the cells **(C)**, similar to the exposure to 20 nm PPP. Mean ± SD are presented.

3.2.2 Assay on apoptosis

Low concentrations (< 200 µg / ml) of PPP 20 had no influence on activation of effector caspases 3 and 7 at any time-point. However, exposure to PPP at concentrations of 200 µg / ml induced strong activation already after 4 hours, reaching the maximum of an about 50-fold increase after 8 hours and an almost 30-fold increase after 24 hours as compared to non-exposed cells (Figure 13 A). Exposure of the cells to PPP 200 resulted in an unnotable increase in caspase activation at any time-point (Figure 13 B).

3.2.3 Assay on cytotoxicity based on the release of LDH

A similar dose-dependent effect was observed for membrane disruption upon treatment with PPP 20 (Figure 13 C). Exposure to concentrations ≤ 200 µg / ml for 4 and 8 hours induced a hardly notable release of LDH compared to the lysis control. However, after 24 hours, the LDH release increased to almost same amounts as treatment with lysis solution. Higher concentrations induced an increased LDH release at all time-points.
Exposure of the cells to PPP 200 resulted in a very low release of LDH (up to 15% of the lysis control) at all time-points, irrespective of the employed concentration (Figure 13 D).

A

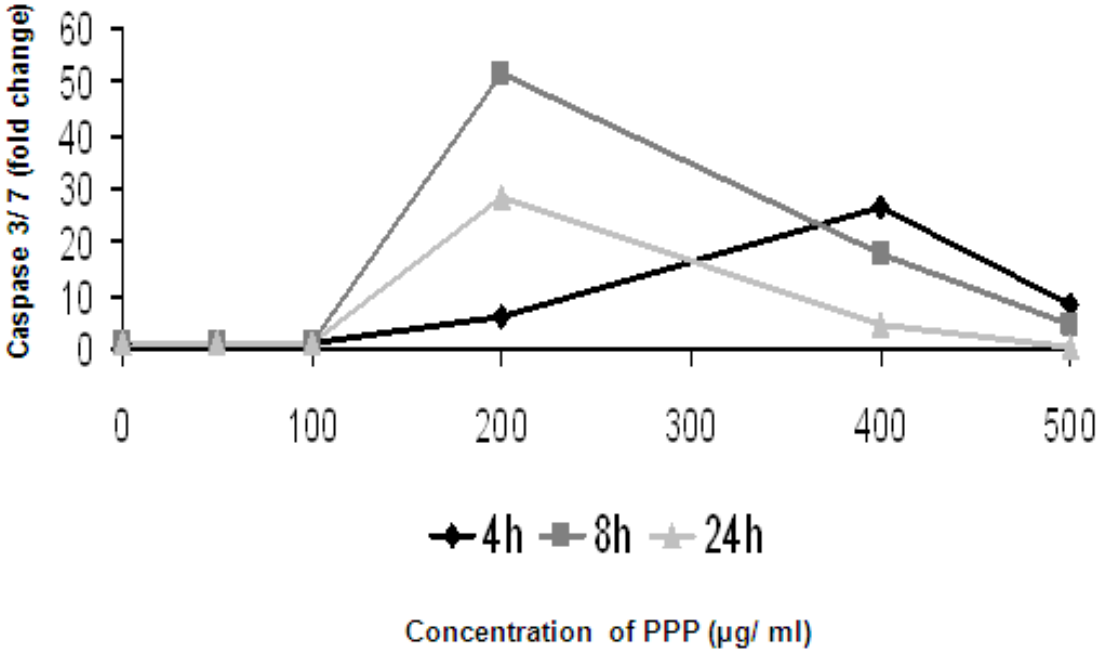
Caspase 3/ 7 (fold change)
60
50
40
30
20
10
0
0
100
200
300
400
500
4h
8h
24h
Concentration of PPP (µg/ ml)

B

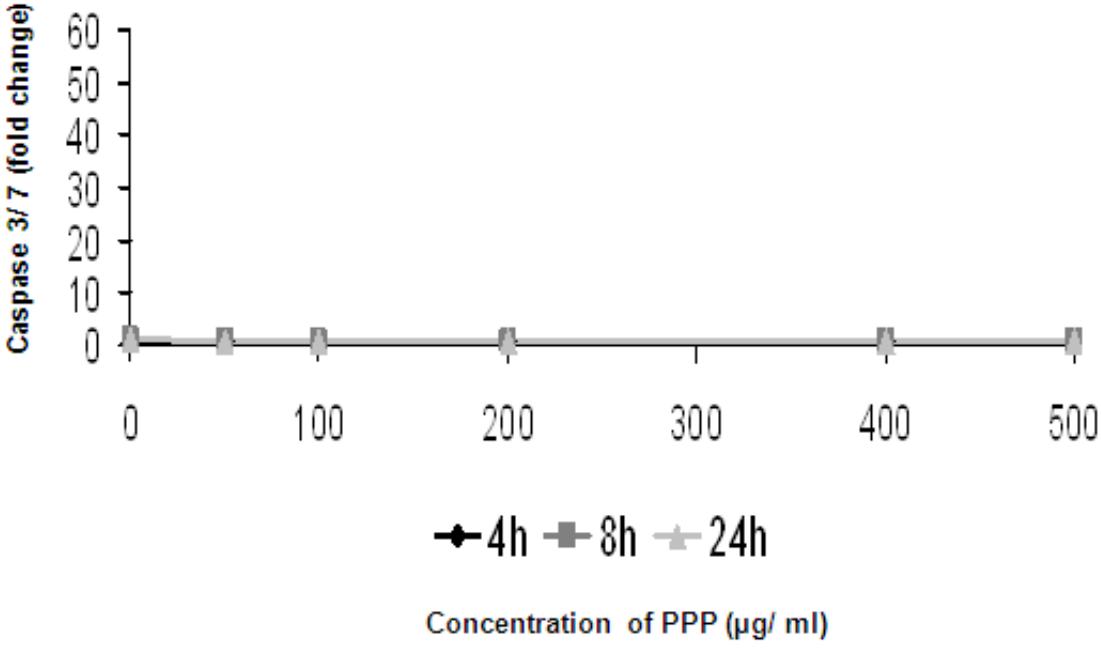
Caspase 3/ 7 (fold change)
60
50
40
30
20
10
0
0
100
200
300
400
500
4h
8h
24h
Concentration of PPP (µg/ ml)

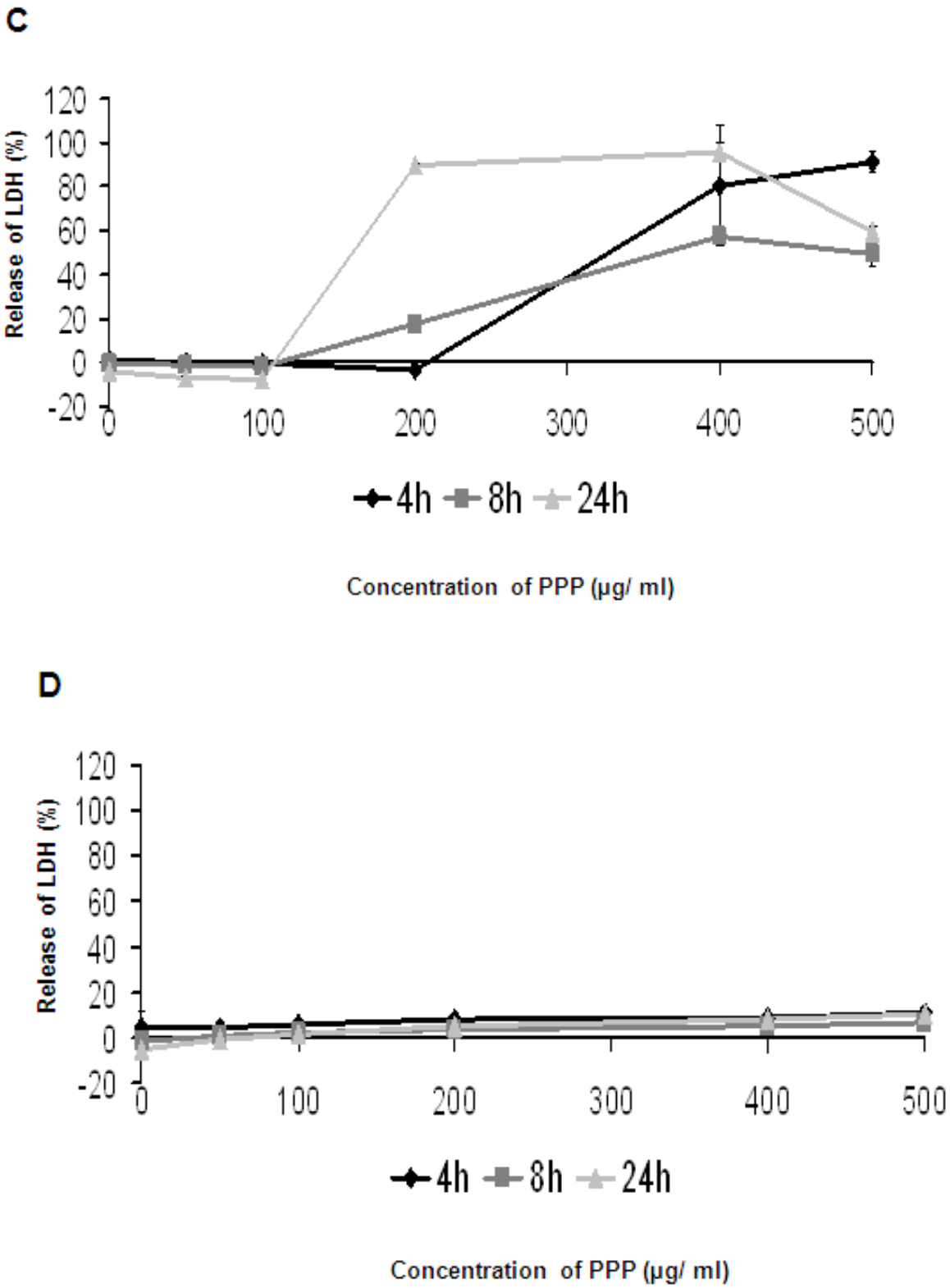

Figure 13. Mode of action of PPP 20 and PPP 200 upon short-term exposure.

Induction of effector caspases 3 and 7 as well as membrane disruption (LDH release) upon exposure to 20 nm PPP **(A and C)** and 200 nm PPP **(B and D)**. Mean ± SD are presented.

3.3 Acute effects on THP-1 cells

3.3.1 Assay on cell viability

Exposure to PPP 20 resulted in a dose-dependent decrease in cell viability. The estimated IC_{50} was approximately 65 µg / ml. Larger particles induced a lesser reduction in cell viability. However, the viability upon exposure to concentration ≤ 500 µg / ml did not drop below 60% (Figure 14).

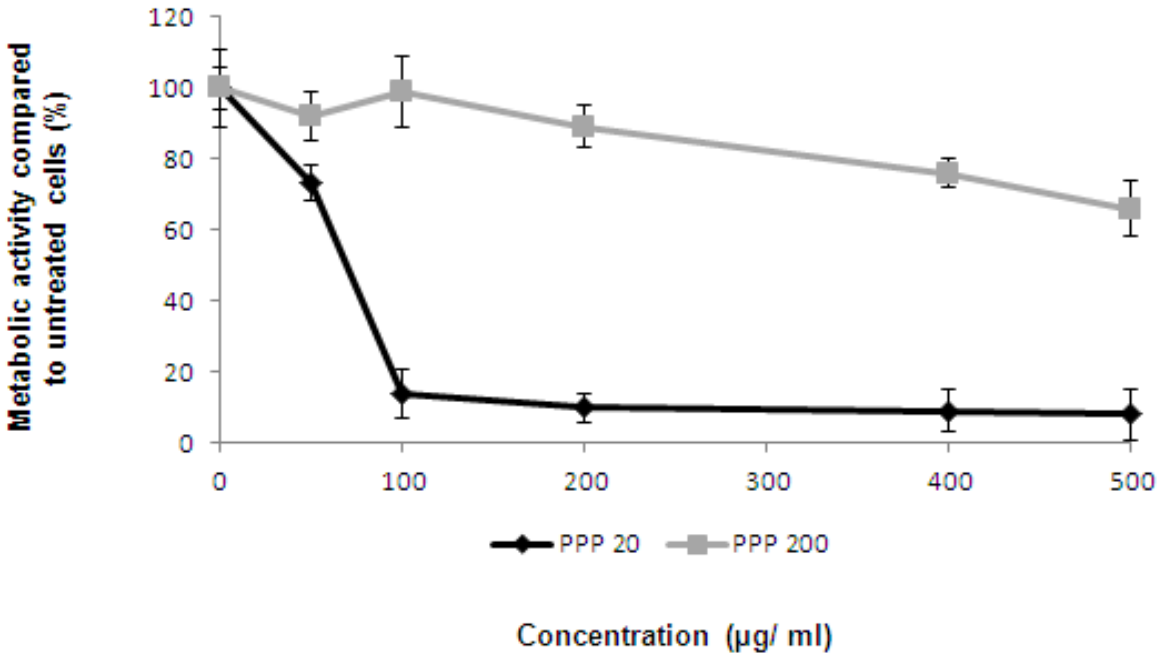

Figure 14. Metabolic activity of THP-1 cells upon short-term exposure to PPP 20 and PPP 200.

Only exposure to PPP 20 induced a dose-dependent decrease in cell viability. Mean ± SD are presented.

3.3.2 Assay on IL release

The maximum amount of IL6 released from treated cells was 10 times lower than the release of IL8. Treatment with LPS resulted in a dose-dependent increase of IL6- and IL8-release. Exposure to PPPs induced a release of both, IL6 and IL8 as compared to untreated cells.

Exposure to concentrations ≤ 75 µg / ml of PPP 20 induced a dose-dependent release of both cytokines. While a delayed addition of 100 ng / ml LPS after exposing the cells to PPP 20 enhanced the effect, a concentration of 1000 ng / ml was shown to be even more effective. However, combined treatment with 1000 ng / ml of LPS and PPP 20 resulted in lower amounts of released cytokines as compared to the delayed addition of LPS (Figure 15 A, C).

Exposure to concentrations of ≤ 50 µg / ml of PPP 200, resulted in a dose-dependent secretion of IL6, but not of IL8. Even higher amounts of IL6 were detected upon a delayed exposure to 1000 ng / ml of LPS (Figure 15 B). The amount of IL8 upon a delayed treatment with 100 ng / ml of LPS decreased in a dose-dependent manner. However, no dose-dependent effects were observed when 1000 ng / ml of LPS were applied. The combined treatment with LPS, however, resulted in a lower amount of IL8 which was increasing with the application of higher concentration of PPP 200 (Figure 15 D).

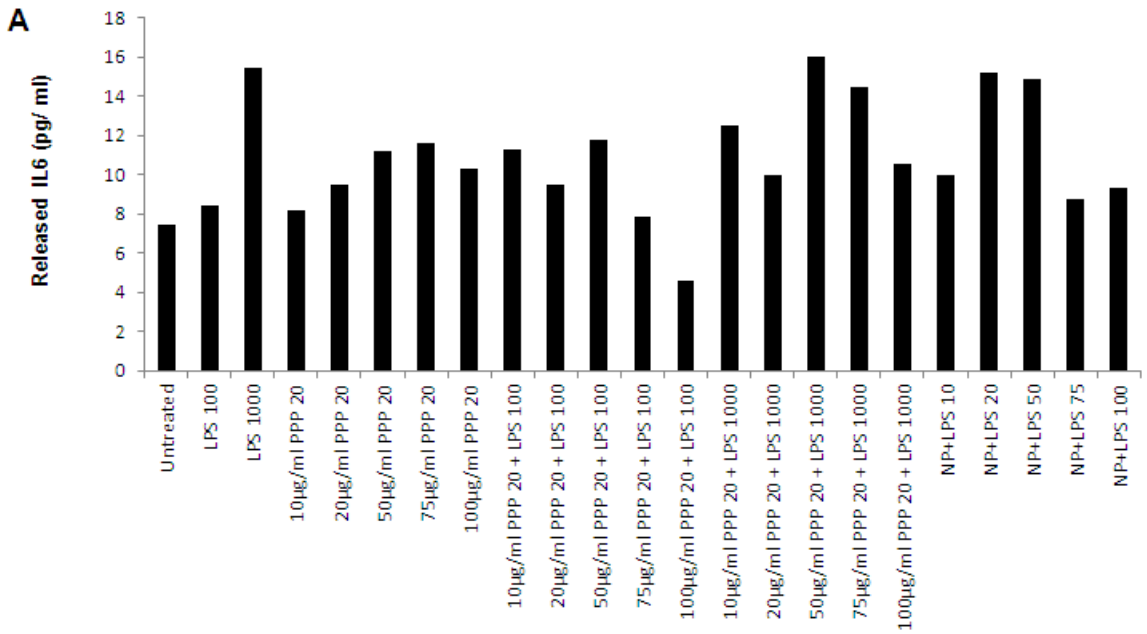

B

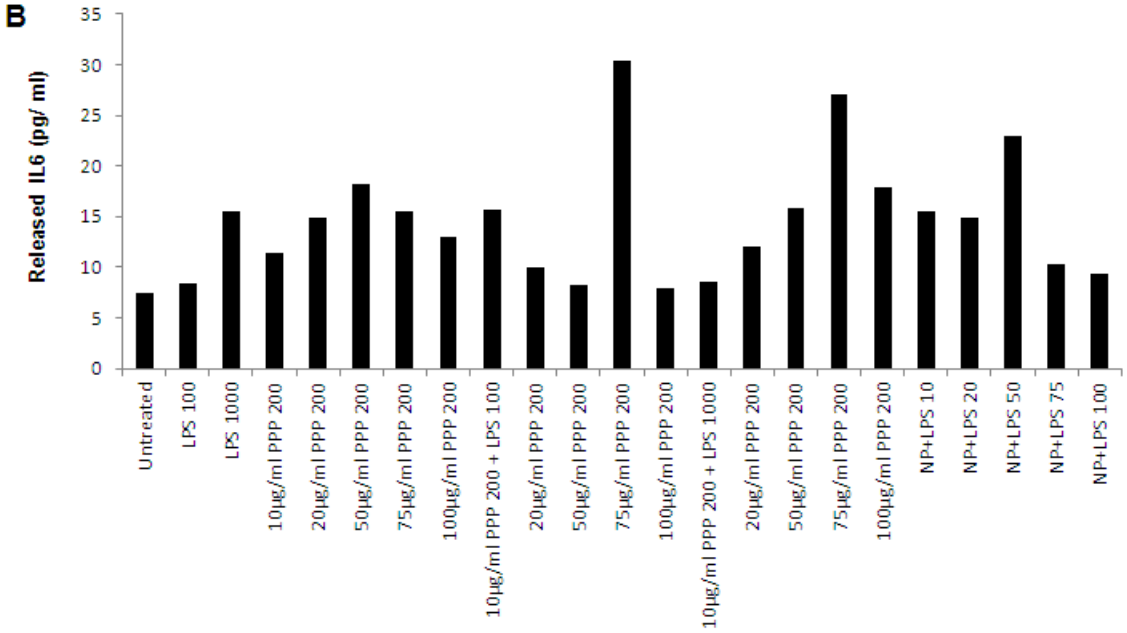
Released IL6 (pg/ ml)
35
30
25
20
15
10
5
0
Untreated
LPS 100
LPS 1000
10µg/ml PPP 200
20µg/ml PPP 200
50µg/ml PPP 200
75µg/ml PPP 200
100µg/ml PPP 200
10µg/ml PPP 200 + LPS 100
20µg/ml PPP 200
50µg/ml PPP 200
75µg/ml PPP 200
100µg/ml PPP 200
10µg/ml PPP 200 + LPS 1000
20µg/ml PPP 200
50µg/ml PPP 200
75µg/ml PPP 200
100µg/ml PPP 200
NP+LPS 10
NP+LPS 20
NP+LPS 50
NP+LPS 75
NP+LPS 100

C

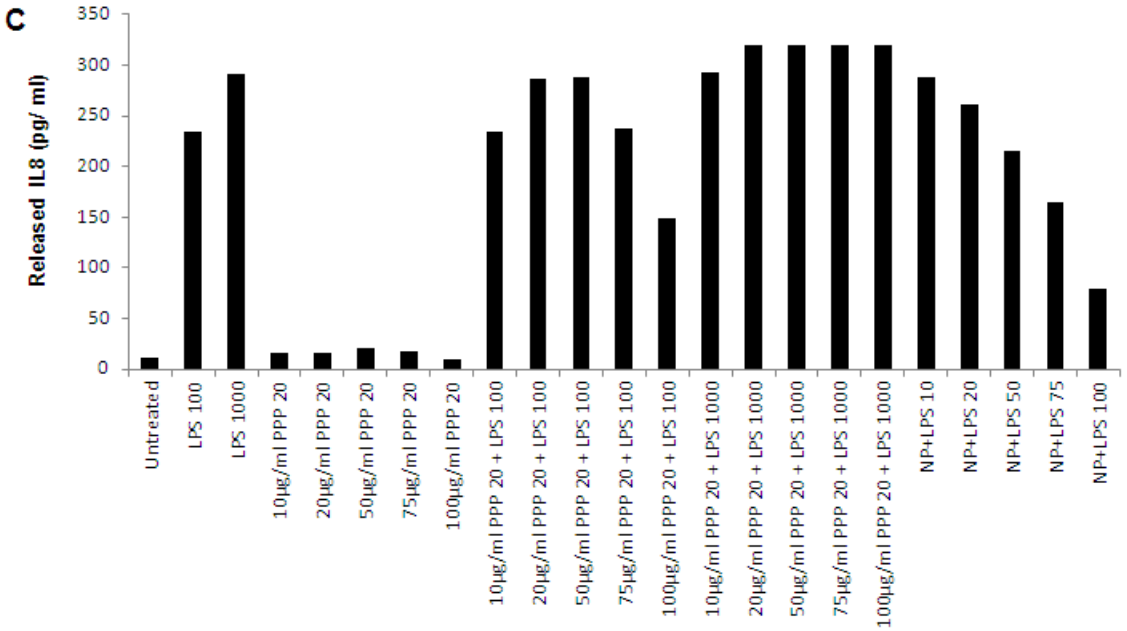
Released IL8 (pg/ ml)
350
300
250
200
150
100
50
0
Untreated
LPS 100
LPS 1000
10µg/ml PPP 20
20µg/ml PPP 20
50µg/ml PPP 20
75µg/ml PPP 20
100µg/ml PPP 20
10µg/ml PPP 20 + LPS 100
20µg/ml PPP 20 + LPS 100
50µg/ml PPP 20 + LPS 100
75µg/ml PPP 20 + LPS 100
100µg/ml PPP 20 + LPS 100
10µg/ml PPP 20 + LPS 1000
20µg/ml PPP 20 + LPS 1000
50µg/ml PPP 20 + LPS 1000
75µg/ml PPP 20 + LPS 1000
100µg/ml PPP 20 + LPS 1000
NP+LPS 10
NP+LPS 20
NP+LPS 50
NP+LPS 75
NP+LPS 100

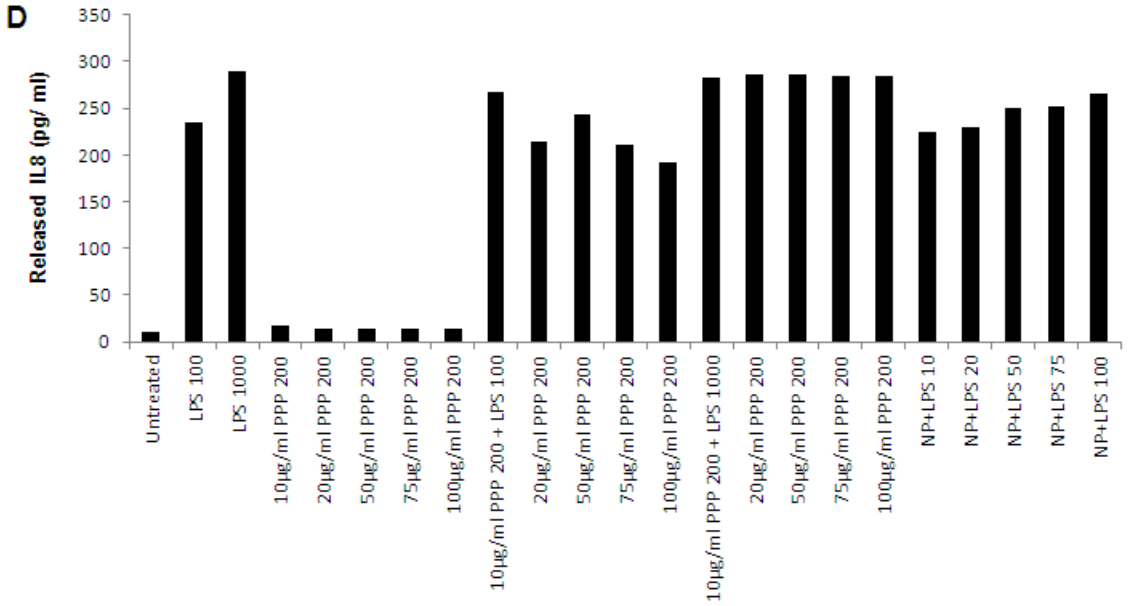

Figure 15. Release of IL6 (A, B) and IL8 (C, D) upon short-term exposure of THP-1 cells to PPP 20 and PPP 200.

As positive control 100 and 1000 ng / ml LPS (LPS 100 and LPS 1000) were applied. Both concentrations of LPS induced an increase in IL-secretion. However, higher amounts were released upon treatment with LPS 1000. NP+LPS: combined treatment with PPP and LPS 1000.

3.4 LDH stability

The stability of LDH (from bovine heart) markedly decreased by about 30% when stored at -20°C as compared to freshly prepared LDH solutions. No LDH could be detected in samples stored at +4°C (data not shown). Only storage at -80°C did not influence the enzyme stability over time. Moreover, addition of BSA, slightly improved the stability, irrespective of the storage temperature (Figure 16).

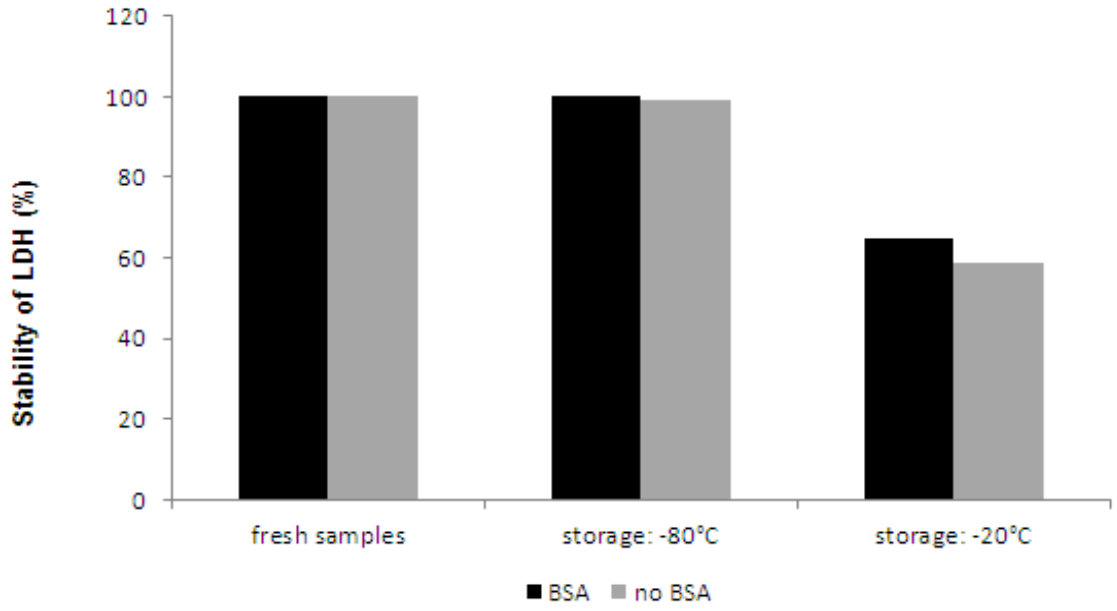

Figure 16. Stability of LDH III from bovine heart.

Three concentrations of the enzyme (0.002 – 0.2 U / ml) were dissolved in different media and were stored at different conditions. The stability of the samples was not changed in samples which were stored at -80°C, but was impaired after storage at -20°C as compared to fresh samples.

3.5 Long-term effects on EAhy 926 cells

3.5.1 Microcarrier cell culture

3.5.1.1 Metabolic activity of EAhy 926 cells

After 24 hours, the viability of cells after exposure to PPP 20 did not decrease when cells were grown on GEM^{TM}. As expected, exposure to PPP 200 did not influence cell viability at any concentration employed (Figure 17 A).
Moreover, no changes in cell viability were detected when cells were exposed to CNTs (Figure 17 B).

A

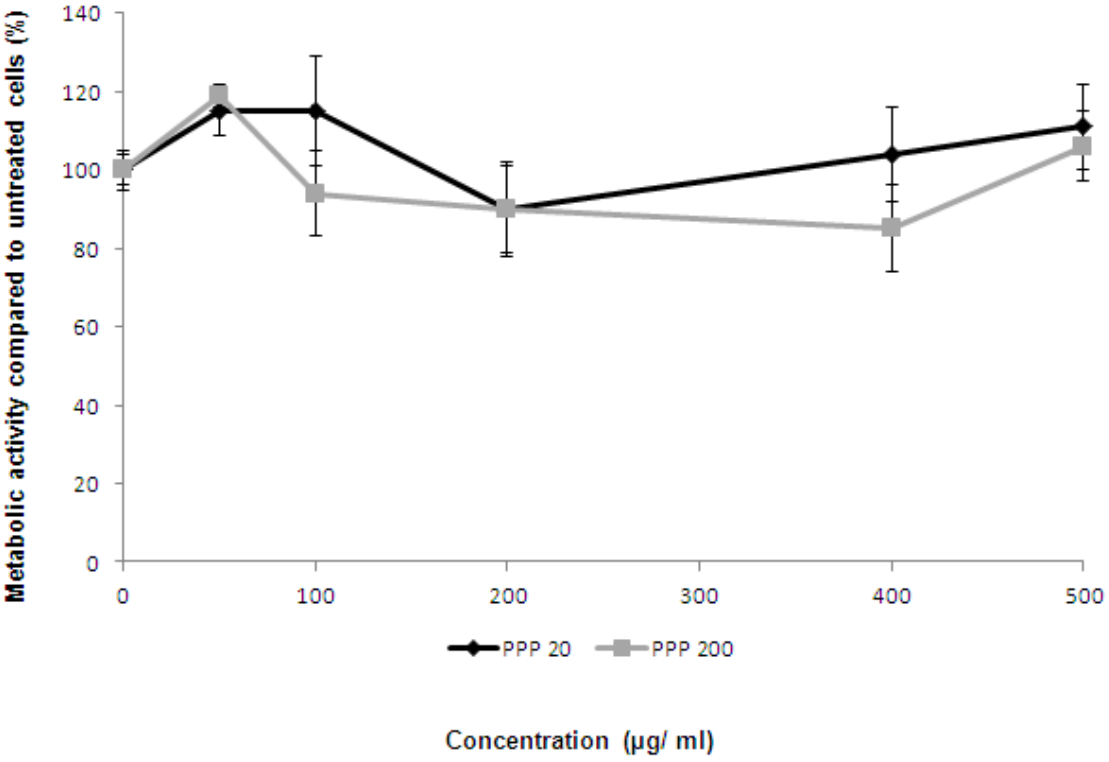
Metabolic activity compared to untreated cells (%)
140
120
100
80
60
40
20
0
0
100
200
300
400
500
PPP 20
PPP 200
Concentration (µg/ ml)

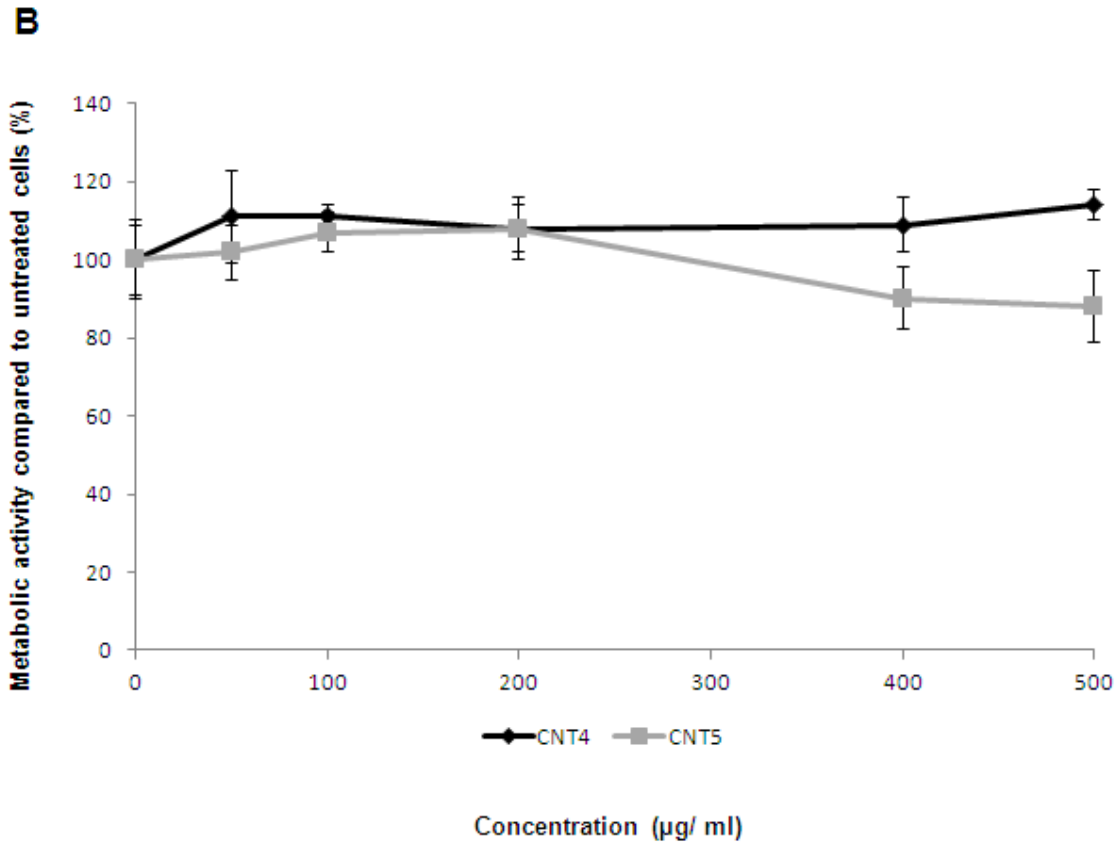

Figure 17. Metabolic activity of EAhy 926 cells grown on microcarriers upon short-term treatment with PPP 20 and PPP 200 (A) aa well as CNT4 and CNT5 (B).

No changes in cell viability was observed irrespective of the NPs and concentrations employed. EAhy 926 cells grown on microcarriers seem to be more resistant to the toxic potential of the NPs. Mean ± SD are presented.

3.5.1.2 Culturing protocol in the BioLevitator™

For optimization of the exposure system, different coatings of the GEM™ (gelatine, laminin, fibronectin, collagen type I and IV, basal membrane) as well as different incubation protocols, pre-defined by the supplier, were compared.
The culturing protocol is presented in Table 8.

	Inoculation	Culture
Rotation period	1 sec	1 sec
Rotation pause	0 sec	1 sec
Rotation speed	50 rpm	80 rpm
Agitation period	40 min	
Agitation pause	2 min	
Duration	12 hrs	∞
Magnet position	0 - 80 mm	0 - 80 mm
Magnet rot. speed	70 mm / sec	70 mm / sec

Table 8. Culturing protocol in the BioLevitator™ for EAhy 926 cells

Cells that were seeded on GEM™ coated with either basal membrane or collagen type IV, and cultured according to the protocol for endothelial cells (HUVEC) reached approximately 4 times higher cell densities compared to which were subjested to the protocol for epithelial cells (HEK 293) (Figure 18). Cultures were maintained for 23 days without sub-culturing.

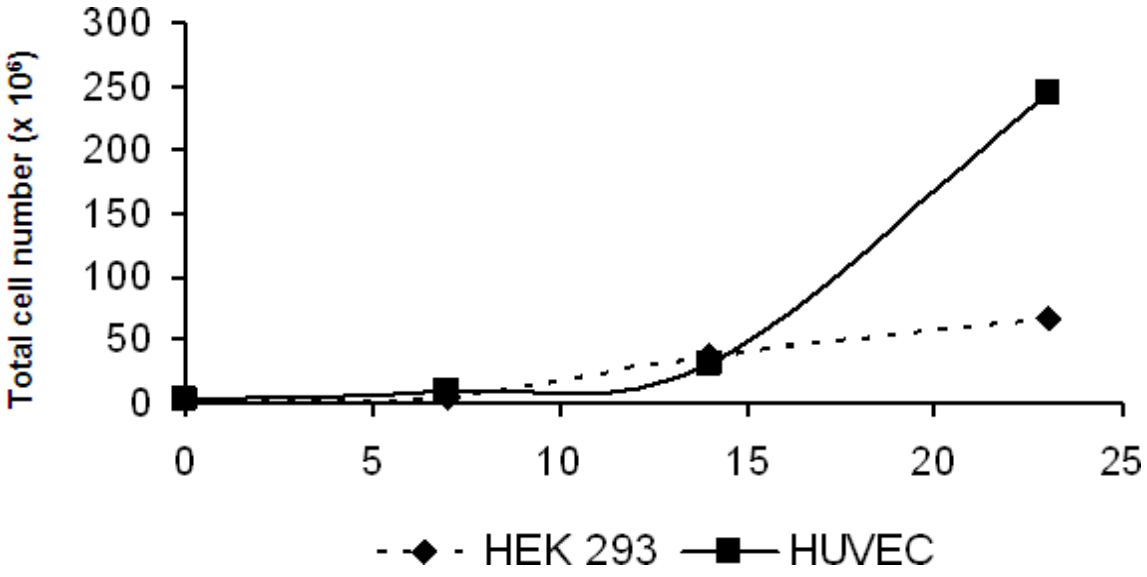

Figure 18. Differences in cell numbers of EAhy 926 cells in the BioLevitator.

Cell culturing according to the protocol for HUVEC (= endothelial) cells, resulted in an approximately 4 times higher cell density after 23 days.

3.5.1.3 Microscopic evaluation of microcarrier cultures

Staining with Hoechst 33342 dye showed an increase in cell proliferation on GEM^{TM} (Figure 19 A). Furthermore, vital staining for mitochondria and endoplasmic reticulum (ER) demonstrated the viability of the cells (Figure 19 B). In addition, cells were exposed to 20 µg / ml of the red fluorescent PPP in order to study cellular localization. R25 were observed within the cells, mainly localized in lysosomes (Figure 19 C).

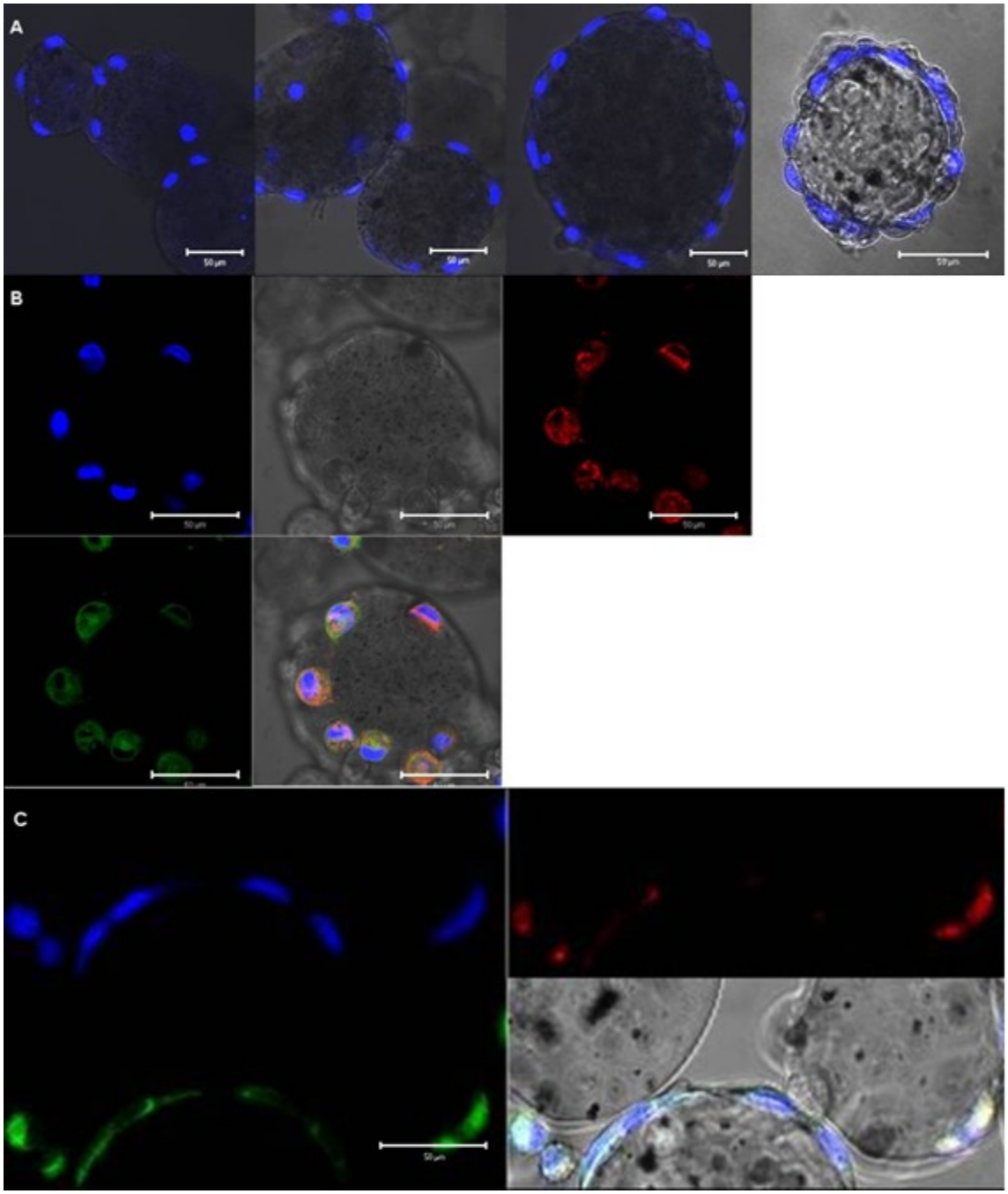

Figure 19. Confocal images of EAhy 926 cells grown on microcarriers.

Cell proliferation (A) was monitored 1, 5, 7, and 14 days after inoculation. Cell viability (B) was demonstrated by mitochondrial (red) and ribosomal (green) staining. Intracellular localization of PPP 20 (red; R25) and co-localization with lysosomes (green) was investigated 14 days after inoculation. Hoechst 33342 (blue) was used in all experiments for nuclear staining.

3.5.1.4 Cellular effects of long-term exposure to NMs

Cells were cultured according to the established protocol (basal membrane or collagen type IV coated GEM, and incubation protocol for endothelial cells) for four weeks with a medium change performed once per week. After inoculation, NPs were added at a concentration 250 times lower than the concentration where cytotoxicity was observed in the acute cytotoxicity setting (24 hours).

Exposure of the cells to 20 µg / ml of PPP 20 resulted in a significantly reduced cell number already after 7 days, showing a decrease in cell numbers of approximately 50%. Even stronger effects were observed at later time-points. No decrease in cell number was observed when the cells were exposed to 20 µg / ml of PPP 200 (Figure 20 A).

Exposure to concentrations of 5 – 20 µg / ml of CNT-COOH decreased cell numbers in a dose-dependent manner at day 7 to approximately 75% - 40% of control cells, respectively. However, with prolonged contact the cell populations recovered. The recovery rate was more rapid for cells exposed to 20 µg / ml than for cells that were exposed to 5 µg / ml; Values reached 90% - 70% of the control after 4 weeks (Figure 20 B). Similar to PPP 200, exposure to plain CNTs did not influence cell numbers at any time point or concentration (Figure 20 C).

Cell viability was not impaired at any time-point, irrespective of the particle type employed.

A

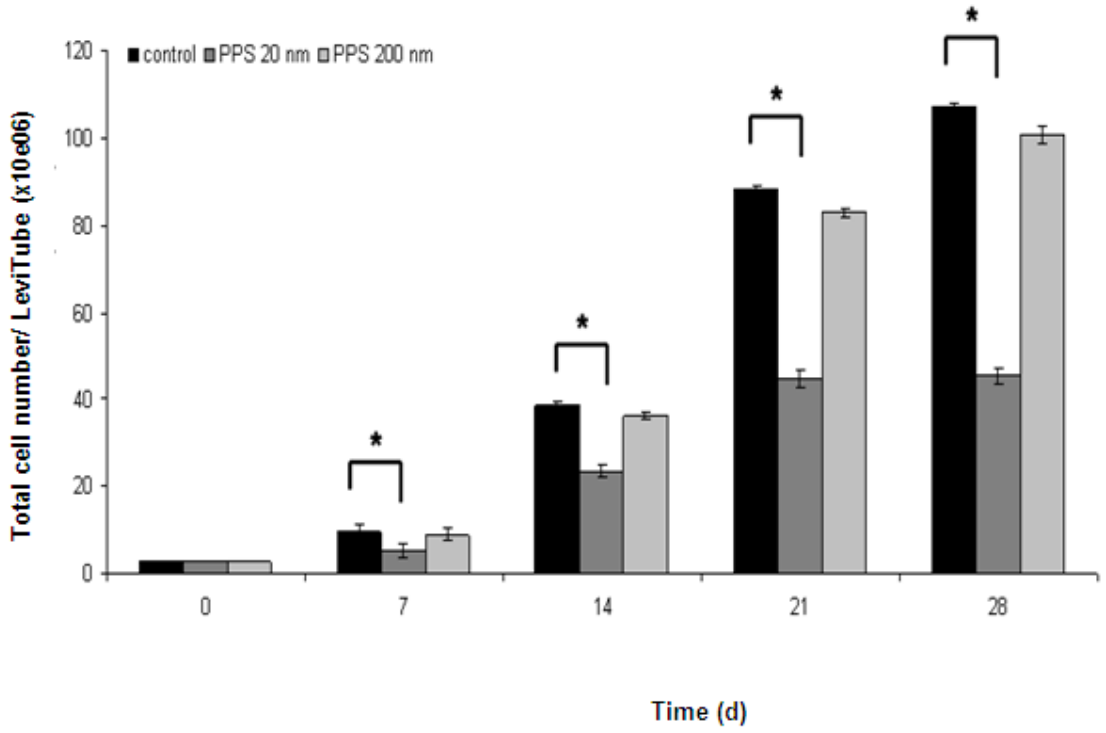
control
PPS 20 nm
PPS 200 nm
Total cell number/ LeviTube (x10e06)
120
100
80
60
40
20
0
0
7
14
21
28
*
*
*
*
Time (d)

B

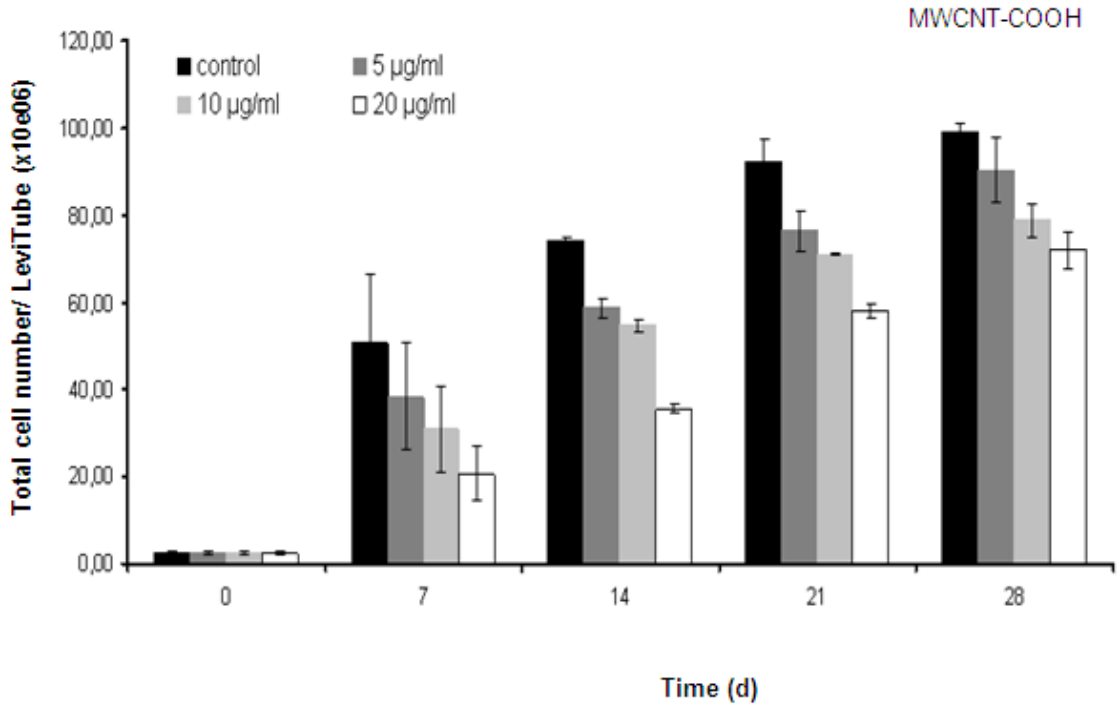
MWCNT-COOH
control
5 µg/ml
10 µg/ml
20 µg/ml
Total cell number/ LeviTube (x10e06)
120,00
100,00
80,00
60,00
40,00
20,00
0,00
0
7
14
21
28
Time (d)

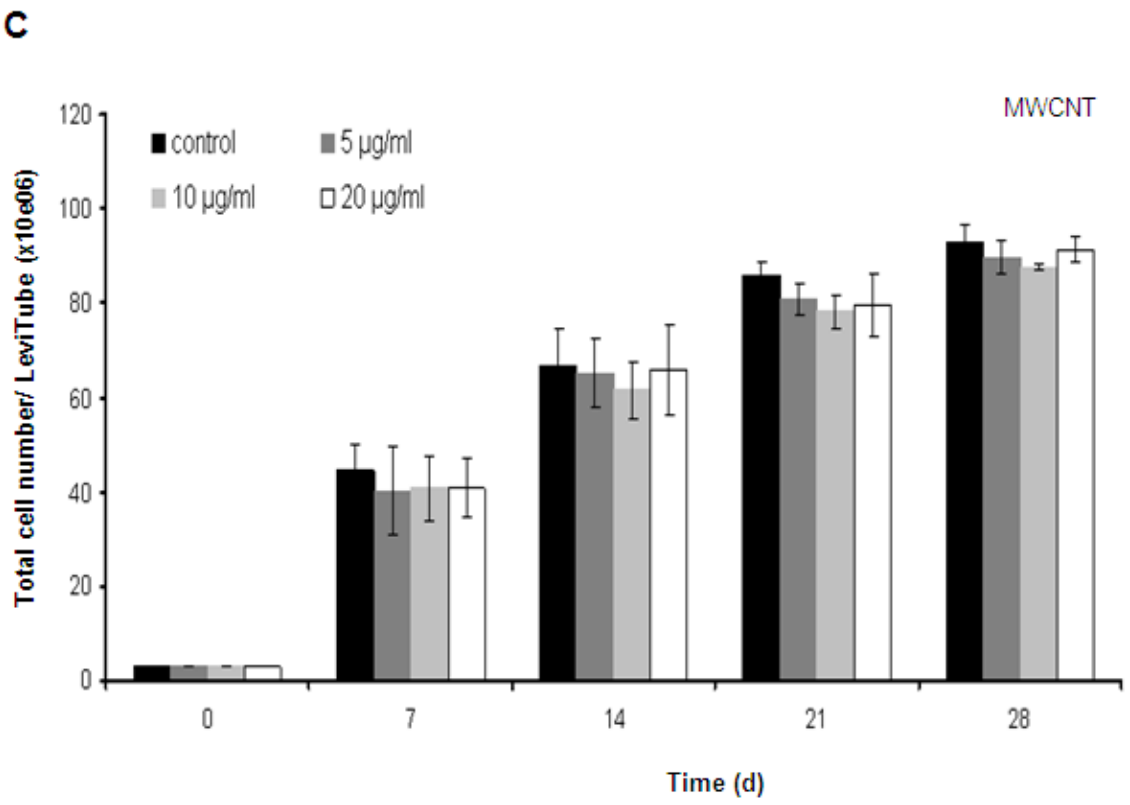

Figure 20. Long-term effects of NPs on EAhy 926 grown on microcarriers.

Statistical significant changes in cell numbers of cells exposed to PPP 20 were detected already 7 days after exposure **(A)**. CNT5 **(B)** induced a dose-dependent effects, while CNT4 **(C)** had no influence on cell proliferation as compared to untreated cells. Mean ± SD are presented.

3.5.1.5 Mode of action of NMs in microcarrier cultures

Long-term exposure to PPP 20 induced an 80% higher activation of the effector caspases 3 and 7 after 7 days as compared to the control cells. Over time, the induction of apoptosis decreased to about 30% of the untreated control (Figure 21 A). PPP 20 induced necrosis with a maximum of LDH release, about 65% higher than in control cells, after 7 days of culturing (Figure 21 C). At later time-points, LDH release slightly dropped by about 15%. However, exposure to PPP 20 resulted in a 2.5- to 5-fold increase in cytotoxicity, while the viability was slightly reduced, as detected by the ApoTox-Glo^{TM} Triplex Assay. No induction of apoptosis was detected (Figure 21 E). Exposure to PPP 200 induced neither apoptosis nor necrosis at any time-point (Figure 21 A, C, E).

Only exposure to MWCNT-COOH induced both, apoptosis and necrosis, in a dose-dependent manner, reaching a 2.5-fold increase as compared to the control upon exposure to a concentration of 20 µg / ml (Figure 21 B, D). Similar to PPP 20, the strongest induction of caspases and the highest release of LDH occurred after 7 days of exposure, after which the levels approached those of control cells.
As shown in Figure 21 F, an 89 kDa fragment representing cleaved PARP-1, indicative for apoptotic cell death, appeared exclusively in the staurosporine treated positive control. Treatment with NPs provoked the appearance of not only un-cleaved (116 kDa), but also additional slight cleaved PARP-1 bands (89 kDa, 72 kDa), which, in combination, occur only after necrosis.

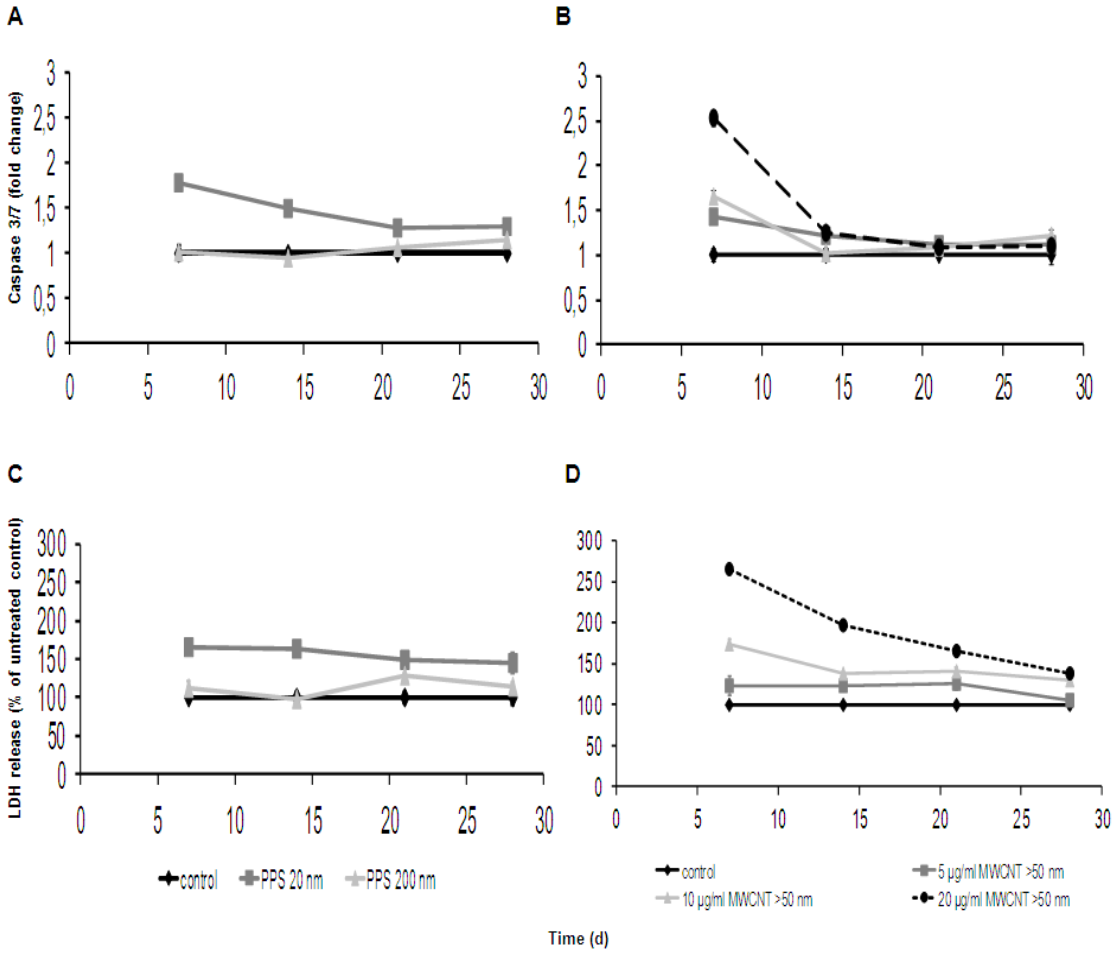

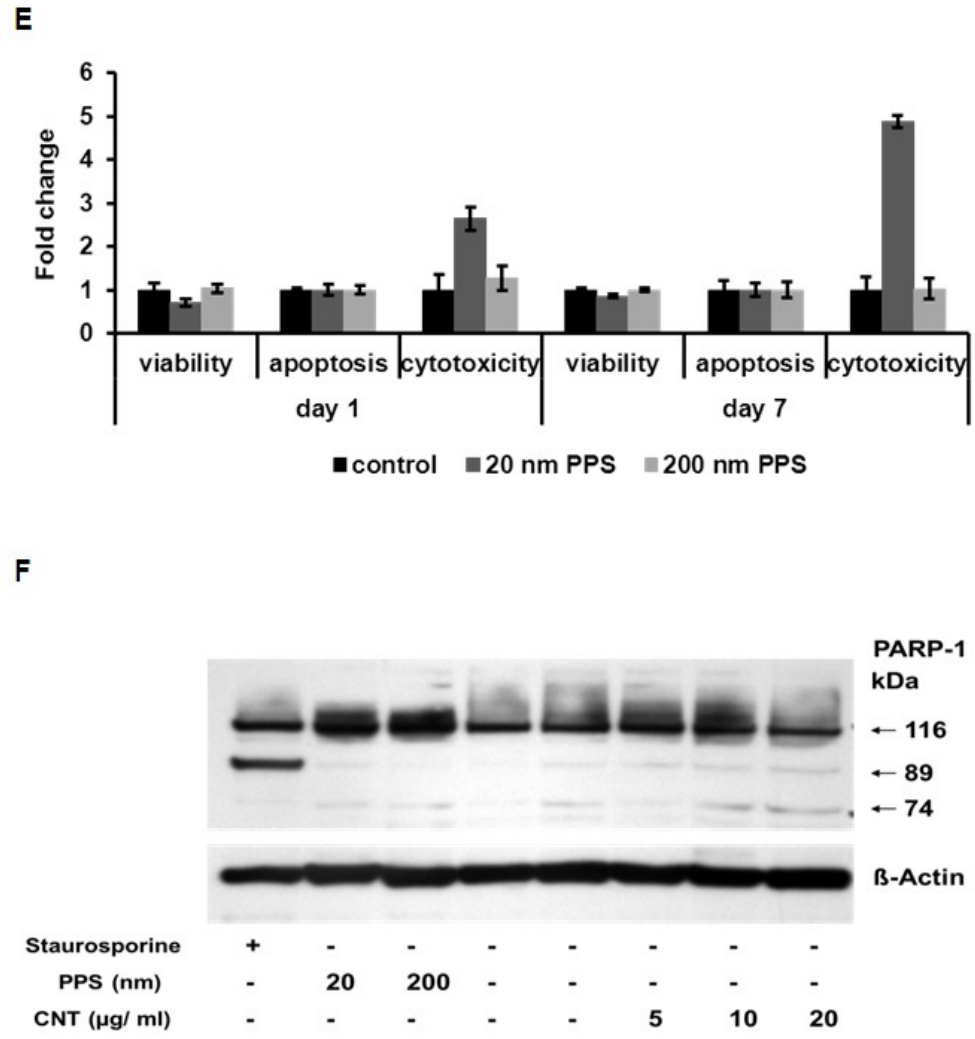

Figure 21. Mode of cell death of PPP and CNT5 in microcarrier cultures.

Necrosis is the main mode of action of both NPs **(C, D, F)**. Furthermore, the data was confirmed for PPP 20 by a simultaneous detection of cell viability, apoptosis, and cytotoxicity **(E)**. Induction of caspase-3 and -7 **(A, B)** seems to be a secondary effect of necrotic cell death. Mean ± SD are presented.

3.5.2 Modified conventional cell culture

3.5.2.1 Cellular effects of long-term exposure to PPP

Exposure of cells to PPP 20 decreased the cell numbers to approximately 80% of the controls. Larger particles did not influence cell numbers as compared to untreated cells (Figure 22). No changes in cell viability were detected.

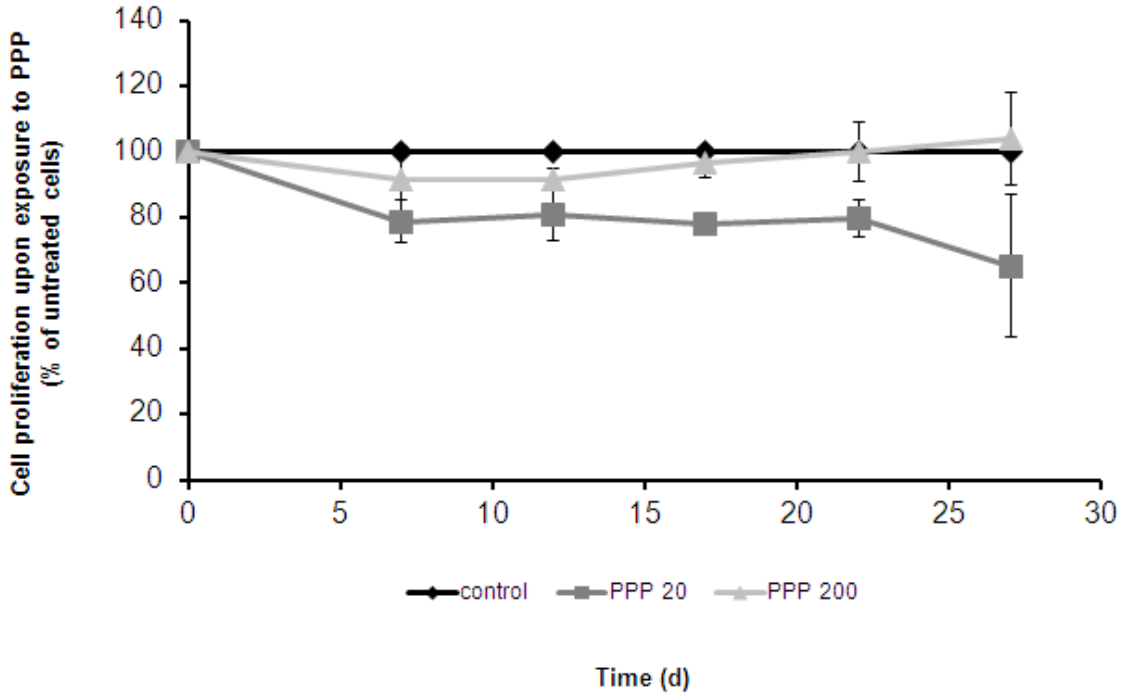

Figure 22. Differences in cell proliferation of sub-cultured EAhy 926 cells upon exposure to PPP.

Cell numbers of cells exposed to PPP 20 dropped by about 20 – 30 % of the controls. PPP 200 did not influence cell proliferation. Mean ± SD are presented.

3.5.2.2 Mode of cell death

As expected, no obvious release of LDH was detected upon exposure of the cells to smaller PPP at all time-points (Figure 23).

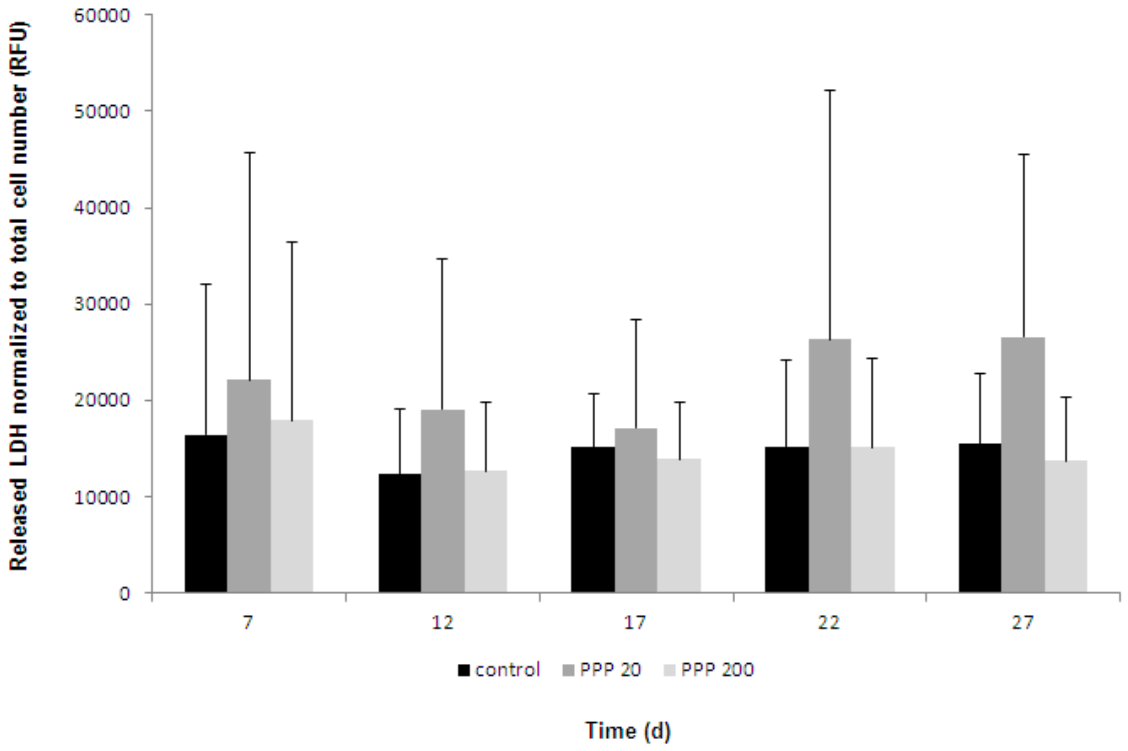

Figure 23. Cytotoxicity of PPP 20 and PPP 200 upon long-term exposure of sub-cultured EAhy 926 cells.

PPP 20 induced a slight increase in the release of LDH as compared to untreated controls. PPP 200 showed no cytotoxicity. Mean ± SD are presented.

3.6 Long-term effects on THP-1 cells

3.6.1 CELLine

3.6.1.1 Establishment of CELLine cultures

The maximal culturing period of 28 days was reached in cultures where 0.25 x 10^5 cells / ml were inoculated. The initial application of 0.5 x 10^5 cells / ml resulted in a reduced culturing period by approximately 2 weeks. Inoculation of 1 x 10^5 cells / ml yielded the shortest culturing period of 12 days (Figure 24)

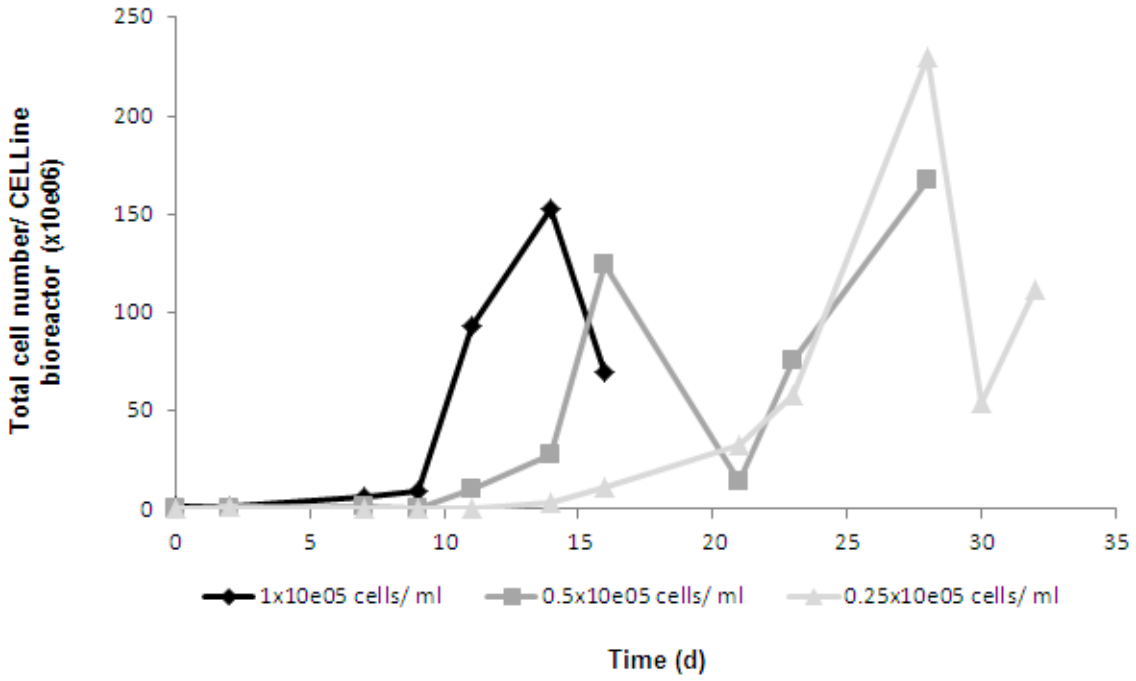

Figure 24. Growth curve of THP-1 cells in a CELLine bioreactor.

Culturing of THP-1 in the CELLine system cells yielded very high cell densities.

3.6.1.2 Cellular effects of long-term exposure to PPP

Data of 7 independent experiments showed that long-term culturing of THP-1 cells in bioreactors CELLine was possible. Untreated cells have reached high cell densities (16 x 10^6 cells / 10 ml medium) already 7 days after inoculation. Even higher cell densities were detected at later time-points. However, after 24 days cell numbers decreased in all cultures but evaluation of the growth curves of untreated cells showed that growth inhibition occurs already at 40 x 10^6 cells / ml.

As expected, treatment with 2% EtOH resulted in a reduction of the cell proliferation. However, this effect was notable only until day 21 after exposure. At later time-points (24 and 28 days), the differences in cell numbers were less pronounced or even inverted (Figure 25 A). Upon treatment with NPs, cell numbers decreased in a dose- and size-dependent manner. However, as presented in Figure 25, the variations between the experiments were very high (Figure 25 B, C).

A

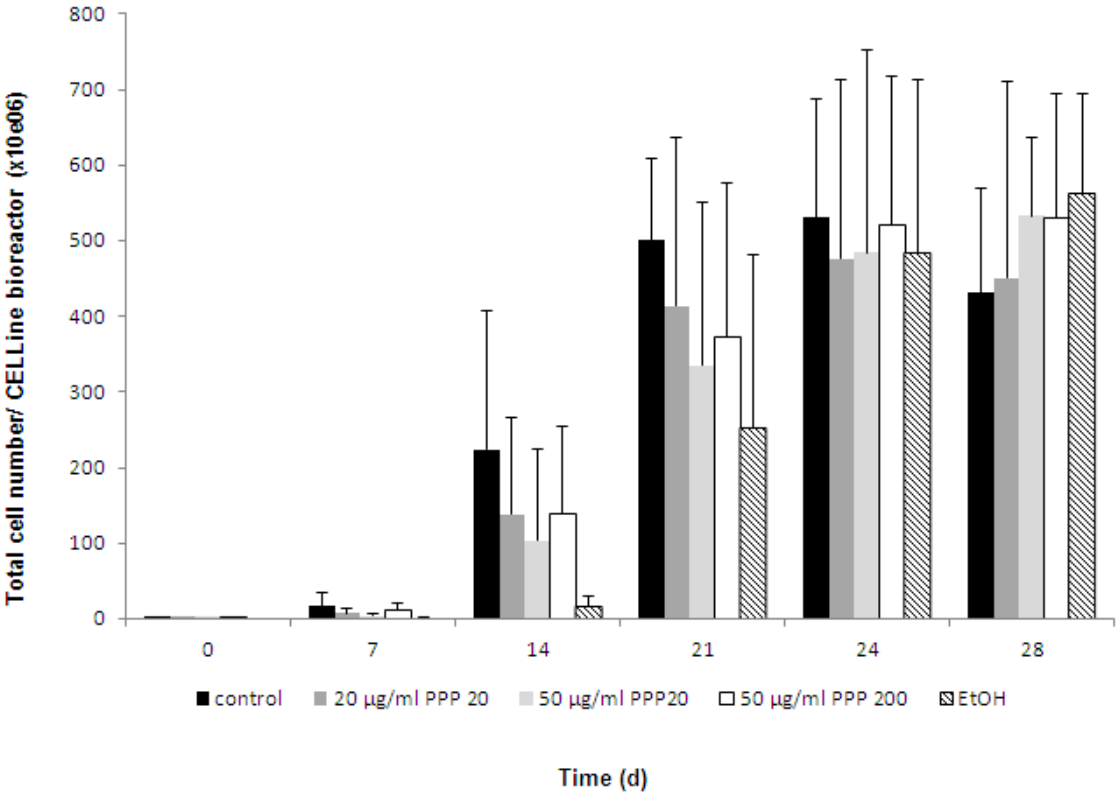
Total cell number/ CELLine bioreactor (x10e06)
800
700
600
500
400
300
200
100
0
0
7
14
21
24
28
control
20 µg/ml PPP 20
50 µg/ml PPP20
50 µg/ml PPP 200
EtOH
Time (d)

B

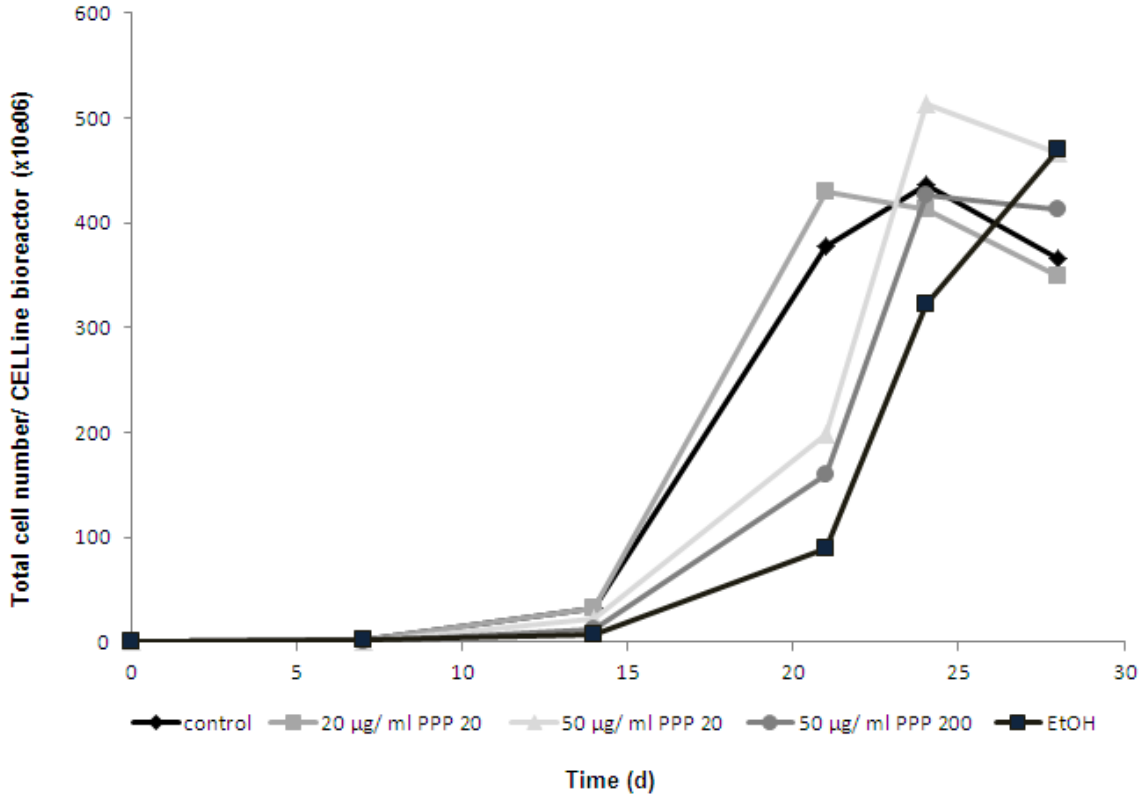
Total cell number/ CELLine bioreactor (x10e06)
600
500
400
300
200
100
0
0
5
10
15
20
25
30
control
20 µg/ ml PPP 20
50 µg/ ml PPP 20
50 µg/ ml PPP 200
EtOH
Time (d)

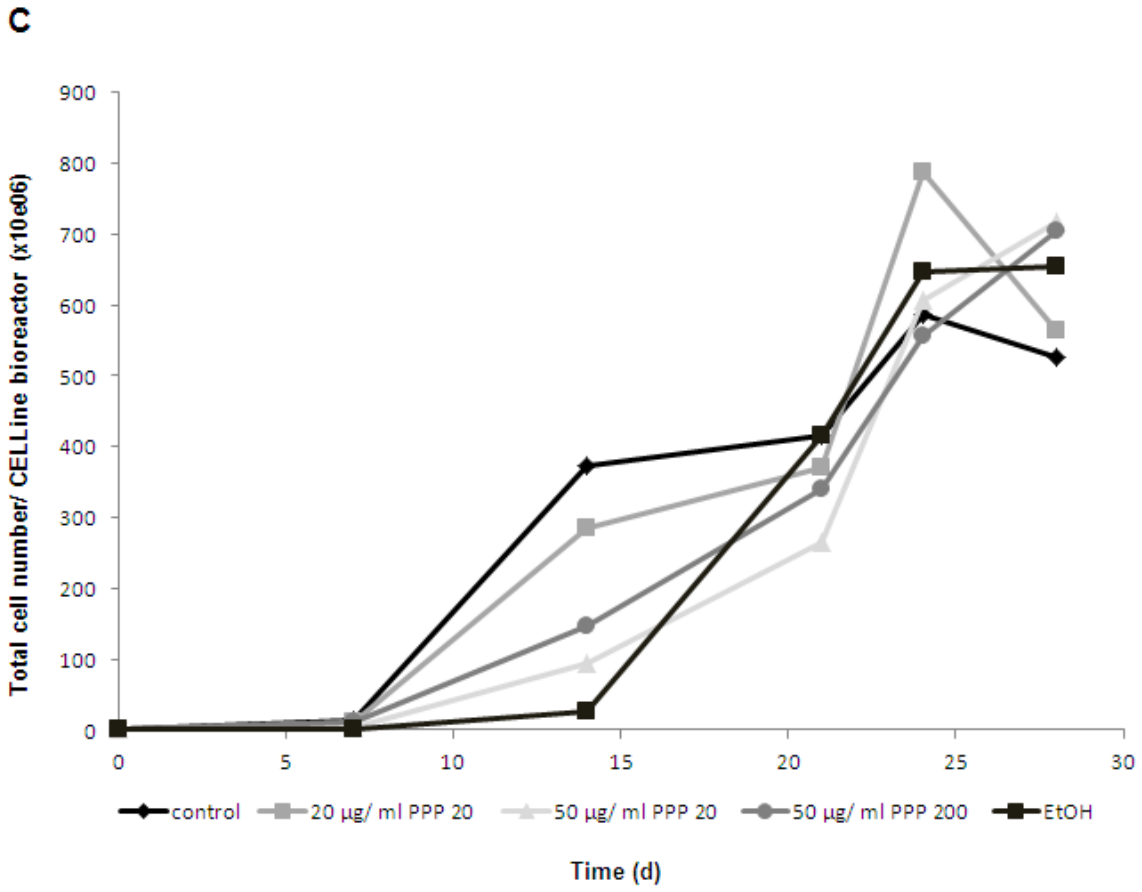

Figure 25. Changes in cell proliferation upon treatment of CELLine cultures to PPP 20, PPP 200, and EtOH.

Mean ± SD of 7 different experiment is presented in (A). Results of two independent experiments (B, C) show the large differences in cell proliferation upon treatment with PPP and EtOH.

3.6.1.3 IL expression upon long-term exposure

Release of IL6 of both, untreated and treated cells was very low. However, the highest amounts were detected 7 days after inoculation. The reaction was dose- and size-dependent. Almost no changes were observed after 7 days when cells were exposed to 20 µg / ml of PPP 20. Thereafter, the release of IL6 increased as compared to the untreated controls. The maximum was reached 28 days after inoculation when a 22-fold increase was detected. Exposure to 50 µg / ml PPP 20 induced a 2.7-fold increase in the release of IL6. PPP 200, however, induced a 1.8-fold increase. At later time-points, the release compared to untreated cells

increased for both conditions, with a maximum release of 14-fold and 3-fold, respectively, at day 21 (Figure 26 A).

The release of IL8 was in general higher than for IL6. Here, too, the highest amounts were detected 7 days after exposure. As expected, the highest amount of approximately 150 pg / ml was assessed in EtOH treated cells (49.8-fold increase). After 14 days, the amount dropped by approximately 145 pg / ml, resulting in a 21.5-fold increase as compared to untreated controls. Even smaller changes were spotted at later time-points. The influence of PPP on the release of IL8 was dose-dependent for small PPP. PPP 200 had no impact at any time-point. 7 days of exposure to higher concentrations of PPP 20 resulted in higher release of IL8. Thereafter, lower concentrations had a greater influence at each time-point (Figure 26 B).

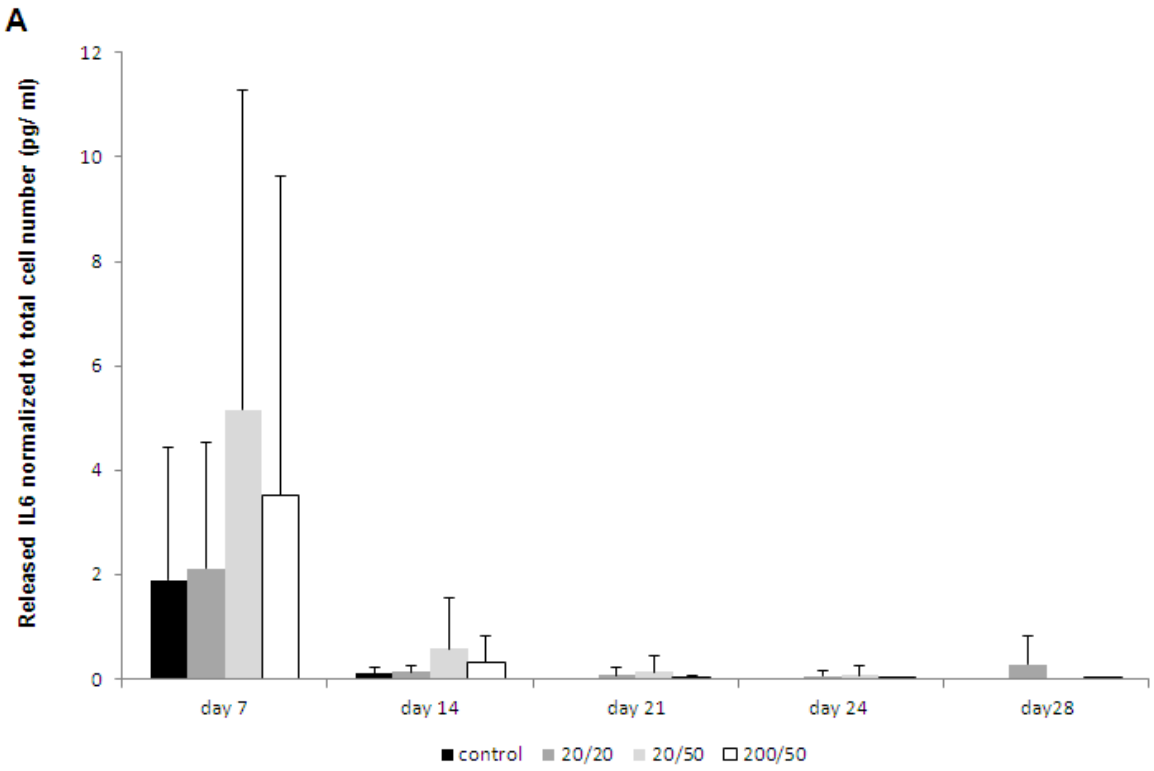

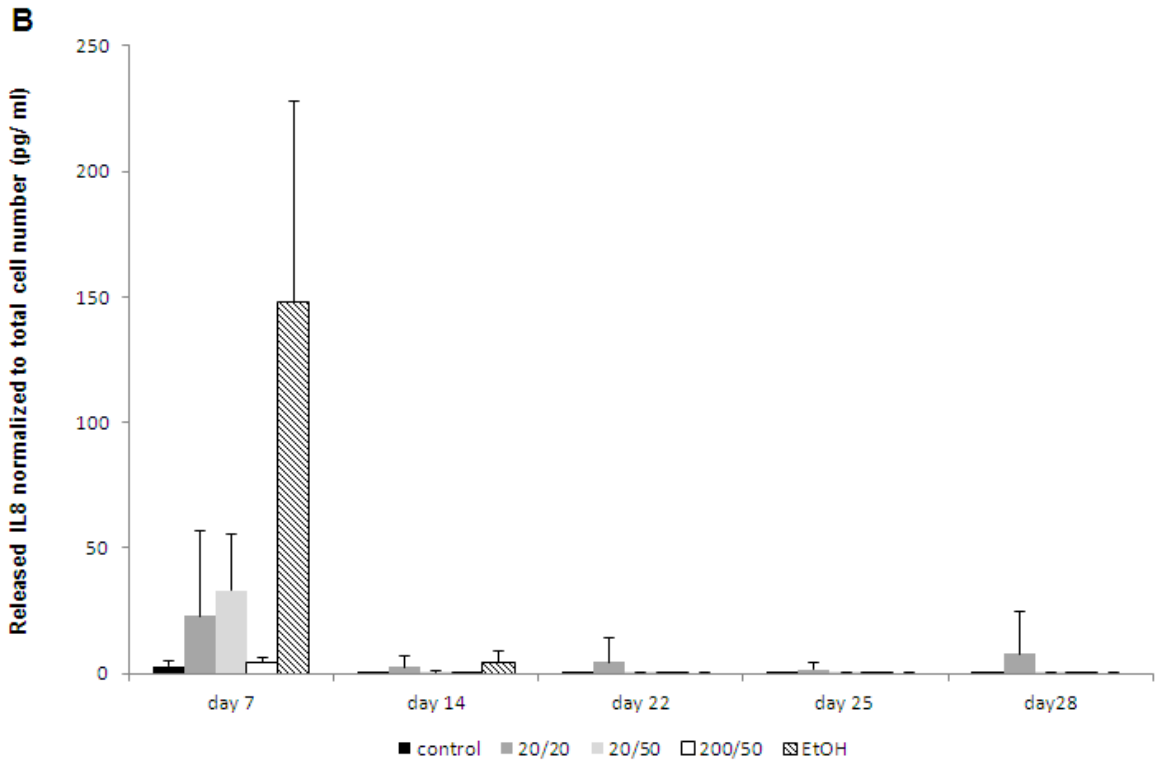

Figure 26. Release of IL6 and IL8 from CELLine cultures exposed to PPP 20 and PPP 200.

The amount of released IL6 (A) was lower compared to IL8 (B). 20/20: 20 µg / ml PPP 20; 20/50: 50 µg / ml PPP 20; 200/50: 50 µg / ml PPP 200. Mean ± SD are presented.

3.6.1.4 LDH-release in CELLine cultures

The highest amount of released LDH was noted at day 7. As expected, exposure to the positive control EtOH revealed the highest increase, followed by the exposure to 50 µg / ml PPP 20. Treatment with 20 µg / ml of PPP 20 and PPP 200, influenced the LDH-release in a similar pattern over the whole culturing period, except at day 28. At day 14 a similar dose- and size-dependent effect was determined even though the amounts of released LDH were lower (Figure 27).

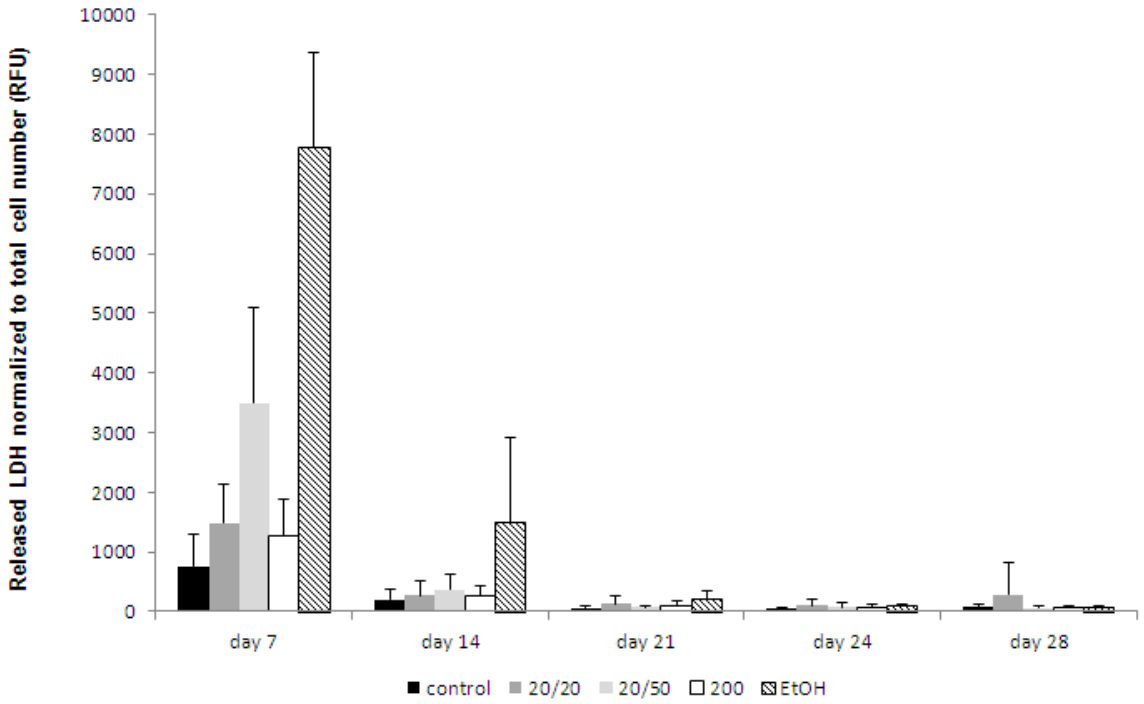

Figure 27. Release of LDH from CELLine cultures exposed to PPP 20 and PPP 200.

20/20: 20 µg / ml PPP 20; 20/50: 50 µg / ml PPP 20; 200/50: 50 µg / ml PPP 200. Mean ± SD are presented.

3.6.1.5 Intracellular localization of PPP

2 days after inoculation, some cells were found to contain R25 particles (Figure 28 A). However, after 7 days, the ratio between cells with and without internalized NPs was higher (Figure 28 B).

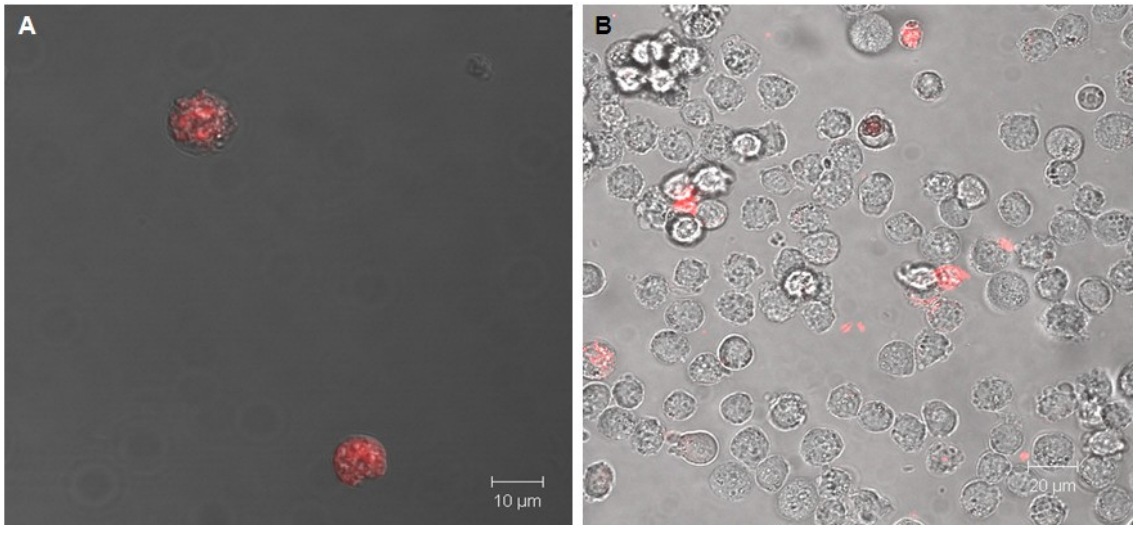

Figure 28. Internalization of R25 particles by THP-1 cells cultured in CELLine.

The ratio between cells which do or do not contain NPs decreases with longer culturing periods. Cells which did not internalize NPs, proliferate faster.

3.6.2 Modified conventional cell culture

3.6.2.1 Cellular effects of long-term exposure to NMs

Similar to CELLine cultures, the untreated cells reached high density already 5 days after inoculation. The maximum in cell numbers of approximately 140 x 10^6 cells per culture vessel was reached at the end of each experiment.

A slight reduction of the cell number by approximately 15% was detected in cells exposed to PPP 200. Moreover, in cells exposed to 50 µg / ml PPP 20 and 2% EtOH the proliferation was reduced by 92% and 95%, respectively. No changes were observed upon exposure to 20 µg / ml of PPP 20 (Figure 29 A).

THP-1 cells exposed to both, CNT4 and CNT5, showed no differences in cell proliferation (Figure 29 B).

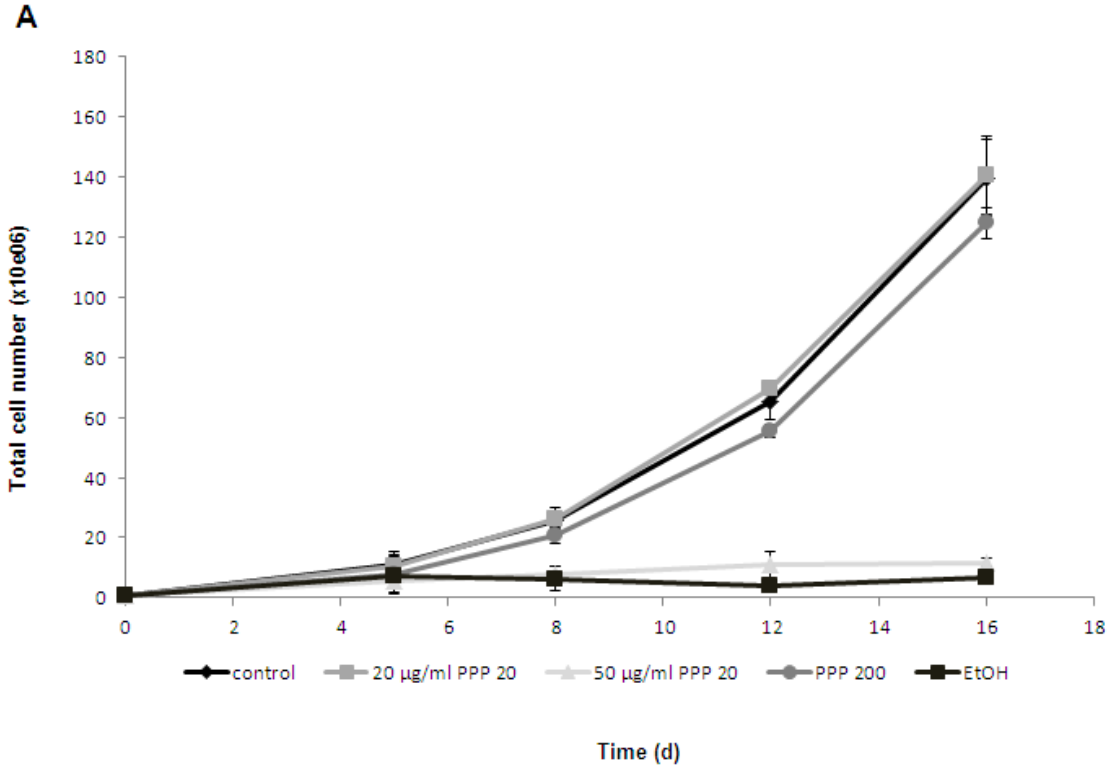

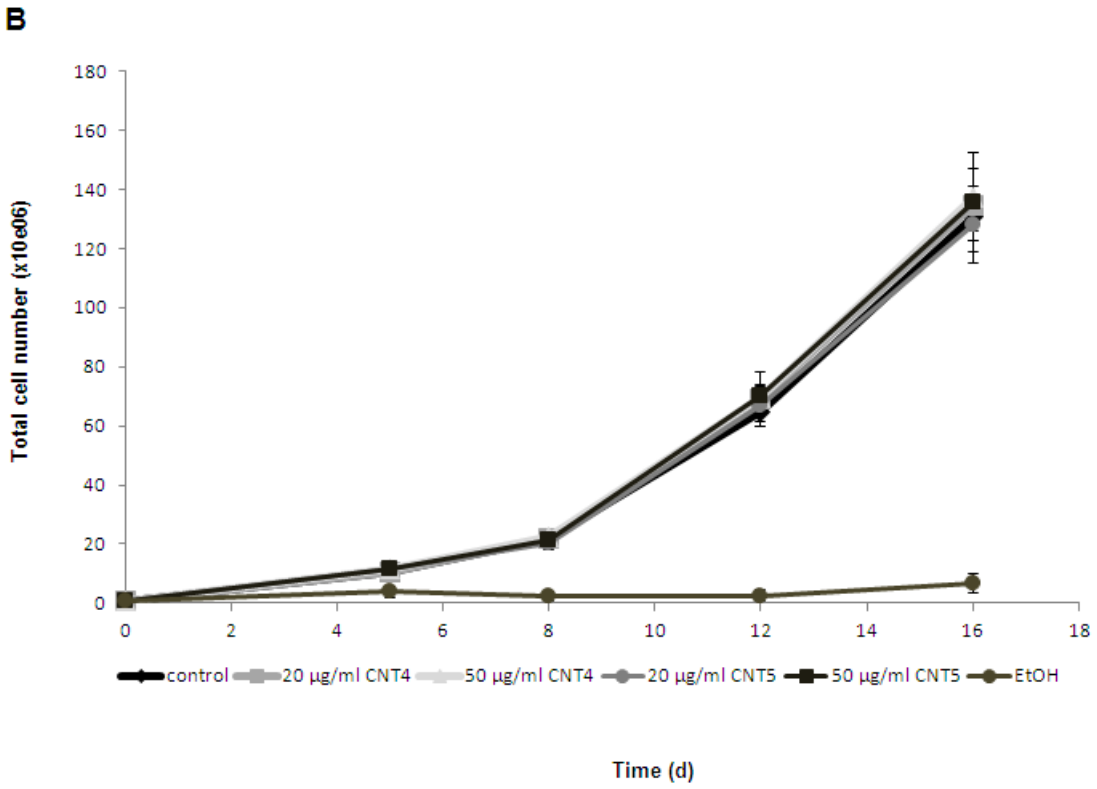

Figure 29. Changes in cell numbers of sub-cultured THP-1 cells exposed to PPP (A) and CNTs (B).

PPP affected cell proliferation in a dose- and size-dependent manner. CNTs did not influence cell numbers at any time-point. Mean ± SD are presented.

3.6.2.2 IL expression upon long-term exposure

The peak amount in released IL6 of untreated cells was detected 5 days after inoculation. With prolonged culture, it dropped by the half at each time-point. Strongest release of IL6 was induced by exposing the cells to 50 µg / ml of PPP 20 as well as to 2% EtOH. Lower concentrations of PPP 20 or larger PPP showed no obvious increase in IL6 at any time-point as compared to untreated controls (Figure 30 A).

A similar dose- and size-dependent effect was noticed for the release of IL8. Again, treatment with EtOH induced the highest release at day 5. However, at later time-points, the amount dropped. 5 days after exposure to PPP, only larger particles induced a 1.4-fold increase of IL8-release as compared to control cells. A

dose-dependent effect of PPP 20 was assessed at day 8 and all later time-points (Figure 30 B).

Similar to data on IL8, the release of IL1-ß following exposure to PPP showed a size-dependent effect at day 5, and a dose-dependent effect of PPP 20 at day 8 and all following time-points. Treatment with EtOH yielded again high amounts of released IL1-ß as compared to untreated cells (Figure 30 C).

Exposure to both types of CNTs induced no changes in the release of both, IL8 and IL1-ß. Only treatment with EtOH induced a strong release of both cytokines as compared to control cells with higher amounts detected for IL1-ß (Figure 31 A, B)

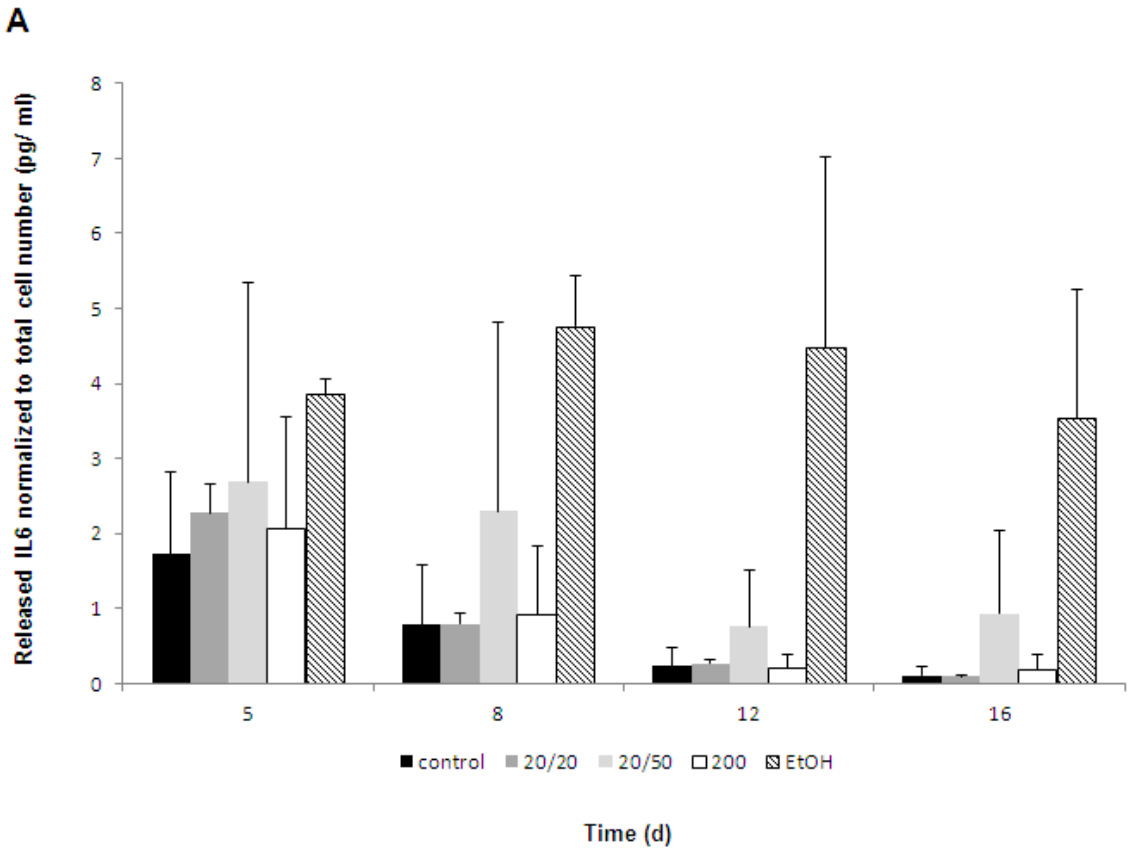

B

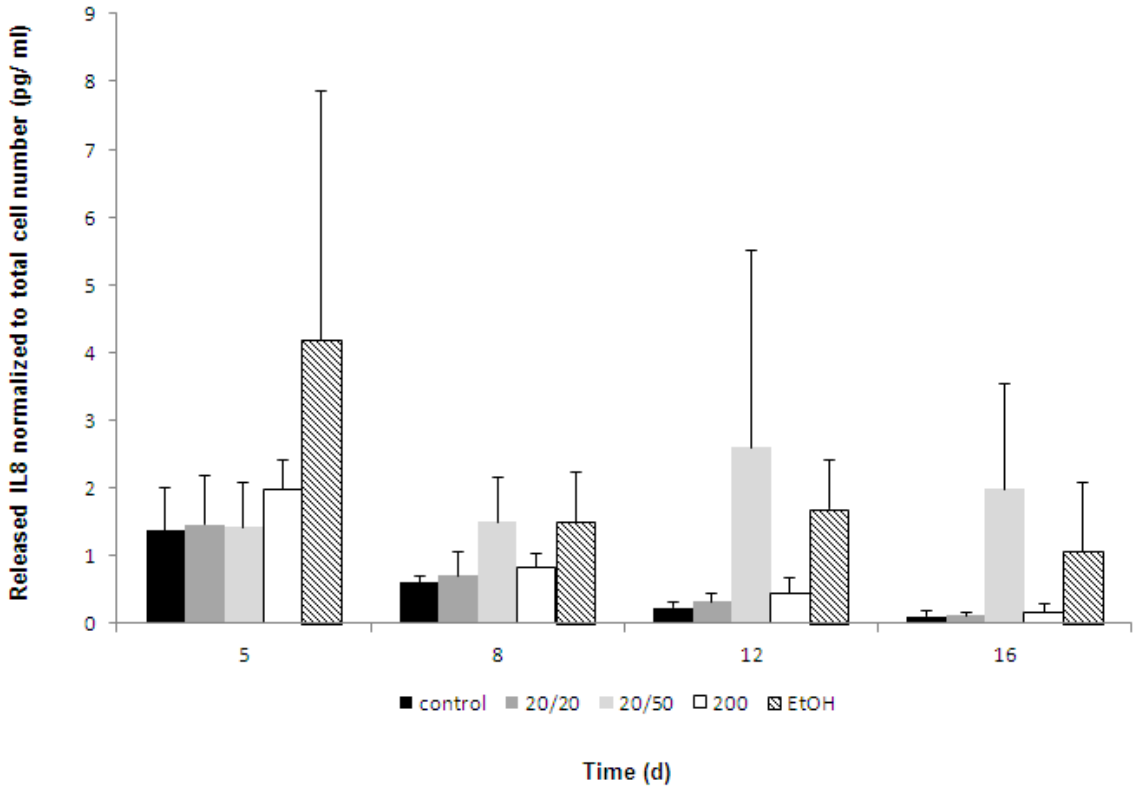
Released IL8 normalized to total cell number (pg/ ml)
9
8
7
6
5
4
3
2
1
0
5
8
12
16
control
20/20
20/50
200
EtOH
Time (d)

C

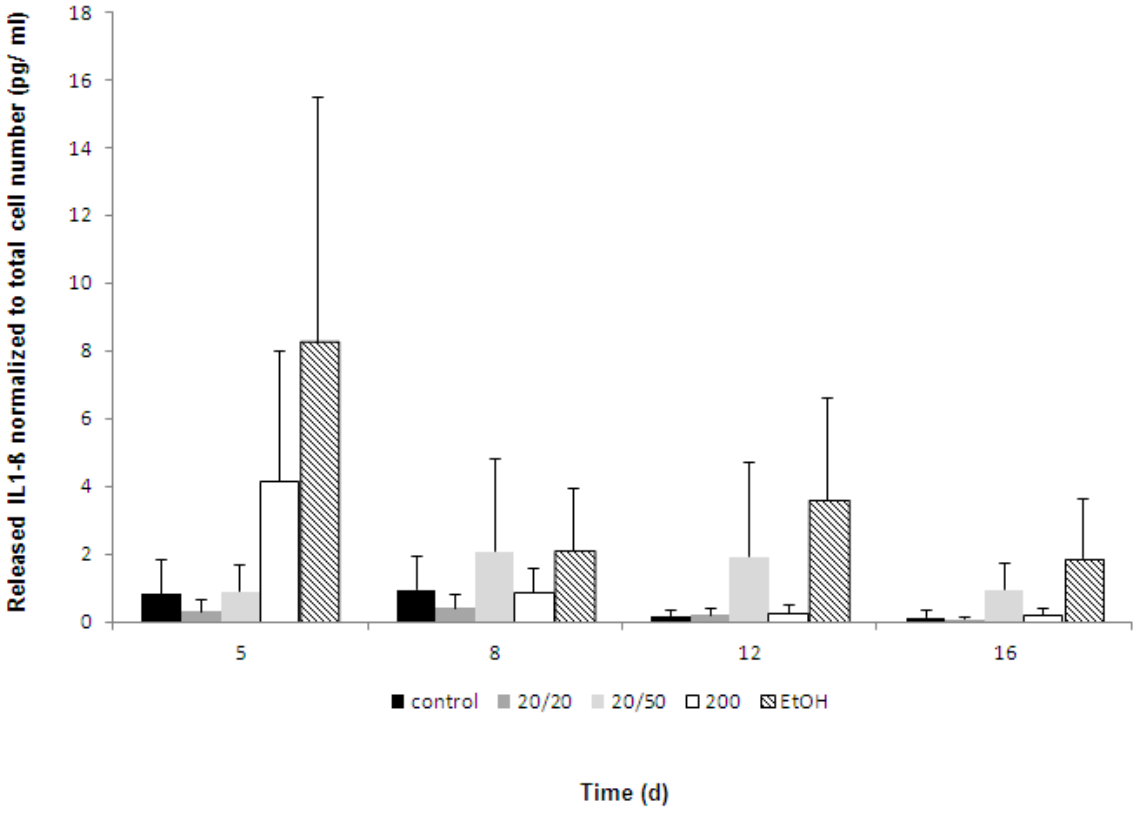
Released IL1-ß normalized to total cell number (pg/ ml)
18
16
14
12
10
8
6
4
2
0
5
8
12
16
control
20/20
20/50
200
EtOH
Time (d)

Figure 30. Release of IL6 (A), IL8 (B), and IL1-ß (C) upon long-term exposure to PPP.

20/20: 20 µg / ml PPP 20; 20/50: 50 µg / ml PPP 20; 200/50: 50 µg / ml PPP 200. Mean ± SD are presented.

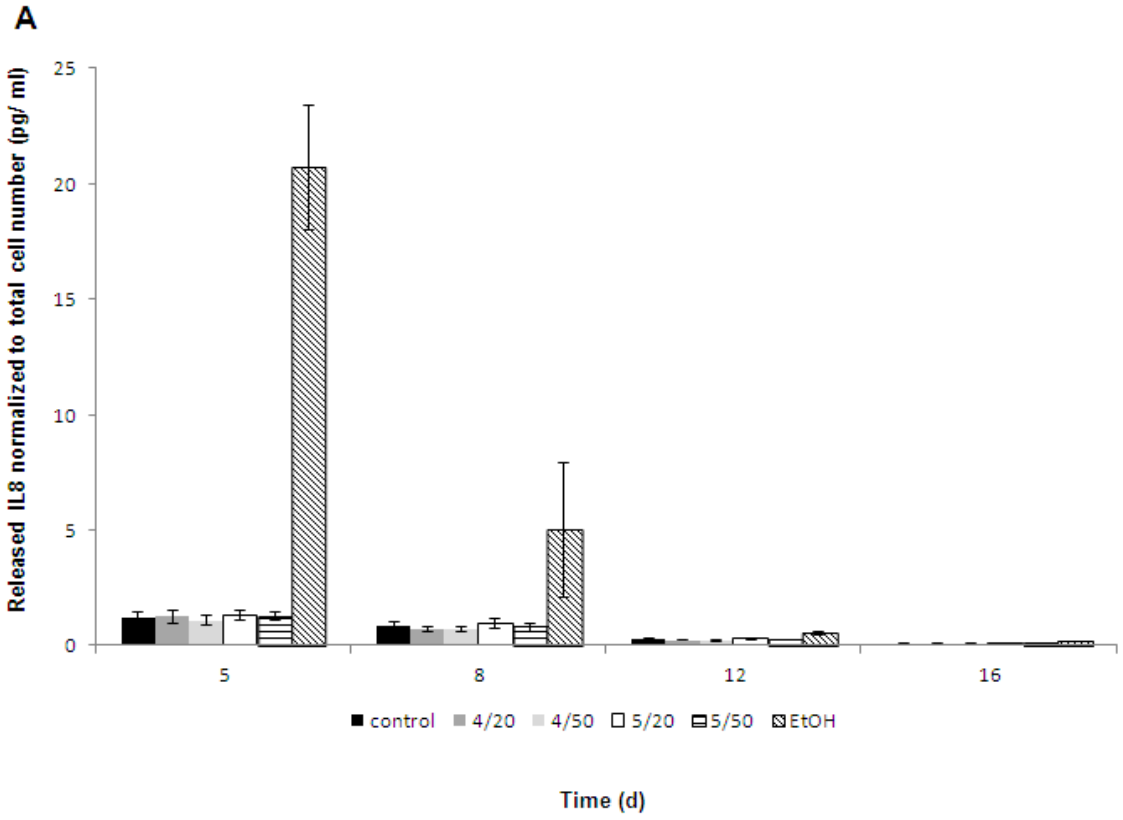

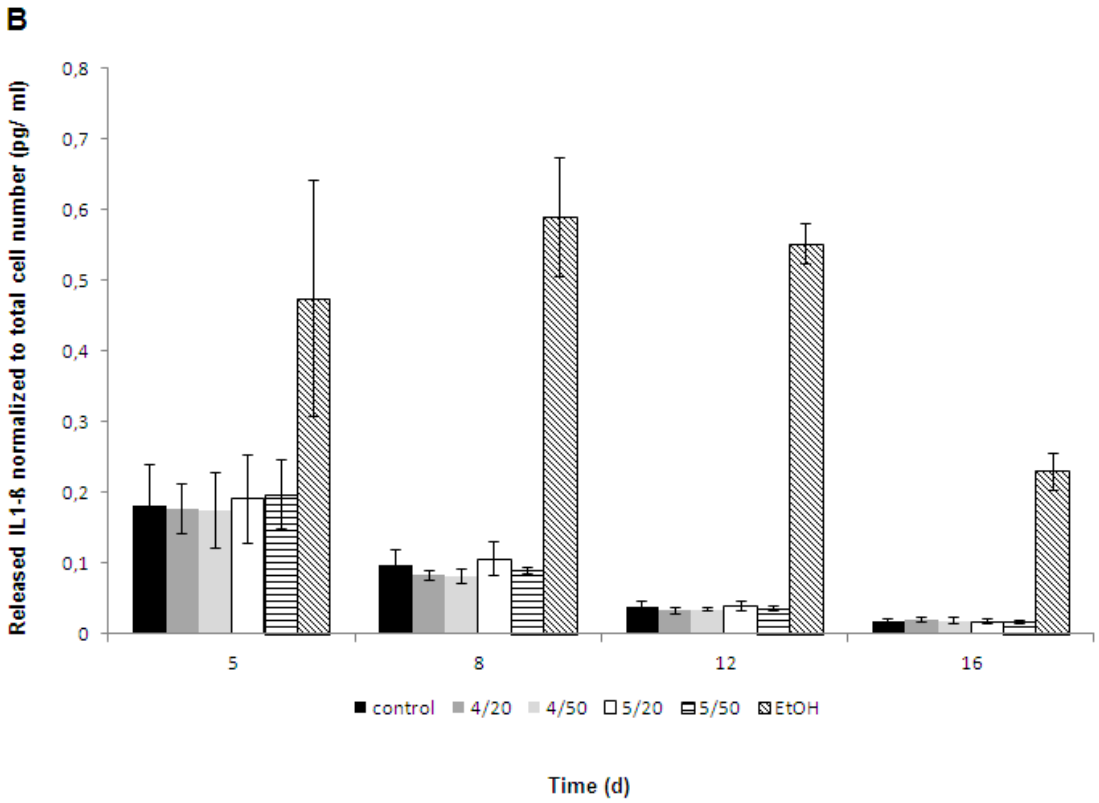

Figure 31. Release of IL8 (A) and IL1-ß (B) upon long-term exposure to CNTs.

4/20: 20 µg / ml CNT4; 4/50: 50 µg / ml CNT4; 5/20: 20 µg / ml CNT5; 5/50: 50 µg / ml CNT5. Mean ± SD are presented.

3.6.2.3 LDH-release in modified conventional cultures

The release of LDH corresponds to cell numbers at each time point: the lower the cell number, the higher was the amount of released LDH. The highest amount of released LDH was detected for EtOH treated cells. However, exposure to PPP resulted in a dose- and size-dependent pattern (Figure 32 A).

Exposure to CNTs induced no release of LDH at any time-point (Figure 32 B).

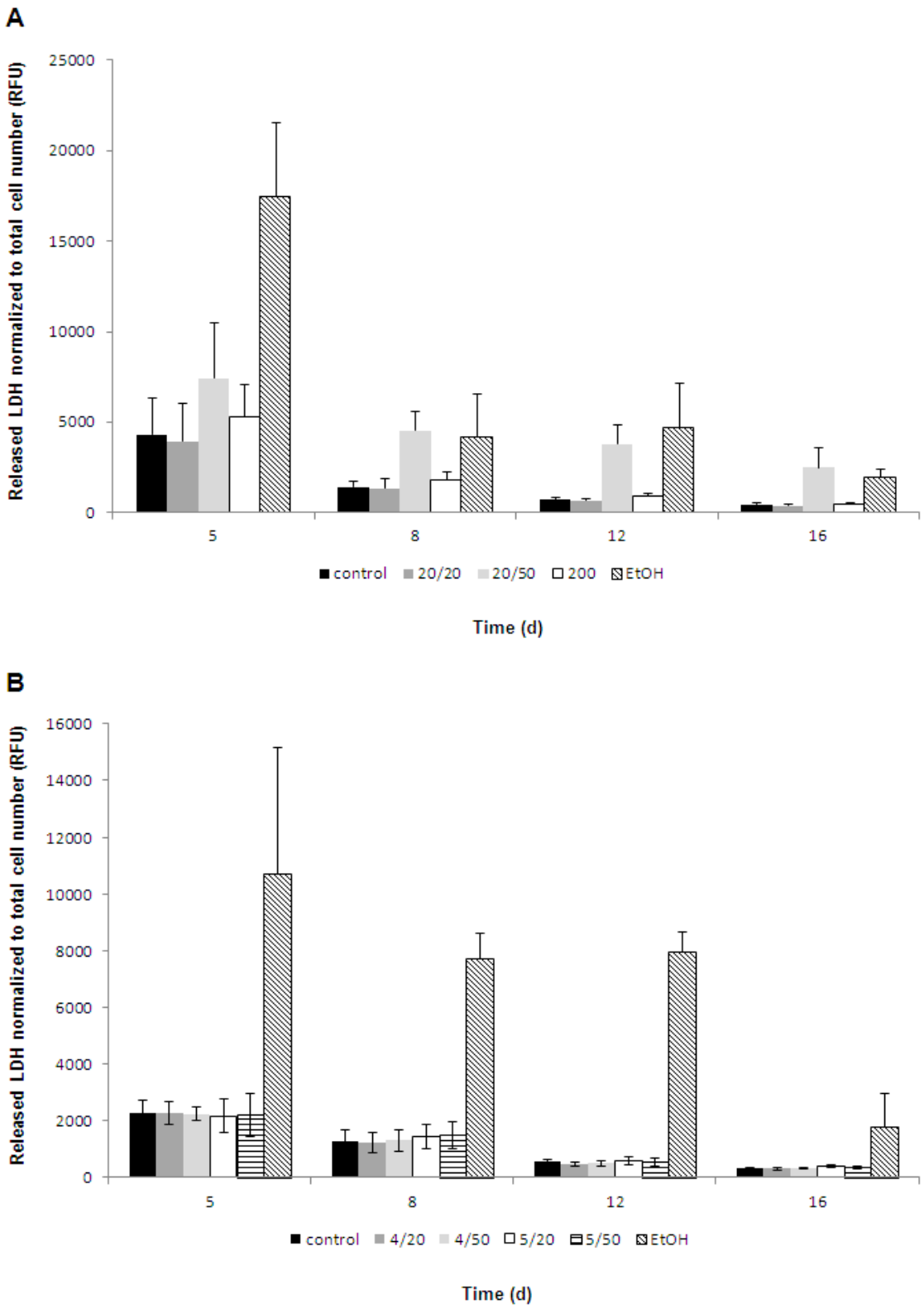

Figure 32. Cytotoxicity of PPP (A) and CNTs (B) to THP-1 cells upon long-term exposure.

20/20: 20 µg / ml PPP 20; 20/50: 50 µg / ml PPP 20; 200/50: 50 µg / ml PPP 200. 4/20: 20 µg / ml CNT4; 4/50: 50 µg / ml CNT4; 5/20: 20 µg / ml CNT5; 5/50: 50 µg / ml CNT5. Mean ± SD are presented.

The results of the long-term exposure of THP-1 cells is presented in Table xy.

	CELLine			
	cell number (x 10e06)			
Day	control	20 µg / ml PPP 20	50 µg / ml PPP 20	50 µg / ml PPP 200
7 - 8	16.9 ± 17.7	7.2 ± 5.7	4.0 ± 3.2	11.2 ± 10.0
14 - 16	223.4 ± 183.2	137.9 ± 128.4	103.9 ± 121.4	137.9 ± 116.4
	IL6 (pg / ml)			
7 - 8	1.9 ± 2.6	2.1 ± 2.4	5.2 ± 6.1	3.5 ± 6.1
14 - 16	0.1 ± 0.1	0.1 ± 0.1	0.6 ± 0.9	0.3 ± 0.5
	IL8 (pg / ml)			
7 - 8	2.9 ± 1.9	22.8 ± 34.1	33.0 ± 22.5	4.5 ± 1.7
14 - 16	0.2 ± 0.2	2.4 ± 4.5	0.6 ± 0.5	0.3 ± 0.2
	LDH (RFU)			
7 - 8	757.5 ± 533.0	1483.2 ± 645.0	3492.9 ± 1587.6	1265.2 ± 625.3
14 - 16	197.2 ± 165.6	271.8 ± 235.7	369.6 ± 250.3	265.6 ± 164.5

	Conventional culture			
	cell number (x 10e06)			
Day	control	20 µg / ml PPP 20	50 µg / ml PPP 20	50 µg / ml PPP 200
7 - 8	25.6 ± 4.2	25.9 ± 3.2	7.9 ± 2.6	20.6 ± 2.7
14 - 16	139.7 ± 12.7	140.5 ± 13.1	11.7 ± 1.4	124.7 ± 5.0
	IL6 (pg / ml)			
7 - 8	0.8 ± 0.8	0.8 ± 0.2	2.3 ± 2.5	0.9 ± 0.9
14 - 16	0.1 ± 0.1	0.1 ± 0.0	0.9 ± 1.1	0.2 ± 0.2
	IL8 (pg / ml)			
7 - 8	0.6 ± 0.1	0.7 ± 0.4	1.5 ± 0.7	0.8 ± 0.2
14 - 16	0.1 ± 0.1	0.1 ± 0.0	2.0 ± 1.6	0.2 ± 0.1
	LDH (RFU)			
7 - 8	1426.7 ± 340.1	1326.9 ± 516.3	4515.8 ± 1045.2	1816.3 ± 428.9
14 - 16	443.2 ± 77.0	372.5 ± 77.3	2495.9 ± 1112.4	449.1 ± 80.5

Changes > 25% of the control value
Changes > 50% of the control value
Changes > 75% of the control value

Table 9. Summary of the results on long-term exposure of THP-1 cells to PPP.

Mean ± SD are presented.

4. DISCUSSION

4.1 Effects on endothelial cells EAhy 926

One aim of this study was the establishment of a suitable system to investigate long-term cellular effects of NMs on endothelial cells. The bench-top bioreactor and incubator hybrid BioLevitator^{TM} was used for the identification of potential chronic effects of NPs on endothelial cells EAhy 926, and was compared to conventional cell culture. This system enabled the culture of viable cells to high densities and identified adverse cellular effects of PPP 20 and of > 50 nm CNT-COOH.

A microcarrier cell culture system enables cell culturing at higher cell densities for a longer time-period. The polarized cell growth, in a more physiologic environment than in conventional cell culture vessels, allows a better differentiation of the cells. The mimicked *in vivo* situation slows down proliferation and therefore the nutrients are depleted more slowly. In addition, due to their structure, the porous microcarrier facilitates long-term cell culturing as the nutrients from the medium and the molecules secreted from the cells (e.g. growth factors) are retained inside the beads. Due to the small volume of medium required to feed the cells over the entire culturing period compared to conventional cell culture methods, it is a very cost- and material-saving method.

Bioreactors were initially developed to increase the yield of cellular products (e.g. antibodies) (Xiao *et al*., 1999). This culture method may also be suitable for toxicity testing and / or the identification of long-term effects. This is particularly important for NPs because they have been shown to persist in organisms (Wu *et al*., 2009), and are influenced by several factors, such as medium composition, binding of proteins, mechanical pre-treatment, and pH, which makes it very laborious to evaluate all these parameters *in vivo*.

The endothelial cells EAhy 926 can be exposed to relatively high concentrations (100 µg/ ml) of 20 nm PPP for 24 hours without showing any apparent damage in a conventional culture. In microcarrier cultures, the resistance to the toxic action of PPP is even higher. Two mechanisms could be suggested that may explain the lower cytotoxicity of PPP in microcarrier culture: (I) a more physiological growth

with a better supply of nutrients, and (II) the fact that a smaller area of the cell membrane is accessible to the NPs because cells are more densely packed (Lee *et al*., 2009).

Upon longer incubation times, however, the situation is inversed. The low concentrations of the NPs did not have a strong influence on the proliferation of cells maintained in conventional cell culture, but pronounced cytotoxicity was detected in the microcarrier culture. This difference may be caused by a higher dilution of the intracellular concentration of NPs due to proliferation. Our experiments demonstrated very clearly that the doubling rate of EAhy 926 cells in conventional culture was 2.3 times higher than in the microcarrier culture.

At concentrations higher than 100 µg / ml, 20 nm PPP decreased the metabolic activity of the cells in conventional culture and induced the activation of effector caspases 3 and 7. In addition, an increased release of LDH, as an indicator of membrane damage, was also observed after exposure to these doses of PPP for 24 hours. Particles of 200 nm did not exert any effect upon culturing under the same conditions.

Upon acute exposure, the main modes of PPP induced cell death were found to be apoptosis and necrosis. In 2009, Fröhlich *et al*. investigated the impacts of 20 nm carboxylated polystyrene (CPS) NPs in the same cell line, grown in conventional cell culture for 24 hours, which also demonstrated induction of necrosis and apoptosis. This similarity between 20 nm CPS and 20 nm PPP may be linked to their similar physicochemical parameters: the differences in size [42 nm (CPS) vs. 73 nm (PPP)] were small and the surface charge of both particles was slightly negative.

Upon prolonged exposure to PPP in microcarrier cultures, not only the LDH release was increased as compared to controls, but also the activation of caspases. However, it is very unlikely that both modes of cell death are induced at the same time. The contradictory findings on caspase activation (Figure 21 A) could be explained by the normalization of very small differences in assay values (caspase 3 / 7) between untreated and treated cells versus larger differences in total cell numbers of the respective culture. Moreover, all other data supported the induction of necrosis as the predominant mode of action of PPP 20 upon long-term exposure. Collectively, we detected no induction of apoptosis and only low induction of necrosis at each time-point in cells exposed to 20 µg / ml of PPP 20.

As both cell death mechanisms should occur within 24 hours (van Nieuwenhuijze *et al*., 2003), we presume that the reduction in cell numbers observed upon long-term exposure was also caused by the decreased cell proliferation in the BioLevitator^{TM}. The lower doubling rate of the cells in microcarrier cultures promotes the accumulation of NPs.

The BioLevitator^{TM} bioreactor used in this study, also appears suitable for the assessment of biological effects upon exposure to other NMs. CNTs could find broad medical application, particularly in imaging and treatment (vaccination, hyperthermia) provided they are not overtly toxic (Turnherr *et al*., 2011). Long-term exposure to CNT-COOH in the microcarrier culture showed a dose-dependent decrease in cell numbers after 7 days. With prolonged contact the cell populations recovered. These findings were supported by our data on the mode of action since the peak levels of induction of apoptosis and/ or necrosis were also detected at day 7. At later time-points, activation of caspases or a notable release of LDH was not detected. However, no differences in any outcome were noted when cells were exposed to pristine CNTs of the same size.

The BioLevitator^{TM} bioreactor may also be used for the toxicological assessment of conventional compounds. The action of drugs on CYP enzymes is important for the metabolization by hepatocytes. Testing is complicated by the fact that CYP enzyme activities are low or absent not only in hepatocyte cell lines but also in cultured primary hepatocytes (Guillouzo *et al*., 2007). In preliminary experiments on HepG2 cells growing on microcarriers, we observed very high cell density and a higher activity of the enzyme CYP1A1, important for many pathways (e.g. steroid hormone biosynthesis, tryptophan metabolism, retinol metabolism, metabolism of xenobiotics, and metabolic pathways) (data not shown). Findings on HepG2 cells grown in a 3 dimensional cell culture and the advantage of that culturing method were described in many other studies (Bokhari *et al*., 2007; Li *et al*., 2008). Long-term culture in the BioLevitator^{TM} may therefore also be suitable to evaluate certain aspects of metabolization by hepatocytes.

Similar to HepG2 cells, H295R cells, which are used as an *in vitro* model for testing endocrine disruption chemicals, were employed to investigate the potential effects of 20 nm PPP on the aromatase activity of the CYP1A1 enzyme. Here, too, an increase of the enzyme activity was detected in microcarrier cultures as compared to conventional approaches. The similarity of both cell types may be

further supported by their growth characteristics. Both cell types are growing as a monolayer in conventional cultures. In the BioLevitator™, the cells were overgrowing each other, thus leading to pronounced increases in cell densities. However, no differences in cell number were detected in H295R cells upon exposure to NPs at all time-points. In contrast, EAhy 926 cells grow in a monolayer, irrespective of the culturing approach. In addition, a pronounced decrease of cell numbers in exposed cultures was observed already at day 7. This variation in the responses of different cells upon the exposure to the same concentration of the same NPs might be explained by the fact that the BioLevitator™ system supports the growth characteristics of the individual cell type. In a monolayer, all cells are accessible to the NPs. However, when cells grow multi-layered, only the layer on the top is accessible to NMs, while the layers in the deep may be protected. Therefore, there are no changes in cell numbers when exposing multi-layered cultures to NMs or other chemicals.

The GEM™ technology and the BioLevitator™ allowed the culture of viable cells with high reproducibility. As expected, the physiological growth on basal membrane or collagen type IV coated microcarriers slowed down the proliferation rate of EAhy 926 cells, which is advantageous for the study of NP accumulation. However, one potential limitation of the system is that high-throughput testing is not possible because only four experiments can be performed in a single bioreactor. Moreover, it is a barely adequate approach to investigate the interaction between different anchorage-dependent cell types. Therefore, the investigation of long-term effects *in vivo* will remain unavoidable.

4.2 Effects on monocytes THP-1

The second important question that should be answered was the determination of cellular effects in monocytes upon exposure to NPs. In order to investigate long-term cellular effects on THP-1 cells, the two-chamber bioreactor CELLine was used. CELLine bioreactors are used for a rapid production (within few days) of high amount of biological products (e. g. antibodies). Since cytotoxicity studies using CELLine bioreactors were not performed before, its suitability was evaluated in this study. The findings were compared to data from conventional cell culture approaches.

Upon short-term exposure of THP-1 cells to PPP 20, the metabolic activity of the cells decreased in a dose-dependent manner. In contrast to adherent growing cells (EAhy 926), even PPP 200 diminished the cell viability. Similar findings were observed when applying CPS (Fröhlich *et al*., 2012). The authors could show that smaller CPS excerted cytotoxicity in all tested cell lines, while larger CPS (≥ 200 nm) acted cytotoxic only in phagocytic cells. Interestingly, Lankoff *et al*. (2012) have demonstrated that THP-1 cells were more resistant to metal NMs of different sizes compared to adherent growing cells. This contradiction could be explained by the employed materials.

Following exposure to different allergens and NPs, immune cells and cell lines (e.g. peripheral blood monocytes, THP-1 cells, macrophages) produce pro-inflammatory cytokines such as IL1-ß, IL8, TNFα, IL6, etc. (Yang *et al*., 2012; Hanley *et al*., 2009; Cachinho *et al*., 2013; Segat *et al*., 2011; Miyazawa *et al*., 2007; Chang, 2010; Lucarelli *et al*., 2004). Moreover, also anti-inflammatory cytokines (IL10) may be released from exposed cells (Pollice *et al*., 1998). Interestingly, Kim *et al*. (2007) could show no release in IL1-ß while other cytokines, such as IL6, TNF-α, were detected upon exposure of THP-1 cells to titanium particles and discs.

Here, we demonstrate that upon short-term exposure to PPP, the production of IL6 but not IL8 was induced. In 2011, Park *et al*. demonstrated a size-dependent effect in the release of cytokines (TNF-α, IL6, IL10, etc.) in RAW 264.7 murine macrophages upon exposure to different sizes of silver NPs. The authors could show that all cytokines except IL10 were induced by 20 nm NPs. Interestingly, in our study only the release of IL8 but not of IL6 was induced by exposing the cells

to PPP 20. Addition of LPS could increase the amount of the released cytokines. Similar results were obtained by Morishige *et al*. (2010) after exposing PMA-primed macrophage-like THP-1 cells to nano-TiO_2. Treatment of LPS-primed RAW 264.7 macrophages with silica NPs also induced the release of IL1-ß (Sandberg *et al*., 2012). However, the release of both IL was decreased upon combined treatment with LPS and PPP compared to subsequent exposure. These findings could suggest that PPP adsorb LPS. This NP-LPS conjugation may induce apoptosis in cells (Ashwood *et al*., 2007) which could explain the lower amounts of released cytokines.

Long-term cell culturing in CELLine yielded unreliable findings. The proper cell density for inoculation was identified in a pilot experiment. However, not only exposed, but also untreated cells behaved differently at each assay. At the early period (up to 21 days), exposure to PPP resulted to a dose- and size-dependent decrease in cell proliferation. At later time-points, almost no differences were detected, suggesting growth inhibition by high cell densities in the controls, an effect that had been observed for other cell lines (Schumpp and Schlaeger, 1990). These variations could be explained by the fact that only a few cells actually ingested NPs. Hence, no alteration in cell proliferation was expected. In 2011, Lunov *et al*. demonstrated the uptake of functionalized polystyrene particles of 100 nm by naïve THP-1 cells which occurred via dynamin II-dependent endocytosis. However, the amount of internalized NPs was 4 times lower as compared to macrophages. In addition, the age of the cells applied in each CELLine bioreactor, was a crucial factor of each experiment. Older cells showed an impaired proliferation and stopped growing much earlier than cells of earlier passages (data not shown).

Exposed CELLine cultures also showed a dose- and size-dependent increase in the release of the pro-inflammatory cytokine IL6. Release of the chemokine IL8 was only induced by PPP 20 in a dose-dependent manner. Usually, the production of IL6 from exposed cells was very low as compared to the secretion of IL8 or IL1-ß. Additionally, cytotoxicity, detected by the release of LDH, was induced in a similar manner, suggesting that the measured IL levels might be caused by cell damage. Moreover, the decreased cell numbers of exposed cells to PPP 20 was clearly linked to an increased release of LDH.

In contrast, exposure of THP-1 cells in conventional cultures identified severe effects upon treatment with PPP. Exposure to lower concentrations of PPP 20 did not affect the cells. However, treatment with 50 µg / ml of PPP 20 induced a tremendous decrease in cell numbers and cell viability as compared to untreated controls. Similar effects were detected upon treating THP-1 cells with ethanol. Exposure to PPP 200 induced a slight decrease in cell numbers, but did not alter cell viability.

The amount of released markers of cytotoxicity and inflammation following treatment of conventional cultures with 50 µg / ml PPP 20 and ethanol increased with prolonged exposure. However, no changes were observed upon treatment with 20 µg / ml of PPP 20. PPP 200 induced a 4-fold increased in the production of IL1-ß as well as a slight increase in other markers at day 5. These findings suggest that long-term exposure to higher concentrations of PPP 20 and PPP 200 induce inflammatory responses in THP-1 cells, and led to necrotic cell death.

Long-term exposure to CNTs did not influence the cells at any time-point. No induction of cytotoxicity or inflammatory response to CNTs was detected. These data are also supported by Brown *et al*. (2010) who investigated the effects of MWCNTs of different lengths and sizes on THP-1 cells. Upon short-term exposure, the authors could show an increase in the production of IL1-ß following treatment with long but not with short CNTs. They suggested oxidative stress as a crucial mechanism. Our findings suggest that short CNTs are less toxic as compared to polystyrene NPs. This would make them suitable for the application in various biomedical and other day-to-day products. Nevertheless, our findings have to be confirmed by other investigators first.

In both long-term culturing approaches, EtOH was used as a positive control. In sub-cultured cells, EtOH induced cytotoxicity already after one week of exposure. Chronic exposure to EtOH may induce an increase in reactive oxygen and nitrogen species which might shift the balance between pro- and anti-apoptotic factors. This could further lead to increased cell death in hepatocytes (Bailey, 2003; Venkatraman *et al*., 2003). In CELLine cultures, however, only the cell numbers decreased compared to the untreated controls. No changes in cell viability could be detected at any time-point. The adaptation of cells to EtOH could be confirmed by many other studies which were conducted in order to investigate the effect of chronic EtOH exposure on different cell types. Han *et al*. (2012)

suggested mitochondrial plasticity in the liver to be an adaptive response to the metabolic stress caused by EtOH. In addition, neuronal cells have been reported previously to show an adaptation to EtOH exposure (Vagts *et al*., 2003; Guo *et al*., 2012).

Overall, the conventional approach was identified to be more suitable to investigate the long-term effects of NPs on monocytes. It allowed the culture of viable cells with high reproducibility. Cellular effects upon repeated exposure could get evaluated easier than in CELLine cultures. Moreover, it is a less expensive and a less material consuming method compared to CELLine bioreactors. However, one limitation of this approach could be the extended risk of missing the potential growth inhibition of untreated controls. Thereby, toxic effects of NPs may be underestimated.

4.3 Conclusions and outlook

In conclusion, our findings could show that repeated exposure to NPs may alter different cell functions such as cell proliferation and cell viability. The study demonstrated that PPP could be used as model particles in order to investigate accumulation of NPs in human cells. PPP affected both cell types in a dose- and size-dependent manner. Reduction in cell numbers was accompanied by release of LDH suggesting necrosis to be the main mode of cytotoxic action. In addition, PPP induced inflammatory responses in THP-1 cells.
In contrast to PPP, CNTs seemed to be less toxic to both cell types. In microcarrier cultures, only CNT-COOH induced a decrease in cell numbers. This indicated that the surface functionalization of NPs is an important physicochemical property and plays a crucial role in particle toxicity. In THP-1 cells, no alterations in different cell functions were detected upon exposure to both, plain and carboxylated CNTs. These findings implicate short MWCNTs to be well-tolerated by human cells.

However, data suggest that assays on monocultures of THP-1 cells may lead to false negative results as compared to co-cultures of monocytes and endothelial cells (Liu *et al*., 2012). Future studies should consider the use of co-cultures of THP-1 and EAhy 926 cells. For this task, the BioLevitator™ system would be an ideally suitable approach – the endothelial cells which grow on microcarriers could be easily co-cultured with monocytes in one LeviTube™.

5. REFERENCES

Abdelmoez A. A., Thurner G. C., Wallnöfer E. A., Klammsteiner M., Kremser C., Talasz H., Mrakovcic M., Fröhlich E., Jaschke W., and Debagge P. (2010) Albumin-based nanoparticles as magnetic resonance contrast agents: II. Physicochemical characterization of purified and standardised nanoparticles. Histochem Cell Biol 134(2); 171 – 196

Ai J., Biazar E., Jafarpour M., Montazeri M., Majdi A., Aminifard S., Zafari M., Akbari H. R., and Rad H. G. (2011) Nanotoxicology and nanoparticle safety in biomedical designs. Int J Nanomedicine 6; 1117 – 1127

Alexis F., Rhee J. W., Richie J. P., Radovic-Moreno A. F., Langer R., and Farokhzad O. C. (2008) New frontiers in nanotechnology for cancer treatment. Urol Oncol 26(1); 74 – 85

Alves P. M., Moreira J. L., Rodrigues J. M., Aunins J. G., and Carrondo J. M. T. (1996) Two-dimensional versus three-dimensional culture systems: Effects on growth and productivity of BHK cells. Biotechnol. Bioeng. 52; 429 - 432

Arora S., Rajwade J. M., and Paknikar K., M. (2012) Nanotoxicology and in vitro studies: the need of the hour. Toxicol Appl Pharmacol 258; 151 – 165

Ashwood P., Thompson R. P. H., and Powell J. J. (2007) Fine particles that adsorb lipopolysaccharide via bridging calcium cations may mimic bacterial pathogenicity towards cells. Exp Biol Med 232; 107 – 117

Bailey S. M. (2003) A review of the role of reactive oxygen and nitrogen species in alcohol-induced mitochondrial dysfunction. Free Radic Res 37(6); 585 – 596

Baktur R., Patel H., and Kwon S. (2011) Effect of exposure conditions on SWCNT-induced inflammatory response in human alveolar epithelial cells. Toxicol In Vitro 25(5); 1153 – 1160

Becker H., Herzberg F., Schulte A., and Kolossa-Gehring M. (2011) The carcinogenic potential of nanomaterials, their release from products and options for regulating them. Int J Hygiene Environ Health 214; 231 – 238

Bexiga M. G., Varela J. A., Wang F., Fenaroli F., Salvati A., Lynch I., Simpson J. C., and Dawson K. A. (2011) Cationic nanoparticles induce caspase 3-, 7- and 9-mediated cytotoxicity in a human astrocytoma cell line. Nanotoxicology 5(4); 557 – 567

Bhattacharya R. and Mukherjee P. (2008) Biological properties of “naked” metal nanoparticles. Adv Drug Deliv Rev 60; 1289 – 1306

Block S. M., Asbury C. L., Shaewitz J. W., and Lang M. J. (2003) Probing the kinesin reaction cycle with a 2D optical force clamp. Proc Natl Acad Sci USA 100; 2351 – 2356

Bokhari, M., Carnachan, R. J., Cameron, N. R., and Przyborski, S. A. (2007) Culture of HepG2 liver cells on three dimensional polystyrene scaffolds enhances cell structure and function during toxicological challenge. J Anat 211, 567 – 576

Borm P. J. A., Robbins D., Haubold S., Kuhlbusch T., Fissan H., Donaldson K., Schins R., Stone V., Kreyling W., Lademann J., Krutmann J., Warheit D., and Oberdörster E. (2006) The potential risk of nanomaterials: a review carried out for ECETOC. Part Fibre Toxicol 3; 1 – 45

Brown D. M., Donaldson K., and Stone V. (2010) Nuclear translocation of Nrf2 and expression of antioxidant defence genes in THP-1 cells exposed to carbon nanotubes. J Biomed Nanotechnol 6(3); 224 – 233

Bruchez M. Jr., Moronne M., Gin P., Weiss S., and Alivisatos A. P. (1998) Semiconductor nanocrystals as fluorescent biological labels. Science 281(5385); 2013 – 2016

Butler, M., Burgener, A., Patrick, M., Berry, M., Moffatt, D., Huzel, N., Barnabé, N., and Coombs, K. (2000) Application of a serum-free medium for the growth of Vero cells and the production of reovirus. Biotechnol. Prog. 16; 854 – 858

Cachino S. C. P., Pu F., and Hunt J. A. (2013) Cytokine secretion from human peripheral blood mononuclear cells cultured in vitro with metal particles. J Biomed Mater Res Part A 101A; 1201 – 1209

Cardinal J., Klune J. R., Chory E., Jeyabalan G., Kanzius J. S., Nalesnik M., and Geller D. A. (2008) Noninvasive radiofrequency ablation of cancer targeted by gold nanoparticles. Surgery 144(2); 125 – 132

Chan W. C., Maxwell D. J., Gao X., Bailey R. E., Han M., and Nie S. (2002) Luminescent quantum dots for multiplexed biological detection and imaging. Curr Opin Biotechnol 13(1); 40 – 46

Chang C. (2010) The immune effects of naturally occurring and synthetic nanoparticles. J Autoimmun 34(3); 234 – 246

Chang M. Y., Shiau A. L., Chen Y. H., Chang C. J., Chen H. H., and Wu C. L. (2008) Increased apoptotic potential and dose-enhancing effect of gold nanoparticles in combination with single-dose clinical electron beams on tumor-bearing mice. Cancer Sci 99(7); 1479 – 1484

Chithrani B. D., Ghazani A. A., and Chan W. C. W. (2006) Determining the size and shape dependence of gold nanoparticle uptake into mammalian cells. Nano Lett 4; 662 – 668

Clift M. J., Bhattacharjee S., Brown D. M., and Stone V. (2010) The effects of serum on the toxicity of manufactured nanoparticles. Toxicol Lett 198(3); 358 – 365

Coles G. V. (1992) Occupational risks. Nature 359; 99

De Jong W. H. and Borm P. J. (2008) Drug delivery and nanoparticles: applications and hazards. Int J Nanomedicine 3(2); 133 – 149

De la Zerda A., Zavaleta C., Keren S., Vaithilingam S., Bodapati S., Liu Z., Levi J., Smith B. R., Ma T. J., and Oralkan O (2008) Carbon nanotubes as photoacoustic molecular imaging agents in living mice. Nat Nanotechnol 3(9); 557 – 562

Dockery D. W., Pope C. A. 3rd, Xu X., Spengler J. D., Ware J. H., Fay M. E., Ferris B. G. Jr, and Speizer F. E. (1993) An association between air pollution and mortality in six U.S. cities. N Engl J Med 329; 1753 – 1759

Donaldson K., Stone V., Tran C. L., Kreyling W., and Borm P. J. A. (2004) Nanotoxicology. Occup Environ Med 61; 727 – 728

Donaldson K., Aitken R., Tran L., Stone V., Duffin R., Forrest G., and Alexander A. (2006) Carbon nanotubes: A review of their properties in relation to pulmonary toxicology and workplace safety. Toxicol Sci 92(1); 5 – 22

Edgell, C. S., McDonald, C. C., and Graham, J. B. (1983) Permanent cell line expressing human factor VIII-related antigen established by hybridization. Proc. Natl. Acad. Sci. USA 80; 3734 – 3737

Elder A., Gelein R., Silvia V., Feikert T., Opanashuk L., Carter J., Potter R., Maynard A., Ito Y., Finkelstein J., and Oberdörster G. (2006) Translocation of inhaled ultrafine manganese oxide particles to the central nervous system. Environ Health Perspect 114; 1172 – 1178

Fadeel B. and Garcia-Bennett A. E. (2010) Better safe than sorry: understanding the toxicological properties of inorganic nanoparticles manufactured for biomedical applications. Adv Drug Deliv Rev 62; 362 – 374

Ferin J., Oberdörster G., Penney D., Sonderholm S., Gelein R. M., et al. (1990) Increased pulmonary toxicity of ultrafine particles. 1. Particle clearance, translocation, morphology. J Aerosol Sci 21; 381 – 384

Fiorito S., Serafino A., Andreola F., and Bernier P. (2006) Effects of fullerenes and single-wall carbon nanotubes on murine and human macrophages. Carbon 44(6); 1100 – 1105

Fröhlich, E., Samberger, C., Kueznik, T., Absenger, M., Roblegg, E., Zimmer, A., and Pieber, T. R. (2009) Cytotoxicity of nanoparticles independent from oxidative stress. J Toxicol Sci 34(4), 363 – 375

Fröhlich E., Kueznik T., Samberger C., Roblegg E., Wrighton C., and Pieber T. R. (2010) Size-dependent effects of nanoparticles on the activity of cytochrome P450 isoenzymes. Toxicol Appl Pharmacol 242; 326 – 332

Fröhlich E., Meindl C., Roblegg E., Griesbacher A., and Pieber T. R. (2012) Cytotoxicity of nanoparticles is influenced by size, proliferation and embryonic origin oft he cells used for testing. Nanotoxicology 6(4); 424 – 439

Fröhlich E., Meindl C., Roblegg E., Ebner B., Absenger M., and Pieber T. R. (2012) Action of polystyrene nanoparticles of different sizes on lysosomal function and integrity. Part Fibre Toxicol 9:26

Fubini B. (1997) Surface reactivity in the pathogenic response to particulates. Environ Health Perspect 105; 1013 – 1020

Gannon C. J., Cherukuri P., Yakobson B. I., Cognet L., Kanzius J. S., Kittrell C., Weisman R. B., Pasquali M., Schmidt H. K., and Smalley R. E. (2007) Carbon nanotube-enhanced thermal destruction of cancer cells in a noninvasive thermal destruction of cancer cells in a noninvasive radiofrequency field. Cancer 110(12); 2654 – 2665

Gannon C. J., Patra C. R., Bhattacharya R., Mukherjee P., and Curley S. A. (2008) Intracellular gold nanoparticles enhance non-invasive radiofrequency thermal destruction of human gastrointestinal cancer cells. J Nanobiotechnol 6; 2

Gebhardt R., Hengstler J. G., Müller D., Glöckner R., Buenning P., Laube B., Schmelzer E., Ullrich M., Utesch D., Hewitt N., Ringel M., Hilz B. R, Bader A., Langsch A., Koose T., Burger H. J., Maas J., and Oesch F. (2003) New hepatocyte in vitro systems for drug metabolism: metabolic capacity and recommendations for application in basic research and drug development, standard operation procedures. Drug Metab Rev 35(2 – 3); 145 – 213

Geiser M., Rothen-Rutishauser B. M., Kapp N., Schürch S., Kreyling W., Schulz H., Semmler M., Im Hof V., Heyder J., and Gehr P. (2005) Ultrafine particles cross cellular membranes by nonphagocytic mechanisms in lungs and in cultured cells. Environ Health Perspect 113; 1555 – 1560

Gradauer K., Vonach C., Leitinger G., Kolb D., Fröhlich E., Roblegg E., Bernkop-Schnürch A., and Prassl R. (2012) Chemical coupling of thiolated chitosan to preformed liposomes improves mucoadhesive properties. Int J Nanomedicine 7; 2523 – 2534

Gradauer K., Dünnhaupt S., Vonach C., Szöllösi H., Pali-Schöll I., Mangge H., Jensen-Jarolim E., Bernkop-Schnürch A., and Prassl R. (2013) Thiomer-coated liposomes harbor permeation enhancing and efflux pump inhibitory properties. J Control Release 165(3); 207 – 215

Guillouzo, A., Corlu, A., Aninat, C., Glaise, D., Morel, F., and Guguen-Guillouzo, C. (2007) The human hepatoma HepaRG cells: A highly differentiated model for studies of liver metabolism and toxicity of xenobiotics. Chem Biol Interact 168, 66 – 73

Guo Y., Chen Y., Carreon S., and Qiang M. (2012) Chronic intermittent ethanol exposure and its removal induce a different miRNA expression pattern in primary cortical neuronal cultures. Alcohol Clin Exp Res 36(6); 1058 – 1066

Hamilton Jr. R. F., Wu N. N., Porte D., Buford M., Wolfarth M., and Holian A. (2009) Particle length-dependent titanium dioxide nanomaterials toxicity an bioactivity. Part Fibre Toxicol 6; 35 – 45

Han D., Ybanez M. D., Johnson H. S., McDonald J. N., Mesropyan L., Sancheti H., Martin G., Martin A., Lim A. M., Dara L., Cadenas E., Tsukamoto H., and Kaplowitz N. (2012) Dynamic adaptation of liver mitochondria to chronic alcohol feeding in mice. J Biol Chem 287(50) 42165 – 42179

Han X., Gelein R., Corson N., Wade-Mercer P., Jiang J., Biswas P., Finkelstein J. N., Elder A., and Oberdörster G. (2011) Validation of an LDH assay for assessing nanoparticle toxicity. Toxicology 287(1 – 3); 99 – 104

Hanley C., Thurber A., Hanna C., Punnoose A., Zhang J., and Wingett D. G. (2009) The influence of cell type and ZnO nanoparticle size on immune cell cytotoxicity and cytokine induction. Nanoscale Res Lett 4; 1409 – 1420

Hartman K. B., Wilson L. J., and Rosenblum M. G. (2008) Detecting and treating cancer with nanotechnology. Mol Diagn Ther 12(1); 1 – 14

Haslam G., Wyatt D., and Kitos P. A. (2000) Estimating the number of viable animal cells in multi-well cultures based on their lactate dehydrogenase activities. Cytotechnology 32; 63 – 75

Heath J. R. and Davis M. E. (2008) Nanotechnology and cancer. Annu Rev Med 59; 251 – 265

Helland A., Scheringer M., Siegrist M., Kastenholz H. G., Wiek A., and Scholz R. W. (2008) Risk assessment of engineered nanomaterials: a survey of industrial approaches. Environ Sci Technol 42; 640 – 646

Hillegass J. M., Shukla A., Lathrop S. A., MacPherson M. B., Fukagawa N. K., and Mossman B. T. (2010) Assessing nanotoxicity in cells in vitro. Interdiscip Rev Nanomed Nanobiotechnol 2(3); 219 – 231

Hoet P. H., Bruske-Hohlfels I., and Salata O. V. (2004) Nanoparticles – known and unknown health risks. J Nanobiotech 2(1); 12

Hyuk Suh W., Suslick S. K., Stucky Galen D., and SuhYH. (2009) Nanotechnology, nanotoxicology, and neuroscience. Pro Neurobiol 87(3); 133 – 170

Iijima S. (1991) Helical microtubules of graphitic carbon. Nature 354; 56 - 58

Jacobsen N. R., Pojana G., White P., Moller P., Cohn C. A., Korsholm K. S., Vogel U., Marcomini A., Loft S., and Wallin H. (2008) Genotoxicity, cytotoxicity, and reactive oxygen species induced by single-walled carbon nanotubes and C_{60} fullerenes in the FE1-Muta^{TM} mouse lung epithelial cells. Environ Mol Mutagen 49; 476 – 487

Jani P., Halbert G. W., Langridge J, and Florence A. T. (1990) Nanoparticle uptake by the rat gastrointestinal mucosa: quantitation and particle size dependency. J Pharm Pharmacol 42(12); 821 – 826

Jia G., Wang H., Yan L., Wang X., Pei R., Yan T., Zhao Y., and Guo X. (2005) Cytotoxicity of carbon nanomaterials: single-wall nanotube, multi-wall nanotube, and fullerene. Environ Sci Technol 39; 1378 – 1383

Jiang X. Y., Ferrigno R., Mrksich M., and Whiteside GM. (2003) Electrochemicaldesorption of self-assembled monolayers noninvasively releases patterned cells from geometrical confinements. J Am Chem Soc 125; 2366 – 2367

Johnston H. J., Semmler-Behnke M., Brown D. M., Kreyling W., Tran L., and Stone V. (2010) Evaluating the uptake and intracellular fate of polystyrene nanoparticles by primary and hepatocyte cell lines in vitro. Toxicol Appl Pharmacol 242; 66 – 78

Justice B. A., Badr N. A., and Felder R. A. (2009) 3D cell culture opens new dimensions in cell-based assays. Drug Discov. Today 14(1/2); 102 – 107

Kim D. H., Novak M. T., Wilkins J., Kim M., Sawyer A., and Reichert W. M. (2007) Response of monocytes exposed to phagocytosable particles and discs of comparable surface roughness. Biomaterials 28(29); 4231 – 4239

Kishore A. S., Surekha P., and Murthy P. B. (2009) Assessment of the dermal and ocular irritation potential of multi-walled carbon nanotubes by using in vitro and in vivo methods. Toxicol Lett 191; 268 – 274

Knight A. E., Veigel C., Chambers C., and Molloy J. E. (2001) Analysis of single.molecule mechanical recordings: application to acto-myosin interactions. Prog Biophys Mol Biol 77; 45 – 72

Krug H. F. and Wick P. (2011) Nanotoxicology: an interdisciplinary challenge. Angew Chem Int Ed 50; 1260 – 1278

Kwon, J. T., Kim, D. S., Minai-Tehrani, A., Hwang, S. K., Chang, S. H., Lee, E. S., Xu, C. X., Lim, H. T., Kim, J. E., Yoon, B. I., An, G. H., Lee, K. H., Lee, J. K., and Cho M. H. (2009) Inhaled fluorescent magnetic nanoparticles induced extramedullary hematopoiesis in the spleen of mice. J. Occup. Health 51, 423 - 431

Lankoff A., Sandberg W. J., Wegierek-Ciuk A., Lisowska H., Refsnes M., Sartowska B., Schwarze P. E., Meczynska-Wielgosz S., Wojewodzka M., and Kruszewski M. (2012) The effect of agglomeration state of silver and titanium dioxide nanoparticles on cellular response of HepG2, A549 and THP-1 cells. Toxicol Lett 208(3); 197 – 213

Larson B., Berry D., Justice B., and Gainer T. (2010) A novel 3D cell culture method for automated drug screening. Biotech international 22; 10 – 12

Lasagna-Reeves C., Gonzalez-Romero D., Barria M. A., Olmedo I., Clos A., Sadagopa Ramanujam V. M., Urayama A., Vergara L., Kogan M. J., and Soto C. (2010) Bioaccumulation and toxicity of gold nanoparticles after repeated administration in mice. Biochem Biophys Res Commun. 393; 649 – 655

Lee J., Lilly D., Doty C., Podsiadlo P., and Kotov N. A. (2009) In vitro toxicity testing of nanoparticles in 3D cell culture. Small 5(10); 1213 – 1221

Lewinski N., Colvin V., and Drezek R. (2008) Cytotoxicity of nanoparticles. Small 4(1); 26 – 49

Li C., Tian T., Nan K., Zhao N., Guo Y., Cui J., Wang J., and Zhang W. (2008) Survival advantages of multicellular spheroids vs. monolayers of HepG2 cells *in vitro*. Oncol Rep 20; 1465 – 1471

Lindl T., Lewandowski B., Schreyögg S., and Stäudte A. (2005) An evaluation of the in vitro cytotoxicities of 50 chemicals by using an electrical current exclusion method versus the neutral red uptake and MTT assays. Altern Lab Anim 33(6); 591 – 601

Linkov I., Satterstrom F. K., and Corey L. M. (2008) Nanotoxicology and nanomedicine: making hard decisions. Nanomedicine: Nanotech Bio and Med 4; 167 – 171

Liu X., Xue Y., Ding T., and Sun J. (2012) Enhancement of proinflammatory and procoagulant responses to silica particles by monocyte-endothelial cell interactions. Part Fibre Toxicol 9; doi: 10.1186/1743-8977-9-36

Liu Y., Li W., Lao F., Liu Y., Wang L., Bai R., Zhao Y., and Chen C. (2011) Intracellular dynemics of cationic and anionic polystyrene nanoparticles without direct interaction with mitotic spindle and chromosomes. Biomaterials 32; 8291 – 8303

Lock L. T., and Tzanakakis E. S. (2009). Expansion and differentiation of human embryonic stem cells to endoderm progeny in a microcarrier stirred-suspension culture. Tissue eng Part A 15(8); 2051 - 2063

Lockman P. R., Koziara J. M., Mumper R. J., Allen D. D. (2004) Nanoparticle surface charges alter blood-brain barrier integrity and permeability. J Drug Target 12; 635 – 641

Long T. C., Saleh N., Tilton R. D., Lowry G. V., and Veronesi B. (2006) Titanium dioxide (P25) produces reactive oxygen species in immortalized brain microglia (BV2): implications for nanoparticle neurotoxicity. Environ Sci Technol 40(14); 4346 – 4352

Lucarelli M., Gatti A. G., Savarino G., Quattroni P., Martinelli L., Monari E., and Boraschi D. (2004) Innate defence functions of macrophages can be biased by nano-sized ceramic and metallic particles. Eur Cytokine Netw (15(4); 339 – 346

Lunov O., Syrovets T., Loos C., Beil J., Delacher M., Tron K., Nienhaus G. U., Musyanovych A., Mailänder V., Landfester K., and Simmet T. (2011) Differential uptake of functionalized polystyrene nanoparticles by human macrophages and a monocytic cell line. ACS Nano 5(3); 1657 – 1669

Mayer A., Vadon M., Rinner B., Novak A., Wintersteiger R., and Fröhlich E. (2009) The role of nanoparticle size in hemocompatibility. Toxicol 258; 139 – 147

Maynard A. D. and Baron P. A. (2004) Aerosols in the industrial environment. In: Aerosols Handbook. Measurment, Dosimetry and Health Effects. CRC Press; 225 – 264

McGuinnes C., Duffin R., Brown S., Mills N. L., Megson I. L., MacNee W., Johnston S., Lu S. L., Tran L., Li R., Wang X., Newby D. E., and Donaldson K. (2011) Surface derivation state of polystyrene latex nanoparticles determines both their potency and their mechanism of causing human platelet aggregation in vitro. Toxicol Sci 119(2); 359 – 368

Michalet, X., Pinaud, F. F., Bentolila, L. A., Tsay, J. M., Doose, S., Li, J. J., Sundaresan, G., Wu, A. M., Gambhir, S. S., and Weiss, S. (2005) Quantum dots for live cells, *in vivo* imaging and diagnostics. Science 307, 538 - 544

Miyazawa M., Ito Y., Yoshida Y., Sakaguchi H., and Suzuki H. (2007) Phenotypic alterations and cytokine production in THP-1 cells in response to allergens. Toxicol In Vitro 21(3); 428 – 437

Moghimi S. M., Hunter A. C., and Murray J. C. (2005) Nanomedicine: current status and future prospects. Faseb J 19(3); 311 – 330

Monteiro-Riviere N. A., and Inman A. O. (2006) Challenges for assessing carbon nanomaterial toxicity to the skin. Carbon 44; 1070 – 1078

Morishige T., Yoshioka Y., Tanabe A., Yao X., Tsunoda S., Tsutsumi Y., Mukai Y., Okada N., and Nakagawa S. (2010) Titanium dioxide induces different levels of IL-1ß production dependent on its particle characteristics through caspase-1 activation mediated by reactive oxygen species and cathepsin B. Biochem Biophys Res Commun 392; 160 – 165

Mosmann T. (1983) Rapid colorimetric assay for cellular growth and survival: application to proliferation and cytotoxicity assays. J Immunol Methods 65; 55 – 63

Mrakovcic M., Absenger M., Riedl R., Roblegg E., and Fröhlich E. (2013) Assessment of long-term effects of nanoparticles in a microcarrier cell culture system. PLoS ONE 8(2); e56791. Doi:10.1371/journal.pone.0056791

Murr L. E., Garza K. M., Soto K. F., Carrasco A., Powell T. G., Ramirez D. A., Guererro P. A., Lopez D. A., and Venzor J (2005) Cytotoxicity assessment of some carbon nanotubes and related carbon nanoparticle aggregates and the implications for anthropogenic carbon nanotube aggregates in the environment. Int J Environ Res Public Health 2; 31 – 42

van Nieuwenhuijze A. E. M., van Lopik T., and Aarden L. A. (2003) Time between onset of apoptosis and release of nucleosomes from apoptotic cells: putative implications for systemic lupus erythematosus. Ann Rheum Dis 62, 10 – 14

Nel A., Xia T., Mädler L., and Li N. (2006) Toxic potential of materials at the nanolevel. Science 311; 622 – 627

Nomura T., Miyazaki J., Miyamoto A., Kuriyama Y., Tokumoto H., and Konishi Y. (2013) Exposure of the Yeast Saccharomyces cerevisiae to functionalized polystyrene latex nanoparticles: Influence of surface charge on toxicity. Environ Sci Technol 47(7); 3417 – 3423

Oberdörster G., Ferin J., Finkelstein G., Wade P., and Corson N. (1990) Increased pulmonary toxicity of ultrafine particles. 2. Lung lavage studies. J Aerosol Sci 21; 384 – 387

Oberdöster G., Elder A., Gelein R., Sharp Z., Atudorei V., Kreyling W., and Cox C. (2004) Translocation of inhaled ultrafine particles to the brain. Inhal Toxicol 16(6 – 7); 437 – 445

Oberdörster G., Oberdörster E., and Oberdörster J. (2005) Nanotoxicology: an emerging discipline evolving from studies of ultrafine particles. Environ Health Perspect 113(7); 825 – 839

Oberdörster G., Maynard A., Donaldson K., Castranova V., Fitzpatrick J, Ausman K., Carter J., Karn B., Kreyling W., Lai D., Olin S., Monteiro-Riviere N., Warheit D., and Yang H. (2005) Principles for characterizing the potential human health effects from exposure to nanomaterials: elements of a screening strategy. Part. Fibre Toxicol 2: doi: 10.1186/1743-8977-2-8.

O'Neal D. P., Hirsch L. R., Halas N. J., Payne J.D., and West J. L. (2004) Photo-thermal tumor ablation in mice using near infrared-absorbing nanoparticles. Cancer Lett 209; 171 – 176

Ott M., Robertson J. D., Gogvadze V., Zhivotovsky B., and Orrenius S. (2002) Cytochrome c release from mitochondria proceeds by a two-step process. Proc Natl Acad Sci USA 99; 1259 – 1263

Park M. V. D. Z., Neigh A. M., Vermeulen J. P., de la Fonteyne L. J. J., Verharen H. W., Briedé J. J., van Loveren H., and de Jong W. H. (2011) The effect of particle size on the cytotoxicity, inflammation, developmental toxicity and genotoxicity of silver nanoparticles. Biomaterials 32; 9810 – 9817

Park Y. H., Jeong S. H., Yi S. M., Choi B. H., Kim Y. R., Kim I. K., Kim M. K., and Son S. W. (2011) Analysis for the potential of polystyrene and TiO2 nanoparticles to induce skin irritation, phototoxicity, and sensitization. Toxicol In Vitro 25(8); 1863 – 1869

Pazos P., Fortaner S., and Prieto P. (2002) Long-term in vitro toxicity models: comparisons between a flow-cell bioreactor, a static-cell bioreactor and static cell cultures. Altern Lab Anim 30(5); 515 – 523

Peer D., Karp J. M., Hong S., Farokhzad O. C., Margalit R., and Langer R. (2007) Nanocarriers as an emerging platform for cancer therapiy. Nat Nanotechnol 2(12); 751 – 760

Pollice P. F., Hsu J., Hicks D. G., Bukata S., Rosier R. N., Reynolds P. R., Puzas J. E., and O'Keefe R. J. (1998) Interleukin-10 inhibits cytokine synthesis in monocytes stimulated by titanium particles: evidence of an anti-inflammatory regulatory pathway. J Orthop Res 16; 697 – 704

Pope-Harman A., Cheng M. M., Robertson F., Sakamoto J., and Ferrari M. (2007) Biomedical nanotechnology for cancer. Med Clin North Am 91(5); 899 – 927

Roblegg E., Sinner F., and Zimmer A. (2009) Health Risks of Nanotechnology. EuroNanotox Letters 1; 1 – 18

Rourou S., van der Ark A., van der Velden T., and Kallel H. (2007) A microcarrier cell culture process for propagating rabies virus in Vero cells grown in a stirred bioreactor under fully animal component free conditions. Vaccine 25; 3879 – 3889

Ryman-Rasmussen J. P., Riviere J. E., and Monteiro-Riviere N. A. (2006) Penetration of intact skin by quantum dots with diverse physicochemical properties. Toxicol Sci 91(1); 159 – 165

Ryman-Rasmussen J. P., Cesta M. F., Brody A. R., Shipley-Phillips J. K., Everitt J. I., Tewksbury E. W., Moss O. R., Wong B. A., Doss D. E., Andersen M. E., and Bonner J. C. (2009) Inhaled carbon nanotubes reach the subpleural tissue in mice. Nat Nanotech 4(11); 747 – 751

Sadauskas, E., Jacobsen, N. R., Danscher, G., Stoltenberg, M., Vogel, U., Larsen, A., Kreyling, W., and Wallin, H. (2009) Biodistribution of gold nanoparticles in mouse lung following intratracheal instillation. Chem Cent J. 3, 16

Sandberg W. J., Låg M; Holme J. A., Friede B., Gualteri M., Kruszewski M., Schwarze P. E., Skuland T., and Refsnes M. (2012) Comparison of non-crystalline silica nanoparticles in IL-1ß release from macrophages. Part Fibre Toxicol 9:32

Santra S., Kaittanis C., Grimm J., and Perez J. M. (2009) Drug/dye-loaded, multifunctional iron oxide nanoparticles for combined targeted cancer therapy and dual optical/ magnetic resonance imaging. Small 5(16); 1862 – 1868

Sayes C. M., Fortner J. D., Guo W., Lyon D., Boyd A. M., Ausman K. D., Tao Y. J., Sitharaman B., Wilson L. J., Hughes J. B., West J. L., and Colvin V. L. (2004) The differential cytotoxicity of water-soluble fullerenes. Nano Lett 4; 1881 – 1887

Sayes C. M., Liang F., Hudson J. L., Mendez J., Guo W., Beach J. M., Moore V. C., Doyle C. D., West J. L., Billups W., Ausman K. D., and Colvin V. L. (2004) Functionalizationdensity dependence of single-walled carbon nanotubes cytotoxicity in vitro. Toxicol Lett 161; 135 – 142

Sayes C. M., Gobin A. M., Ausman K. D., Mendez J., West J. L., and Colvin V. L. (2005) Nano-C60 cytotoxicity is due to lipid peroxidation. Biomaterials 26; 7587 – 7595

Schins R. P. F., Duffin R., Hohr D., Ad M. Knaapen A. M., Shi T., Weishaupt C., Stone V., Donaldson K., and Borm P. J. A. (2002) Surface modification of quartz inhibits toxicity, particle uptake, and oxidative DNA damage in human lung epithelial cells. Chem Res Toxicol 15; 1166 – 1173

Schlesinger R. B. (1995) Toxicological evidence for health effects from inhaled particulate pollution: does it support the human experience? Inhal Toxicol 7; 99 – 109

Schlumpp B. and Schlaeger E-J. (1990) Optimization of culture conditions for high cell density proliferation of HL-60 human promyelocytic leukemia cells. J Cell Sci 97; 639 – 647

Segat D., Tavano R., Donini M., Selvestrel F., Rio-Echevarria I., Rojnik M., Kocbek P., Kos J., Iratni S., Sheglmann D., mancin F., Dusi S., and Papini E. (2011) Proinflammatory effects of bare and PEGylated ORMOSIL-, PLGA- and SUV-NPs on monocytes and PMNs and their modulation by f-MLP. Nanomedicine 6(6); 1027 – 1046

Sengupta S., Eavanore D., Capila I., Zhao G., Watson N., Kiziltepe T., and Sasisekharan R. (2005) Temporal targeting of tumour cells and neovasculature with a nanoscale delivery system. Nature 436(7050); 568 – 572

Serra M., Brito C., Leite S. B., Gorjup E., von Briesen H., Carronde M. J. T., and Alves P. M. (2009) Stirred bioreactors for the expansion of adult pancreatic stem cells. Ann. Anat. 191; 104 – 115

Shain S. A., Boesel R. W., Klipper R. W., and Lancaster C. M. (1983) Creatine kinase and lactate dehydrogenase: stability of isoenzymes and their activity in stored human plasma and prostatic tissue extracts and effect of sample dilution. Clin Chem 29(5); 832 – 835

Sharma P., Brown S. C., Bengtsson N., Zhang Q., Walter G. A., Grobmyer S. R., Santa S., Jiang H., Scott E., and Moudgil B. (2008) Gold-speckled multimodal

nanoparticles for noninvasive bioimaging. Chemistry of Materials 20(19); 6087 – 6094

Shimizu Y., Isoda K., Tezuka E., Yufu T., Nagai Y., Ishida I., and Tezuka M. (2012) Influence of 50-nm polystyrene particles in inducing cytotoxicity in mice co-injected with carbon tetrachloride, cisplatin, or paraquat. Pharmazie 67(8); 712 – 714

Shvedova A., Castranova V., Kisin E., Schwegler-Berry D., Murray A., Gandelsman V., Maynard A., and Baron P. (2003) Exposure to carbon nanotube material: assessment of nanotube cytotoxicity using human keratinocyte cells. J Toxicol Environ Health Part A 66(20); 1909 – 1926

Stein R. A. (2010) Transitioning toward three-dimensional cell culture. GEN 30(16), 5

Tinkle S. S., Antonini J. M., Rich B. A., Roberts J. R., Salmen R., DePree K., and Adkins E. J. (2003) Skin as a route of exposure and sensitization in chronic beryllium disease. Environ Health Perpect 111(9); 1202 – 1208

Tsuchiya S., Yamabe M., Yamaguchi Y., Kobayashi Y., Konno T., and Tada K. (1980) Establishment and characterization of a human acute monocytic leukemia cell line (THP-1). Int J Cancer 26(2); 171 – 176

Turnherr, T., Brandenberger, C., Fischer, K., Diener, L., Manser, P., Maeder-Althaus, X., Kaiser, J. P., Krug, H. F., Rothen-Rutishauser, B., and Wick, P. (2011) A comparison of acute and long-term effects of industrial multiwalled carbon nanotubes on human lung and immune cells in vitro. Toxicol Lett 200(3), 176 – 186

Vagts A. J., He D., Yaka R., amd Ron D. (2003) Cellular adaptation to chronic ethanol results in altered compartmentalization and fuction of the scaffolding protein RACK1. Alcohol Clin Exp Res 27(10); 1599 – 1605

Varani J., Piel F., Josephs S., Beals T. F., and Hillegas W. J. (1998) Attachment and growth of anchorage-dependent cells on a novel, charged-surface microcarrier under serum-free conditions. Cytotechnology 28; 101 – 109

Venkatraman A., Shiva S., Davis A. J., Bailey S. M., Brookes P. S., and Darley-Usmar V. M. (2003) Chronic alcohol consumption increases the sensitivity of rat mitochondrial respiration to inhibition by nitric oxide. Hepatology 38; 141 – 147

Volkheimer G. (1974) Passage of particles through the wall of the gastrointestinal tract. Environ Health Perspect 9; 215 – 225

Whitesides GM. (2003) The “right” size in nanobiotechnology. Nature Biothech 21(10); 1161 – 1165

Wick P., Manser P., Limbach L. K., Dettlaff-Weglikowska U., Krumreich F., Roth S., Stark W. J., and Bruinink A. (2007) The degree and kind of agglomeration affect carbon nanotube cytotoxicity. Toxicol Lett 168; 121 – 131

Wick P., Malek A., Manser P., Meili D., Maeder-Althaus X., Diener L., Diener P. A., Zisch A., Krug H. F., and von Mandach U. (2010) Barrier capacity of human placenta for nanosized materials. Environ Health Perspect 118; 432 – 436

Wu J., Liu W., Xue C., Zhou S., Lan F., Bi L., Xu H., Yang X., and Zeng F. D. (2009) Toxicity and penetration of TiO2 nanoparticles in hairless mice and porcine skin after subchronic dermal exposure. Toxicol Lett 191, 1 – 8

Xia T., Kovochich M., Brant J., Hotze M., Sempf J., Oberley T., Sioutas C., Yeh J. I., Wiesner M. R., and Nel A. (2006) Comparison of the abilities of ambient and manufactured nanoparticles to induce cellular toxicity according to an oxidative stress paradigm. Nano Lett 6; 1794 – 1807

Xia T., Kovochich M., Liong M., Zink J. I., and Nel A. E. (2008) Cationic polystyrene nanosphere toxicity depends on cell-specific endocytic and mitochondrial injury pathways. ACS Nano 2(1); 85 – 96

Xiao C., Huang Z., Li W., Hu X., Qu W., Gao L., and Liu G. (1999) High density and scale-up cultivation of recombinant CHO cell line and hybridomas with porous microcarrier Cytopore. Cytotechnology 30, 143 – 147

Yanagisawa R., Takano H., Inoue K. I., Koike E., Sadakane K., and Ichinose T. (2010) Size effects of polystyrene nanoparticles on atopic dermatitislike skin lesions in NC/NGA mice. Int J Immunopathol Pharmacol 23(1); 131 – 141

Yang E-J., Kim S., Kim J. S., and Choi I-H. (2012) Inflammasome formation and IL-1ß release by human blood monocytes in response to silver nanoparticles. Biomaterials 33; 6858 – 6867

Yang X., Skrabalak S. E., Li Z. Y., Xia Y., and Wang L. V. (2007) Photoacoustic tomography of a rat cerebral cortex in vivo with Au nanocages as an optical contrast agent. Nano Lett 7(12); 3798 – 3802

6. APPENDIX

1. Curriculum vitae
2. Assessment of Long-term Effects of Nanoparticles in a Microcarrier Cell Culture System

Curriculum vitae

Maria Fröhlich (formerly Mrakovcic)

Date of Birth March 12th, 1985 in Rijeka, Croatia

Education

1991-1999 Elementary school "Fran Krsto Frankopan"
Punat, Croatia

1999-2003 Secondary school "Hrvatski kralj Zvonimir"
Krk, Croatia
Final examination: Term paper "Human embryonic development"

University of Veterinary Medicine Vienna, Austria:

2003-2006 **BSc. in Biomedicine & Biotechnology**
Bachelor thesis: "Establishment of a chromogen *in situ* hybridization (CISH) for *Lawsonia intracellularis*"
Institute of Pathology; supervisor Dr. Herbert Weissenboeck

2006-2008 **MSc. in Biomedicine & Biotechnology**
Master thesis: "Identification of *Brachyspira sp.* upon multiple infections in pigs"
Institute of Pathology; supervisor Dr. Herbert Weissenboeck

Medical University of Graz, Austria:

Since 2009 **PhD in Cell Biology and Nanotoxicology**
PhD topic: "Long-term cytotoxicity upon chronic exposure to nanomaterials"
Center for Medical Research; supervisor Priv.-Doz. Dr. Eleonore Fröhlich

Research & Professional Experience

Practical courses in Biomedicine and Biotechnology:

Jan 2003 "Investigation of parameters of gut physiology using the Ussing chamber"

Apr 2004 "Isolation and identification of thyroid peroxidase by gel electrophoresis"

Dec 2004 "Measurement of α-tocopherol in chicken liver"

May 2005 "Detection of *Cryptosporidium sp.* in domestic geese"

Nov 2005 "Detection of Circoviruses in geese"

May 2007 "Bisulfite methylation analysis: Molecular cloning and sequencing of several differentially methylated regions of the Gsα (*Gnas*) locus in mice"

Sep 07- Sep 08 "Identification of *Brachyspira sp.* upon multiple infections in pigs"

Medical University of Vienna:

Oct 08 - Sep 09 Technical Assistant in Cellular and Molecular Biology
Center for Brain Research, Vienna; Dept. of Neuronal Cell Biology

Teaching Experience

University of Veterinary Medicine Vienna:

Supervision of bachelor students for laboratory course

Medical University of Graz:

Supervision of bachelor/ diploma students (FH Joanneum, Graz; FH Steyr, Steyr)

Awards and Prices

2004-2008 Stipend of Punat, Croatia

Membership

Since 2011 Erwin Schrödinger Society for Nanosciences

Since 2012 Austrian Association of Molecular Life Sciences and Biotechnology ÖGMBT

Languages German & Croatian (both first language), English, Italian

Publications

1. Weissenböck H, **Mrakovcic M**, Ladinig A, Fragner K. *In situ* hybridization for *Lawsonia intracellularis*-specific 16S rRNA sequence in paraffin embedded tissue using a digoxigenin-labeled oligonucleotide probe. J Vet Diagn Invest 2007 May; 19(3): 282-285

2. Fröhlich LF, **Mrakovcic M**, Steinborn R, Chung U, Bastepe M, Jüppner H. Targeted deletion of the Nesp55 DMR defines another *Gnas* imprinting control region and provides a mouse model of autosomal dominant PHP-Ib. Proc Natl Acad Sci USA. 2010; 107(20): 9275-9280

3. Abdelmoez AA, Thurner GC, Wallnöfer EA, Klammsteiner M, Kremser C, Talasz H, **Mrakovcic M**, Fröhlich E, Jaschke W, Debagge P. Albumin-based nanoparticles as magnetic resonance contrast agents: II. Physicochemical characterization of purified and standardised nanoparticles. Histochem Cell Biol. 2010; 134(2): 171-196

4. **Mrakovcic M**, Absenger M, Roblegg E, Riedl R, Fröhlich E. Assessment of long-term cellular effects of nanoparticles on endothelial cells in a 3D cell culture system. PLoS ONE 2013; 8(2); doi: 10.1371/journal.pone.0056791.

5. ***Mrakovcic M,*** *Neudecker M, Meindl C, Ferk F, Knasmüller S, Roblegg E, Fröhlich E. Plain and carboxylated short carbon nanotubes may act genotoxic by different mechanisms. In preparation*

Presentations

1. **Mrakovcic M**. Assessing chronic cytotoxicity: microcarrier culture vs. compartment culture. 1st Cell Culture Day; June 2010; Graz, Austria (**Oral presentation**)

2. **Mrakovcic M**, Absenger M, Meindl C, Mujk D, Fröhlich E. Evaluation of cell culture models for the assessment of chronic cytotoxic effects of nanoparticles. Joint ZMF and Doctoral Days; November 2010; Graz, Austria (**Poster presentation**)

3. **Mrakovcic M**, Absenger M, Riedl R, Pieber TR, Fröhlich E. Assessment of long-term cellular effects of nanoparticles on endothelial cells in a 3D cell culture system. Nanotechitaly 2011; November 2011; Venice, Italy (**Poster presentation**)

4. **Mrakovcic M**, Absenger M, Meindl C, Riedl R, Roblegg E, Fröhlich E. Assessing long-term effects of nanomaterials in a 3D cell culture system. 9th International Conference on Nanosciences and Nanotechnologies; July 2012; Thessaloniki, Greece (**Oral presentation**)

5. **Mrakovcic M**, Froehlich LF, Smole C, Chowdhury P, Fröhlich E, Zatloukal K. TP53 mutational status determines uterine tumor cell response towards histone deacetylase inhibitor induced apoptosis or autophagy. Gordon Research Conference “Cell death”; July 2012; Lucca, Italy (**Poster presentation**)

6. **Mrakovcic M**, Absenger M, Riedl R, Roblegg E, Fröhlich E. Assessing long-term effects of nanomaterials on endothelial cells in a microcarrier cell culture system. 4th ÖGMBT Annual Meeting; September 2012; Graz, Austria (**Poster presentation**)

7. **Mrakovcic M,** Fröhlich LF, Smole C, Fröhlich E, and Zatloukal K. TP53 mutational status determines uterine tumor cell response towards histone deacetylase inhibitor induced apoptosis or autophagy. 4th ÖGMBT Annual Meeting; September 2012; Graz, Austria (**Oral presentation**)

8. **Mrakovcic M,** Fröhlich LF, Smole C, Fröhlich E, and Zatloukal K. TP53 mutational status determines uterine tumor cell response towards histone deacetylase inhibitor induced apoptosis or autophagy. 4th ÖGMBT Annual Meeting; September 2012; Graz, Austria (**Poster presentation**)

9. **Mrakovcic M**, Absenger M, Meindl C, Riedl R, Roblegg E, Fröhlich E. Assessing long-term effects of nanomaterials in a 3D cell culture system. Intl. Cong. on Safety of Engineered Nanoparticles and Nanotechnologies; November 2012; Helsinki, Finland (**Poster presentation**)

10. **Mrakovcic M**. Microcarrier Cell Culturing for the Assessment of Long-term Cytotoxicity. ZMF Days 2012; November 2012; Graz, Austria (**Invited oral presentation**)

11. **Mrakovcic M,** Neudecker M, Meindl C, Ferk F, Knasmüller S, Roblegg E, Fröhlich E. Plain and carboxylated short carbon nanotubes may act genotoxic by different mechanisms. BioNanoMed; March 2013; Krems at the Danube, Austria (**Invited oral presentation**)

Assessment of Long-term Effects of Nanoparticles in a Microcarrier Cell Culture System

Maria Mrakovcic[1], Markus Absenger[1], Regina Riedl[2], Claudia Smole[3], Eva Roblegg[4], Leopold F. Fröhlich[3], Eleonore Fröhlich[1, *]

[1] Center for Medical Research, Medical University of Graz, Graz, Austria

[2] Institute for Medical Informatics, Statistics and Documentation, Medical University of Graz, Graz, Austria

[3] Institute of Pathology, Medical University of Graz, Graz, Austria

[4] Institute of Pharmaceutical Sciences, Department of Pharmaceutical Technology, Karl-Franzens-University of Graz, Graz, Austria

[*] **Corresponding author**: E-mail: eleonore.froehlich@medunigraz.at

ABSTRACT

Nano-sized materials could find multiple applications in medical diagnosis and therapy. One main concern is that engineered nanoparticles, similar to combustion-derived nanoparticles, may cause adverse effects on human health by accumulation of entire particles or their degradation products. Chronic cytotoxicity must therefore be evaluated. In order to perform chronic cytotoxicity testing of plain polystyrene nanoparticles on the endothelial cell line EAhy 926, we established a microcarrier cell culture system for anchorage-dependent cells (BioLevitator^{TM}). Cells were cultured for four weeks and exposed to doses, which were not cytotoxic upon 24 hours of exposure. For comparison, these particles were also studied in regularly sub-cultured cells, a method that has traditionally been used to assess chronic cellular effects. Culturing on basal membrane coated microcarriers produced very high cell densities. Fluorescent particles were mainly localized in the lysosomes of the exposed cells. After four weeks of exposure, the number of cells exposed to 20 nm polystyrene particles decreased by 60% as compared to untreated controls. When tested in sub-cultured cells, the same particles decreased cell numbers to 80% of the untreated controls. Dose-dependent decreases in cell numbers were also noted after exposure of microcarrier cultured cells to 50 nm short multi-walled carbon nanotubes. Our findings support that necrosis, but not apoptosis, contributed to cell death of the exposed cells in the microcarrier culture system. In conclusion, the established microcarrier model appears to be more sensitive for the identification of cellular effects upon prolonged and repeated exposure to nanoparticles than traditional sub-culturing.

Keywords: Microcarrier cell culture, Long-term effects, Nanoparticle, Cytotoxicity

INTRODUCTION

In nanotechnology, a nanoparticle (NP) is defined as a small object that behaves as a whole unit in terms of its transport and properties. NPs are natural, incidental or manufactured particles with one or more external dimensions that range from 1 to 100 nm [1, 2]. NPs are of great scientific interest as they bridge bulk materials and atomic or molecular structures. Properties of nanomaterials (NMs) change as their size approaches the nanoscale [3]. Because of quantum size and large surface area, NMs have unique properties compared with their larger counterparts. Even when made of inert elements (e.g. gold), NMs become highly (re)active or even catalytic at nanometer dimensions [4], mostly because of their high surface to volume ratio. Oberdörster et al. discovered that the toxic effect of NMs is influenced by several properties, such as size, surface charge, hydrophobicity, shape and contamination [5]. Size and surface characteristics of NPs are no constants, but vary according to the concentration of salts and proteins as well as to mechanical pre-treatment [6]. The danger of inhaling particulate matter (fume or smoke particles) has been recognized since ancient times, but it was not until the early 1990s when associations between particle inhalation and diseases of the respiratory or cardiovascular systems were uncovered [7]. At that time, researchers started to systematically study the effects of (natural) NPs on human health [8, 9], especially the association between NP size and its response in lung tissue [10 - 12]. However, due to their properties, engineered NMs are increasingly often used in consumer products. But the same advantageous size-dependent properties of NMs lead to the possibility of harmful size-dependent biological interactions [13]. Therefore, the need to assess the potential risk of NMs on human health is rapidly growing.

NPs can display acute cytotoxic action at the site of entry. Cells important in this regard are epithelial cells of the respective organ, and cells of the innate immune system. Upon exposure to NMs, such as carbon black (CB), carbon nanotubes (CNTs), or zinc oxide, cells may be acutely damaged and their functionality may be compromised [14 - 17]. Both, bio-persistent (e.g. CNTs) and bio-degradable (e.g. iron oxide) NPs may cause severe

problems [2, 18]. In addition to acute toxic effects, chronic exposure may result in selective cytotoxicity affecting specific cell functions [19]. However, testing of chronic effects *in vitro* is rarely done for conventional substances. Drugs are usually metabolized, excreted and degraded within cells and cellular accumulation is not expected. Consequently, models to assess chronic toxicity have not been developed and chronic toxicity is usually studied in animals. Nevertheless, data suggest that some NMs are not sufficiently cleared from the organism [20, 21]. If an organism is exposed over a long period to low concentrations of NPs, the function of cells may be compromised. Most indications for organ damage by repeated exposure to NPs were obtained in animal studies. Repeated exposure to gold NPs and magnetic NPs caused not only accumulation and histopathological changes in various organs but also weight loss and marked alterations in blood count [22 - 24]. Therefore, the assessment of toxic effects is becoming of outmost importance.

In short-term cytotoxicity studies, cell lines are usually employed, but these generally cannot be studied much longer than 72 hours in conventional culture. Subsequently, the cells need medium change and / or the cultures are in the stationary state. To assess longer time-periods, cells have been sub-cultured and again exposed to the tested compound [21]. Other systems such as bioreactors have to be used when observations over longer time-periods are needed [25, 26]. Dependent on their growth characteristics (adherent or in suspension), cells in bioreactors are either dispersed in medium or cultured on scaffolds, matrices or microcarriers.

In microcarrier cell cultures, anchorage-dependent cells are grown on the surface of small spheres which are maintained in stirred suspension cultures. In comparison to conventional monolayer cell culture, this technology provides the advantage that high cell densities and higher yields of cellular products such as antibodies can be obtained. Main advantages of the microcarrier system are reduced costs and reduced risk of contamination, increased culture periods without sub-culturing [27] as well as the imitation of the *in vivo* situation due to a more physiologic environment. This technique is therefore

a good choice where cells are used for the production of biologicals, cells, cell products, and viral vaccines. Other applications include studies of cell structure, function and differentiation, enzyme-free sub-cultivation, and implantation studies [28 - 30]. Several cell lines (e.g. MDCK, Vero cells, Cos-7, stem cells, HEK 293T) were described to grow and differentiate on microcarriers [31 - 34].

In this study, we describe a microcarrier cell culture system to monitor cellular effects of NPs for a period of four weeks. We used plain polystyrene particles (PPS) as model NPs, as they are not bio-degradable; thus, the effect of accumulation can be studied. To investigate the suitability of the microcarrier system for other NMs, multi-walled CNTs were also evaluated. Cytotoxicity was assessed in microcarrier culture as well as in repeatedly sub-cultured cells. Moreover, the intracellular localization and the mode of cell death were investigated.

MATERIAL AND METHODS

Cell culture

All experiments were performed on the endothelial cell line EAhy 926 which was kindly provided by Dr. C.J. Edgell [35]. Cells were cultured in high glucose Dulbeco's Modified Earls Medium (DMEM) supplemented with 10% fetal bovine serum (FBS), 2 mM L-Glutamine and 1% penicillin / streptomycin (P/ S) (PAA, Austria).

Nanoparticles

Non-functionalized PPS "Nanosphere Size Standards" 1% (w/v) 20 nm and 200 nm, red fluorescent PPS "Fluoro-Max Red Aqueous Fluorescent Particles" R25 1% (w/v) 25 nm (Thermo Scientific, USA), and short (0.5-2 µm) carboxyl-functionalized >50 nm diameter CNTs (MWCNT >50 nm COOH) (CheapTubes Inc., Brattleboro, Vermont) were used. CNTs were synthesized by catalytic chemical vapour deposition, acid purified, and were functionalized through repeated reductions and extractions in concentrated acids. As

indicated by the supplier, CNTs were of high purity (> 95%) with low amount of contaminants (ash <1.5 wt %).

Characterization of particles

Particle characterization was performed by dynamic light scattering with a Malvern Zetasizer 3000 HS. Size and surface charge were determined after sonification for 20 minutes in distilled water, and in cell culture medium (DMEM) with or without 10% FBS.

Cytotoxicity screening

1.4-1.7 x 10^5 cells per ml were seeded in 96-well plates (Corning Costar, The Netherlands) and were incubated overnight at 37°C and 5% CO_2 to allow cell attachment. For cytotoxicity screening on Global Eucaryotic Microcarrier GEM™ (Global Cell Solutions, Virginia, USA), 2 x 10^5 cells per ml were seeded in 96-well plates (Corning Costar) coated with a 5% poly (2-hydroxyethyl methacrylate) (poly-HEMA) solution (Sigma, Austria) to block cell attachment onto the plate. Cultures were exposed to different concentrations of 20 nm and 200 nm PPS as well as CNTs for 4 and 24 hours. After treatment, the viability of the cells was assessed by a formazan bioreduction (MTS) assay (CellTiter 96® AQueous Non-Radioactive Cell Proliferation Assay, Promega, Germany) according to the manufacturer's protocol. After two hours of incubation with the MTS-solution, the absorbance was measured on a SpectraMAX plus 384 (Molecular Devices, Austria) at 490 nm. Wells without cells but with the respective medium, in which the NPs were dissolved, were used as blank control. To investigate whether the NPs interfere with the assay, an interference control (= highest concentration of each NP without cells) was included. In addition, after exposure to CNT, cells were washed three times with pre-warmed phosphate buffered saline (PBS) (PAA) prior to adding staining solution.

Mode of action of PPS in conventional cell culture

After exposure of cells to the PPS for 4, 8, and 24 hours, the integrity of the cell membrane was determined using the CytoTox-ONE™Homogeneous Membrane Integrity Assay (Promega), based on the release of lactate dehydrogenase (LDH). The fluorescence was recorded with an excitation wavelength of 560 nm and an emission wavelength of 590 nm on a FLUOstar Optima (BMG Labtech, Germany). As positive control, the cells were treated with a lysis solution of equal amounts of Triton X-100 and 70% ethanol for 10 minutes at room temperature. Induction of apoptosis was assessed after treatment of cells under same conditions as for the LDH measurement by using the Caspase-Glo 3/7 Assay (Promega). Measurements were read on a Lumistar (BMG Labtech). Both assays were carried out according to manufacturer's instructions.

Assays on long-term effects in conventional cell culture

Cells were plated in 25 cm² cell culture dishes in complete DMEM and were incubated at 37°C and 5% CO2 to allow cell attachment. After 24 hours, the media were exchanged and NPs at a final concentration of 20 µg/ ml were added. Controls received no NPs. Cell numbers and cell viability were assessed at time-points when controls reached 100% confluence to avoid bias by growth inhibition. In parallel, assays on the membrane integrity and apoptosis were assessed as described above and the cells were sub-cloned in a 1:10 ratio.

Microcarrier cell culture

For the establishment of a three dimensional model, basal membrane coated GEM™ were used. Cells were incubated in specialized culture vessels (LeviTubes™) in the bench-top bioreactor BioLevitator™ (Hamilton Company, Switzerland) at 37°C and 5% CO_2. Two pre-installed culturing protocols (for epithelial and endothelial cells) were compared with respect to cell proliferation. 3 x 10^6 cells were seeded on a 50% bead slurry in medium with 10% FBS. After an overnight inoculation period, LeviTubes™ were filled with additional medium. 20 nm and 200 nm PPS, in concentrations where no acute toxicity was

observed after 24 hours, were added to the medium. For untreated controls no NPs were added. In parallel, red fluorescent labelled PPS were used in order to identify the sub-cellular localization of the NPs.

In pilot experiments, we investigated the effects on cell growth, viability, as well as on the toxic action of 20 nm PPS by changing the medium every other day (as in conventional cultures), and once per week. Since no differences on any outcome were observed, the medium was changed once per week in all further experiments.

Microscopical evaluation of endothelial cells in microcarrier culture

Cell attachment was recorded at regular intervals by staining the nuclei with 5 µg/ ml Hoechst 33342 staining solution (Invitrogen, Austria) for 15 minutes at room temperature. The viability of cells was determined by labelling different cell organelles (nucleus, endoplasmic reticulum and mitochondria). An aliquot of the microcarrier cultures was stained with Hoechst 33342, 1 µM ER-Tracker green and 200 mM MitoTracker DeepRed 633 (Invitrogen). After incubation for 20 minutes at 37 °C and 5% CO_2, staining was documented on a LSM510 Meta confocal laser scanning microscope (Zeiss, Germany). Changes in cell number and viability were recorded weekly. GEM™ were dissolved in pre-warmed trypsin/ EDTA (PAA). Detachment of the cells was observed under a CKX41 light microscope (Olympus, Japan). Cell number and viability was determined using a CasyONE® cell counter (Inovatis, Germany) [36].

Mode of NP action in microcarrier cell cultures

Induction of apoptosis and / or necrosis of the long-term exposed cultures were assessed weekly and were compared to untreated controls. Mean values were normalized to total cell numbers in the culture vessels at each time point. To determine the main mode of cell death in PPS-exposed cultures, an ApoTox-Glo™ Triplex Assay (Promega) was performed. Thereby, the effects on viability, cytotoxicity, and apoptosis induction were

assessed simultaneously at 24 hours and 7 days after exposure. The assay was performed according to manufacturer's instructions.

Western blot analysis for PARP-1

In order to discriminate between apoptotic and necrotic cell death, a Western blot for poly (ADP-ribose) polymerase (PARP-1) was performed 7 days after exposing microcarrier cultures to both, PPS and CNTs. To obtain a positive control, cells were treated with 1 µg/ ml staurosporine for 5 hours. Upon washing cells with ice-cold PBS, cell lysates were prepared in RIPA buffer (50 mM Tris-HCl pH 8.0, 150 mM NaCl, 1% Triton X-100, 0.5% sodium deoxycholate, 0.1% SDS; Sigma) overnight at 4°C with the addition of protease and phosphatase inhibitor cocktails (1 tablet each was dissolved in 10 ml RIPA buffer) (Roche Diagnostics, Austria). The protein concentration was determined photometrically by a Bradford Assay (Bio-Rad Laboratories, California). 20 µg of the protein lysate was separated by SDS-PAGE (NuPage 4- 12% Bis-Tris gels; Life Technologies, Austria) and transferred to nitrocellulose membrane (Bio-Rad). Following primary antibodies were used: PARP (dilution: 1:750; Cell Signaling Technology, Massachusetts), and as a loading control beta-Actin (diluted 1:1000; Sigma). As secondary antibody we used a goat anti-rabbit (Cell Signaling Technologies) or rabbit anti-mouse HRP-conjugated antibody, respectively (DAKO, Denmark) at a final concentration of 1 µg/ ml. An overnight incubation at 4°C was performed for both primary antibodies, followed by incubation with secondary antibodies at room temperature for 2 hours. Specific protein bands were visualized by the enhanced chemiluminescence assay (Amersham Biosciences, Germany).

Statistical analysis

All experiments, except long-term exposure to PPS, were repeated three times. At least triplicates were assessed for each sample. Due to the small sample size (n = 3), all data are described descriptively, as mean ± standard deviation (SD). To investigate the effects

of PPS on cell growth over time (n = 5), repeated measurements ANOVA was performed. For post-hoc analysis, a Bonferroni correction was conducted. A p-value <0.05 was considered to indicate statistical significance. The statistical analysis was performed by using the statistical software SPSS Version 20.

RESULTS

Prior to the assessment of the long-term effects in 3D culture, NPs were characterized according to their physicochemical parameters and to their acute cytotoxic action in conventional culture.

Particle characterization

The hydrodynamic sizes of PPS were larger when diluted in medium, especially in the presence of FBS than indicated by the supplier. The differences between the indicated size and the hydrodynamic radius in medium with 10% FBS, were more pronounced for the 20 nm PPS than for the 200 nm PPS. All particles were negatively charged except 200 nm PPS when dissolved in DMEM with 10% FBS. Sizes of the > 50 nm CNTs increased markedly when protein-free medium was used. A summary of the particle properties is presented in Table 1.

Acute cytotoxicity

After exposure of cells to 20 nm PPS for 24 hours, the cell viability was reduced in a dose-dependent manner (Fig. 1 A). Addition of serum to the medium decreased the cytotoxicity of the particles. The estimated IC_{50} was approximately 120 µg/ ml in DMEM supplemented with 10% FBS and 30 µg/ ml in medium without FBS. The viability of cells after exposure to 20 nm PPS did not decrease when cells were grown on GEM^{TM}. 200 nm PPS exhibited no cytotoxicity, irrespective of the medium used (Fig. 1 A - C). Exposure of cells to CNT dissolved in serum-containing DMEM decreased cell viability similarly to 20 nm PPS (Fig

1 B); the estimated IC_{50} was approximately 125 µg/ ml. No changes in cell viability were detected when cells were seeded onto GEM™ (Fig 1 C).

Mode of action

Low concentrations (< 200 µg/ ml) of 20 nm PPS had no influence on membrane integrity or on activation of caspases 3 and 7 at any time-point. However, PPS at 200 µg/ ml induced strong activation already after 4 hours, reaching the maximum of an about 50-fold increase after 8 hours and an almost 30-fold increase after 24 hours as compared to non-exposed cells (Fig. 2 A). A similar dose-dependent effect was observed for membrane disruption (Fig. 2 C). Exposure of the cells to 200 nm PPS resulted in a very low release of LDH (up to 15% of the lysis control) and no notable increase in caspase activation at any time-point (Fig. 2 B and D).

Establishment of the microcarrier cell culture system

For optimization of the exposure system, different coatings of the GEM™ (gelatine, laminin, fibronectin, collagen type I and IV, basal membrane) as well as different incubation protocols, pre-defined by the supplier, were compared. Cells that were seeded on basal membrane coated microcarriers and cultured according to the protocol for endothelial cells (HUVEC) reached approximately 4 times higher cell densities compared to those when the protocol for epithelial cells (HEK 293) was used (Fig. 3). Cultures were maintained for 23 days without sub-culturing. The doubling time of EAhy cells was lower in the microcarrier culture system (70 h) than in conventional cultures (30 h). Staining with Hoechst 33342 dye showed an increase in cell proliferation on GEM™ (Fig. 4 A). Furthermore, vital staining for mitochondria and endoplasmic reticulum (ER) demonstrated the viability of the cells (Fig. 4 B).

Intracellular localization of PPS

Cells were exposed to 20 µg/ ml of the red fluorescent PPS in order to study cellular localization. R25 were observed within the cells, mainly localized in lysosomes (Fig. 4 C).

Long-term effects of NPs in microcarrier culture

Cells were cultured according to the established protocol (basal membrane coated GEM™, and incubation protocol for endothelial cells) for four weeks with a medium change performed once per week. After inoculation, NPs were added at a concentration 250 times lower than the concentration where cytotoxicity was seen in the acute cytotoxicity setting (24 hours). Exposure of the cells to 20 µg/ ml of 20 nm PPS resulted in a significantly reduced cell number already after 7 days, showing a decrease in cell numbers of approximately 50%. Even stronger effects were observed at later time-points. No decrease in cell number was observed when the cells were exposed to 20 µg/ ml of 200 nm PPS (Fig. 5 A).

Exposure to concentrations of 5 – 20 µg/ ml of CNT decreased cell numbers in a dose-dependent manner at day 7 to approximately 75% - 40% of control cells, respectively. However, with prolonged contact the cell populations recovered. The recovery rate was more rapid for cells exposed to 20 µg/ ml than for cells that were exposed to 5 µg/ ml and the values reached 90% - 70% of the control after 4 weeks (Fig 5 B). Cell viability was not impaired at any time-point.

Mode of action in microcarrier cultures

Long-term exposure to 20 nm PPS induced an 80% higher activation of the effector caspases 3 and 7 after 7 days as compared to the control cells. Over time, the induction of apoptosis decreased to about 30% of the untreated control (Fig. 6 A). 20 nm PPS induced necrosis with a maximum of LDH release, about 65% higher than in control cells, after 7 days of culturing (Fig. 6 C). At later time-points, LDH release slightly dropped by about 15%. However, exposure to 20 nm PPS resulted in a 2.5- to 5-fold increase in cytotoxicity, while the viability was slightly reduced, as detected by the ApoTox-Glo™

Triplex Assay. No induction of apoptosis was detected (Fig. 6 E). Exposure to 200 nm PPS induced neither apoptosis nor necrosis at any time-point (Fig. 6 A, C, E). CNT induced both, apoptosis and necrosis, in a dose-dependent manner, reaching a 2.5-fold increase as compared to the control upon exposure to a concentration of 20 µg/ ml (Fig 6 B and D). Similar to PPS, the strongest induction of caspases and the highest release of LDH occurred after 7 days of exposure, after which the levels approached those of control cells.

Western blot for PARP-1

As shown in Fig. 6 F, an 89 kDa fragment representing cleaved PARP-1, indicative for apoptotic cell death, appeared exclusively in the staurosporine treated positive control. Treatment with NPs provoked the appearance of not only un-cleaved (116 kDa), but also additional slight cleaved PARP-1 bands (89 kDa, 72 kDa), which, in combination, occur only after necrosis.

DISCUSSION

In this study, the long-term cytotoxicity testing with the BioLevitator™ was used for the identification of potential chronic effects of NPs on cells and was compared to conventional cell culture. This system enabled the culture of viable cells to high densities and identified adverse cellular effects of 20 nm PPS and of > 50 nm CNTs.

A microcarrier cell culture system enables cell culturing at higher cell densities for a longer time period. The polarized cell growth, in a more physiologic environment than in conventional cell culture vessels, allows a better differentiation of the cells [37]. The mimicked *in vivo* situation slows down proliferation and therefore the nutrients are depleted more slowly. In addition, due to their structure, the porous microcarrier facilitates long-term cell culturing as the nutrients from the medium and the molecules secreted from the cells (e.g. growth factors) are retained inside the beads. Due to the small volume of

medium required to feed the cells over the entire culturing period compared to conventional cell culture methods, it is a very cost- and material-saving method. Bioreactors were initially developed to increase the yield of cellular products (e.g. antibodies) [38]. This culture may also be suitable for toxicity testing and / or the identification of long-term effects. This is particularly important for NPs because they have been shown to persist in organisms [39], and are influenced by several factors, such as medium composition, binding of proteins, mechanical pre-treatment, and pH, which makes it very laborious to evaluate all these parameters *in vivo*. The GEM^{TM} technology and the BioLevitator^{TM} allowed the culture of viable cells with high reproducibility. As expected, the physiological growth on basal membrane coated microcarriers slowed down the proliferation of EAhy 926 cells, which is advantageous for the study of NP accumulation. One potential limitation of the system is that high-throughput testing is not possible because only four experiments can be performed in parallel.

The endothelial cells EAhy 926 can be exposed to relatively high concentrations (100 µg/ml) of 20 nm PPS for 24 hours without showing any apparent damage in a conventional culture. In microcarrier culture, the resistance to the toxic action of PPS is even higher. Two mechanisms could be suggested that may explain the lower cytotoxicity of PPS in microcarrier culture: a more physiological growth with a better supply of nutrients and the fact that a smaller area of the cell membrane is accessible to the PPS because cells are more densely packed [40]. Upon longer incubation times, however, the situation is inversed. The low concentrations of the NPs did not have a strong influence on the proliferation of cells maintained in conventional cell culture, but pronounced cytotoxicity was detected in microcarrier culture. This difference may be caused by a higher dilution of the intracellular concentration of NPs due to proliferation. Our experiments proved that the doubling rate of EAhy 926 cells in conventional culture was 2.3 times higher than in the microcarrier culture. At concentrations higher than 100 µg/ml, 20 nm PPS decreased the metabolic activity of the cells in conventional culture and induced the activation of caspases 3 and 7. In addition, an increased release of LDH, as an indicator of membrane

damage, was also observed after exposure to these doses of PPS for 24 hours. Particles of 200 nm did not exert any effect upon culturing under the same conditions. Upon acute exposure, the main modes of PPS induced cell death were found to be apoptosis and necrosis. Fröhlich *et al*. investigated the impacts of 20 nm carboxylated polystyrene (CPS) NPs in the same cell line, grown in conventional cell culture for 24 hours, and also demonstrated induction of necrosis and apoptosis [41]. This similarity between 20 nm CPS and 20 nm PPS may be linked to their similar physicochemical parameters: the differences in size (42 nm (CPS) vs. 73 nm (PPS)) were small and the surface charge of both particles was slightly negative. Upon prolonged exposure to PPS, not only LDH release was increased as compared to controls, but also the activation of caspases. However, it is very unlikely that both modes of cell death are induced at the same time. The contradictory findings on caspase activation (Fig. 6 A) could be explained by the normalization of very small differences in assay values (caspase 3/ 7) between untreated and treated cells versus larger differences in total cell numbers of the respective culture. Moreover, all other data supported the induction of necrosis as the predominant mode of action of 20 nm PPS upon long-term exposure. Collectively, we detected no induction of apoptosis and only low induction of necrosis at each time-point in cells exposed to 20 µg/ ml of 20 nm PPS. As both cell death mechanisms should occur within 24 hours [42], we presume that the reduction in cell number observed upon long-term exposure was also caused by the decreased cell proliferation in the BioLevitator^{TM}, as the lower doubling rate of the cells in microcarrier cultures promotes the accumulation of NPs.

The BioLevitator^{TM} bioreactor used in this study, also appears suitable for the assessment of biological effects upon exposure to other NMs. CNTs could find broad medical application, particularly in imaging and treatment (vaccination, hyperthermia) provided they are not overtly toxic [21]. Long-term exposure in the microcarrier culture showed a dose-dependent decrease in cell numbers after 7 days. With prolonged contact the cell populations recovered. These findings were supported by our data on the mode of action since the peak levels of induction of apoptosis and/ or necrosis were also detected at day

7. At later time-points, activation of caspases or a notable release of LDH was not detected. The BioLevitator™ bioreactor may also be used for the toxicological assessment of conventional compounds. The action of drugs on cytochrome P450 (CYP) enzymes is important for the metabolization by hepatocytes. Testing is complicated by the fact that CYP enzyme activities are low or absent not only in hepatocyte cell lines but also in cultured primary hepatocytes [43]. In preliminary experiments on HepG2 cells growing on microcarriers, we observed high cell density and a higher activity of the enzyme CYP1A1, important for many pathways (e.g. steroid hormone biosynthesis, tryptophan metabolism, retinol metabolism, metabolism of xenobiotics, and metabolic pathways) (data not shown). Findings on HepG2 cells grown in a three dimensional cell culture and the advantage of that culturing method were described in many other studies [44, 45]. Long-term culture in the BioLevitator™ may therefore also be suitable to evaluate certain aspects of metabolization by hepatocytes.

In summary, our findings suggest that non-biodegradable NPs persist in cells and may cause cell damage. Due to the localization of the NPs in lysosomes, as supported by our data on fluorescent labelled particles, it is necessary to investigate their effect on lysosomes. Lysosomes are potential targets for drug-induced damage, such as for drug-induced lysosomal phospholipidosis resulting in lysosomal dys-function [46].

ACKNOWLEDGEMENTS

The authors would like to thank Sandra Blass and Claudia Meindl for excellent technical assistance, as well as Daniel Portsmouth for critically reading the manuscript.

REFERENCES

1. The European Commission. Commission Recommendation of 18 October 2011 on the definition of nanomaterials. Official Journal of the European Union

(2011/696/EU). http://eur-lex.europa.eu/LexUriServ/LexuriServ.do?uri=OJ:L:2011:275:0038:0040:EN:PDF.

2. Lewinski N, Colvin V, Drezek R (2008) Cytotoxicity of Nanoparticles. Small 4(1): 26-49
3. Whitesides GM (2003) The “right” size in nanobiotechnology. Nature Biotech. 21(10): 1161-1165.
4. Ai J, Biazar E, Jafarpour M, Montazeri M, Majdi A, et al. (2011) Nanotoxicology and nanoparticle safety in biomedical designs. Int. J. Nanomedicine 6: 1117-1127.
5. Oberdörster G, Maynard A, Donaldson K, Castranova V, Fitzpatrick J, et al. (2005) Principles for characterizing the potential human health effects from exposure to nanomaterials: elements of a screening strategy. Part. Fibre Toxicol 2: doi: 10.1186/1743-8977-2-8.
6. Bihari P, Vippola M, Schultes S, Praetner M, Khandoga AG, et al. (2008) Optimized dispersion of nanoparticles for biological *in vitro* and *in vivo* studies. Part. Fibre Toxicol. 5: 14.
7. Dockery DW, Pope CA 3rd, Xu X, Spengler JD, Ware JH, et al. (1993) An association between air pollution and mortality in six U.S. cities. N Engl J Med. 329: 1753-1759.
8. Oberdörster G, Ferin J, Finkelstein G, Wade P, Corson N (1990) Increased pulmonary toxicity of ultrafine particles. 2. Lung lavage studies. J Aerosol Sci. 21: 384-387.
9. Ferin J, Oberdörster G, Penney D, Sonderholm S, Gelein RM, et al. (1990) Increased pulmonary toxicity of ultrafine particles. 1. Particle clearance, translocation, morphology. J Aerosol Sci. 21: 381-384.
10. Oberdörster G, Gelein RM, Ferin J, Weiss B (1995) Association of particulate air pollution and acute mortality: involvement of ultrafine particles? Inhal Toxicol. 7: 111-124.

11. Lison D, Lardot C, Huaux F, Zanetti G, Fubini B (1997) Influence of particle surface area on the toxicity of insoluble manganese dioxide dusts. Arch Toxicol. 71: 725-729.
12. Donaldson K, Stone V, Gilmour PS, Brown DM, MacNee W (2000) Ultrafine particles: mechanisms of lung injury. Phil Trans R Soc Lond A. 358: 2741-2749.
13. Nel A, Xia T, Madler L, Li N (2006) Toxic potential of materials at the nanolevel. Science 311: 622-627.
14. Renwick LC, Donaldson K, Clouter A (2001) Impairment of alveolar macrophage phagocytosis by ultrafine particles. Toxicol. Appl. Pharmacol. 172: 119-127.
15. Yang H, Liu C, Yang D, Zhang H, Xi Z (2009) Comparative study of cytotoxicity, oxidative stress and genotoxicity induced by four typical nanomaterials: the role of particle size, shape and composition. J. Appl. Toxicol. 29: 69-78.
16. Kishore AS, Surekha P, Murthy PB (2009) Assessment of the dermal and ocular irritation potential of multi-walled carbon nanotubes by using *in vitro* and *in vivo* methods. Toxicol. Lett. 191: 268-274.
17. Seaton A, Tran L, Aitken R, Donaldson K (2010) Nanoparticles, human health hazard and regulation. J. R. Soc. Interface 7: 119-129.
18. Rodriguez-Yañez Y, Muñoz B, Albores A (2012) Mechanisms of toxicity of carbon nanotubes. Toxicol mech Methods 29: doi:10.3109/15376516.2012.754534.
19. Seibert H, Balls M, Fentem JH, Bianchi V, Clothier RH, et al. (1996) Acute toxicity testing in vitro and the classification and labelling of chemicals. ATLA 24: 499-510.
20. Michalet X, Pinaud FF, Bentolila LA, Tsay JM, Doose S, et al. (2005) Quantum dots for live cells, *in vivo* imaging and diagnostics. Science 307: 538-544.
21. Turnherr T, Brandenberger C, Fischer K, Diener L, Manser P, et al. (2011) A comparison of acute and long-term effects of industrial multiwalled carbon nanotubes on human lung and immune cells in vitro. Toxicol. Lett. 200(3): 176-186.

22. Sadauskas E, Jacobsen NR, Danscher G, Stoltenberg M, Vogel U, et al. (2009) Biodistribution of gold nanoparticles in mouse lung following intratracheal instillation. Chem Cent J. 3: 16.
23. Kwon JT, Kim DS, Minai-Tehrani A, Hwang SK, Chang SH, et al. (2009) Inhaled fluorescent magnetic nanoparticles induced extramedullary hematopoiesis in the spleen of mice. J. Occup. Health 51: 423-431.
24. Lasagna-Reeves C, Gonzalez-Romero D, Barria MA, Olmedo I, Clos A, et al. (2010) Bioaccumulation and toxicity of gold nanoparticles after repeated administration in mice. Biochem Biophys Res Commun. 393: 649-655.
25. Pazos P, Fortaner S, Prieto P (2002) Long-term in vitro toxicity models: comparisons between a flow-cell bioreactor, a static-cell bioreactor and static cell cultures. Altern Lab Anim. 30(5): 515-523.
26. Gebhardt R, Hengstler JG, Müller D, Glöckner R, Buenning P, et al. (2003) New hepatocyte in vitro systems for drug metabolism: metabolic capacity and recommendations for application in basic research and drug development, standard operation procedures. Drug Metab Rev. 35(2-3): 145-213.
27. Lock LT, Tzanakakis ES (2009) Expansion and differentiation of human embryonic stem cells to endoderm progeny in a microcarrier stirred-suspension culture. Tissue eng Part A 15(8): 2051-2063.
28. Alves PM, Moreira JL, Rodrigues JM, Aunins JG, Carrondo JMT (1996) Two-dimensional versus three-dimensional culture systems: Effects on growth and productivity of BHK cells. Biotechnol. Bioeng. 52: 429-432.
29. Rourou S, van der Ark A, van der Velden T, Kallel H (2007) A microcarrier cell culture process for propagating rabies virus in Vero cells grown in a stirred bioreactor under fully animal component free conditions. Vaccine 25: 3879-3889.
30. Justice BA, Badr NA, Felder RA (2009) 3D cell culture opens new dimensions in cell-based assays. Drug Discov. Today 14(1/2): 102-107.

31. Varani J, Piel F, Josephs S, Beals TF, Hillegas WJ (1998) Attachment and growth of anchorage-dependent cells on a novel, charged-surface microcarrier under serum-free conditions. Cytotechnology 28: 101-109.
32. Butler M, Burgener A, Patrick M, Berry M, Moffatt D, et al. (2000) Application of a serum-free medium for the growth of Vero cells and the production of reovirus. Biotechnol. Prog. 16: 854-858.
33. Serra M, Brito C, Leite SB, Gorjup E, von Briesen H, et al. (2009) Stirred bioreactors for the expansion of adult pancreatic stem cells. Ann. Anat. 191: 104-115.
34. Larson B, Berry D, Justice B, and Gainer T (2010) A novel 3D cell culture method for automated drug screening. Biotech international 22: 10-12.
35. Edgell CS, McDonald CC, Graham JB (1983) Permanent cell line expressing human factor VIII-related antigen established by hybridization. Proc. Natl. Acad. Sci. 80: 3734-3737.
36. Lindl T, Lewandowski B, Sheyrogg S, Staudte A (2005). Evaluation of the in vitro cytotoxicities of 50 chemicals by using an electronic current exclusion method versus the neutral red uptake and MTT assays. Altern. Lab. Anim. 33: 591-601.
37. Swiech K, da Silva GMC, Zangirolami TC, Iemma MRC, Selistre-de-Araújo HS, et al. (2007) Evaluating kinetic and physiological features of rCHO-K1 cells cultured on microcarriers for production of a recombinant metalloprotease/disintegrin. Electronic Journal of Biotechnology 10(2): 201-210. Available: http://www.ejbiotechnology.info/content/vol10/issue2/full/15. Accessed 02 July 2012.
38. Xiao C, Huang Z, Li W, Hu X, Qu W, et al. (1999) High density and scale-up cultivation of recombinant CHO cell line and hybridomas with porous microcarrier Cytopore. Cytotechnology 30: 143-147.

39. Wu J, Liu W, Xue C, Zhou S, Lan F, et al. (2009) Toxicity and penetration of TiO2 nanoparticles in hairless mice and porcine skin after subchronic dermal exposure. Toxicol. Lett. 191: 1-8.
40. Lee J, Lilly D, Doty C, Podsiadlo P, Kotov NA (2009) In vitro toxicity testing of nanoparticles in 3D cell culture. Small 5(10): 1213-1221.
41. Fröhlich E, Samberger C, Kueznik T, Absenger M, Roblegg E, et al. (2009) Cytotoxicity of nanoparticles independent from oxidative stress. J. Toxicol. Sci. 34(4): 363-375.
42. van Nieuwenhuijze AEM, van Lopik T, Aarden LA (2003) Time between onset of apoptosis and release of nucleosomes from apoptotic cells: putative implications for systemic lupus erythematosus. Ann. Rheum. Dis. 62: 10-14.
43. Guillouzo A, Corlu A, Aninat C, Glaise D, Morel F, et al. (2007) The human hepatoma HepaRG cells: A highly differentiated model for studies of liver metabolism and toxicity of xenobiotics. Chem. Biol. Interact. 168: 66-73.
44. Bokhari M, Carnachan RJ, Cameron NR, Przyborski SA (2007) Culture of HepG2 liver cells on three dimensional polystyrene scaffolds enhances cell structure and function during toxicological challenge. J. Anat. 211: 567-576.
45. Li C, Tian T, Nan K, Zhao N, Guo Y, et al. (2008) Survival advantages of multicellular spheroids vs. monolayers of HepG2 cells *in vitro*. Oncol. Rep. 20: 1465-1471.
46. Anderson N, Borlak J (2006) Drug-induced phospholipidosis. FEBS Lett. 580(23): 5533-5540.

FIGURE LEGENDS

Fig. 1 Acute cytotoxicity of NPs exerted on EAhy 926 in different cell cultures after 24 hours. Cells in conventional cultures were treated with NPs dissolved in serum-free

medium (A) as well as in medium with 10% FBS (B). Cells cultured on microcarriers were exposed to NMs dissolved in medium with 10% FBS. Data are presented as mean ± SD.

Fig. 2 Mode of action of PPS in conventional cultures. Activation of caspases 3 and 7 (A and B) and release of LDH (C and D) upon exposure of EAhy 926 cells to 20 and 200 nm PPS for 4, 8, and 24 hours compared to untreated cells. Data are presented as mean ± SD. (h), hours.

Fig. 3 Growth curve of EAhy 926 cultured on basal membrane coated GEM^{TM}. Two pre-installed protocols for cell culturing epithelial (HEK 293) and endothelial (HUVEC) cells were compared. (d), days.

Fig. 4 EAhy 926 attached to GEM^{TM}. Nuclear staining with 5 µg/ ml Hoechst 33342 was performed 1, 5, 7, and 14 days after inoculation (A). Vital dye staining for ER and mitochondria five days after inoculation. Hoechst 33342 dye was used as nuclear counterstain (B). Internalized red fluorescent NPs co-localize with the lysosomal dye LysoSensor^{TM} Green DND-189 but not with the nucleus (blue) (C).

Fig. 5 Long-term cytotoxic effects of NPs on EAhy 926. Cultures were exposed to PPS over a period of 28 days, Data are presented as mean ± SD of the total cell number; n =5, *p*-value < 0.05. * indicates statistically significant changes in cell numbers between control and treated cells at each time-point. Long-term effects upon exposure to different concentrations of MWCNT >50 nm are shown in (B). Data are presented as mean ± SD of the total cell number per culture vessel; n=3. (d), days.

Fig. 6 Mode of action of different NPs in microcarrier cultures. Induction of apoptosis (A and B) and necrosis (C and D) after long-term exposure of EAhy 926 grown on GEM^{TM} to NPs. Data are presented as mean ± SD, normalized to the total cell numbers per culture vessel; (d), days. Changes in viability, caspase activation, and cytotoxicity in cells exposed to PPS at early time-points are presented in (E). Data are presented as mean ± SD. Western blot detecting PARP-1 after treatment of microcarrier cultures with both, PPS and CNTs at an early time-point (day 7) is presented in (F). Treatment with 1 µg/ ml staurosporine was used as a control for apoptosis induction.

TABLE

Table 1. Characterization of tested NMs

Particle	Size (nm)			ζ-pot.(mV)		
	Aqua bidest.	DMEM	DMEM+ 10% FBS	Aqua bidest.	DMEM	DMEM+ 10% FBS
PPS 20 nm	22.76	28.89	73.59*/12.37	-37.1	-13.4	-11.7
PPS 200 nm	211.6	211.5	224.8	-57.6	-11.0	8.08
Fluoro-Max 20 nm	22.22	44.56	58.26	-11.1	-28.2	-10.3
MWCNT >50 nm	n.d.‡	602.9	50.41	n.d.‡	-16.9	-11.0

* Predominant peak is indicated first

‡ Not determined due to aggregates

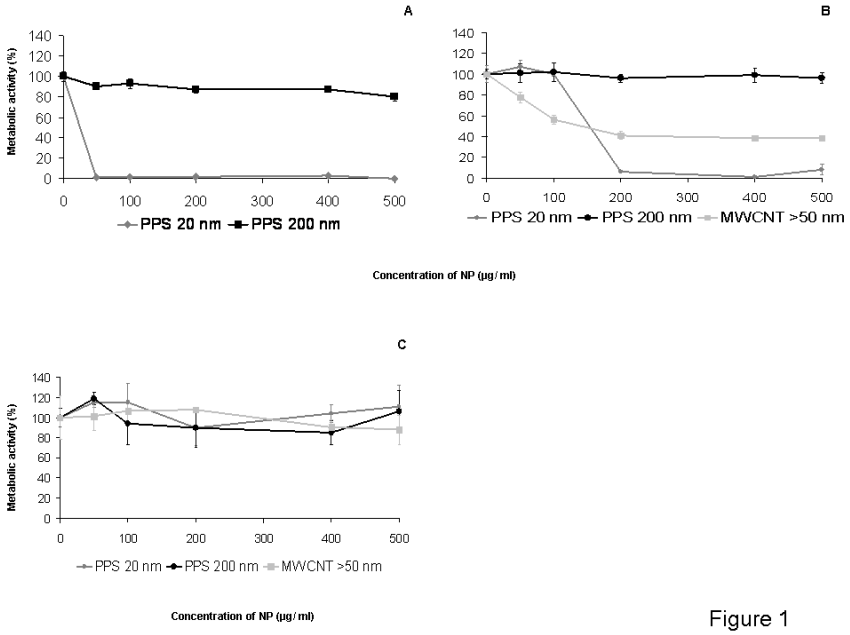

Figure 1

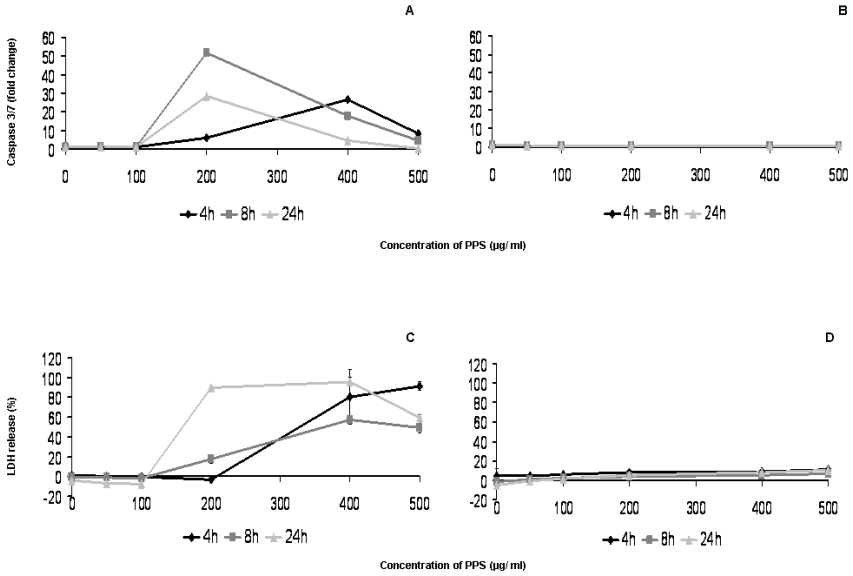

Figure 2

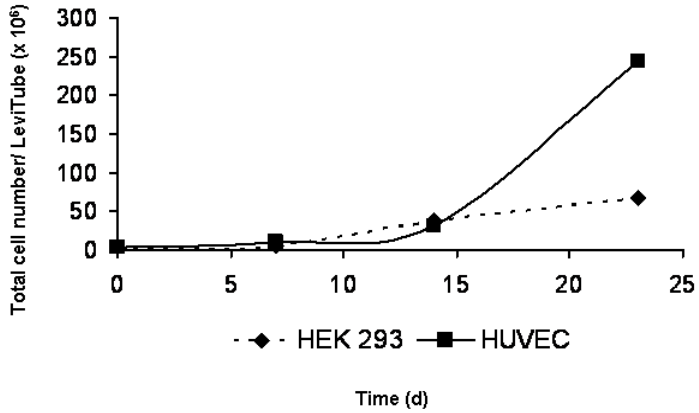
Total cell number/ LeviTube (x 10⁶)
300
250
200
150
100
50
0
0
5
10
15
20
25
HEK 293
HUVEC
Time (d)

Figure 3

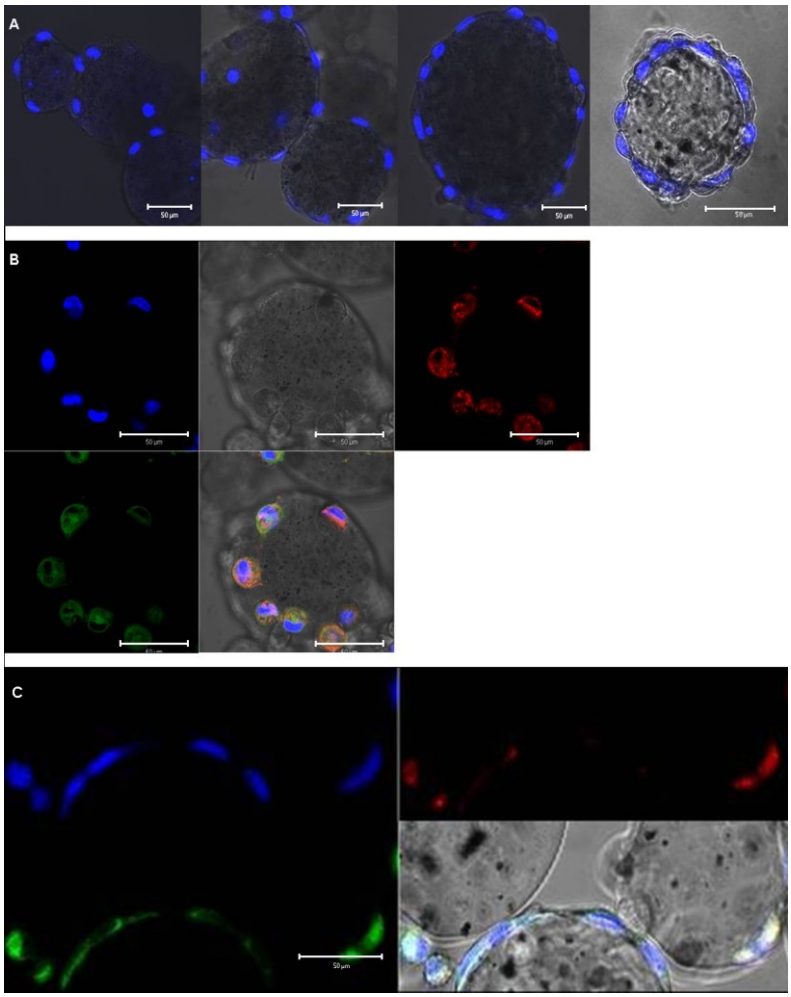
A
B
C

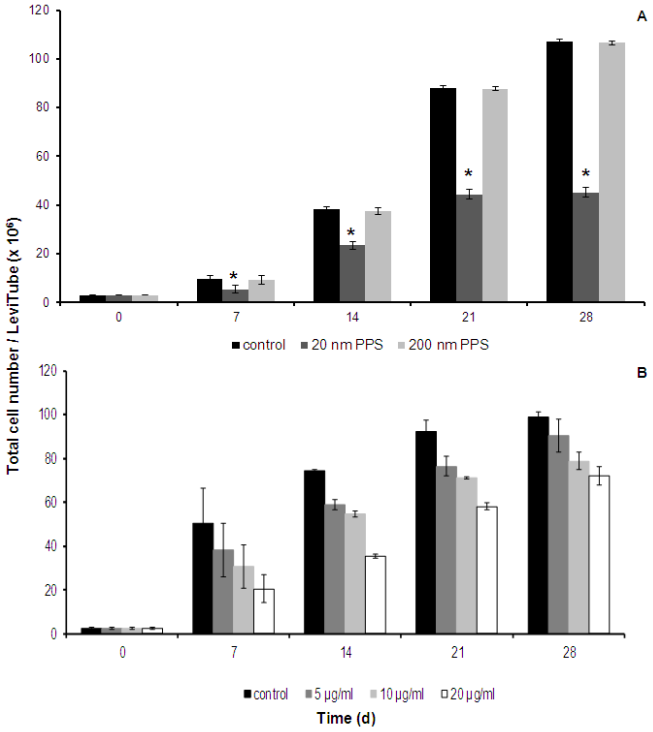

Figure 5

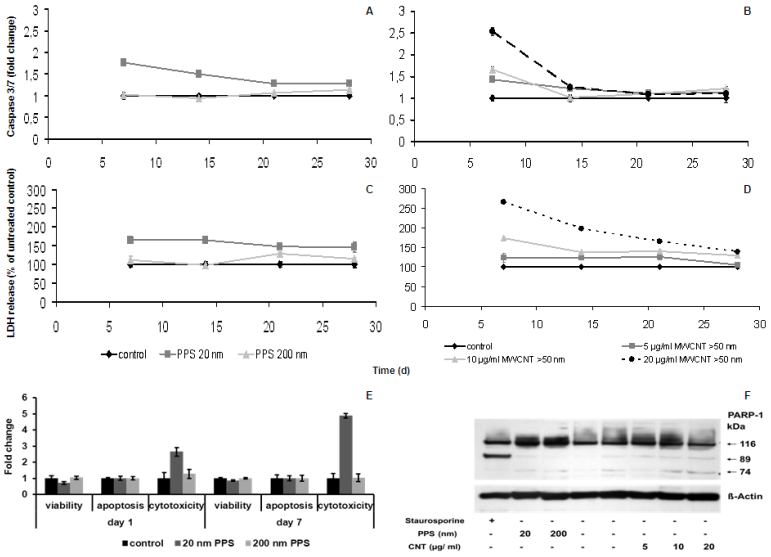

Figure 6